

NEW CHEMISTRY OF MERCAPTOAZULENES AND LOW-VALENT  
COMPLEXES OF ISOCYANOARENES

By

Kolbe Joseph Scheetz

Copyright 2013

Submitted to the graduate degree program in the Department of Chemistry and the Graduate  
Faculty of the University of Kansas in partial fulfillment of the requirements for the degree of  
Doctor of Philosophy.

---

Dr. Mikhail V. Barybin, Chairperson

---

Dr. David R. Benson

---

Dr. Timothy A. Jackson

---

Dr. Helena C. Malinakova

---

Dr. Judy Z. Wu

Date Defended: July 23, 2013

The Dissertation Committee for Kolbe Joseph Scheetz

certifies that this is the approved version of the following dissertation:

NEW CHEMISTRY OF MERCAPTOAZULENES AND LOW-VALENT  
COMPLEXES OF ISOCYANOARENES

---

Dr. Mikhail V. Barybin, Chairperson

Date approved: July 24, 2013

## Abstract

Aryl mercaptans and their coordination complexes contribute to a number of diverse applications including pharmaceutical, surface science, and molecular electronics, and light emitting diodes. Recently the Barybin group has begun to explore the coordination chemistry of mercaptoazulenes. Prior to the work done by Barybin *et. al.* there were no examples of coordination complexes of featuring mercaptoazulenes. Other mercaptoarenes have been utilized in the formation of thin films and featured in materials with luminescent capabilities. Thiolates have also been studied as junction groups used to attach organic compounds with extended  $\pi$  systems to electrodes. Linear asymmetric dimercaptoarenes are rare, but are intriguing for electronics and construction of molecular electronic components such as diodes. In this dissertation coordination chemistry of mercaptoazulenes, synthesis of azulenic derivatives to probe the charge transport dynamics of the asymmetric 2,6-molecular axis of azulene, and the coordination of isocyanoarenes with low valent transition metal complexes will be discussed.

Chapter 1 of the thesis describes the synthesis of the first example of a dimercaptoazulene. Two different synthetic routes were developed for the preparation of this dimercaptan and regioselective metallation was demonstrated for the generation of its mono-nuclear coordination complex. Additionally metallation of the second thiolate termini is also discussed.

Chapter 2 describes the synthesis of isomeric mercaptazulenes featuring cyano substituents. The 6-cyano-2-mercaptoazulene has been prepared. These isomeric molecules offer an opportunity to probe the charge transport dynamics of the asymmetric 2,6-molecular axis of azulene. The cyano substituent could serve as a spectroscopic reporter for additional spectroscopic characterization of these molecules in surface studies.

Chapter 3 describes the coordination studies of iscyanoarenes with electron rich low valent Mo and W metal centers. This investigation focused on whether substitution variations in non-benzenoid aromatic isocyanides would result in the formation of either cis- or trans-  $[M(dppe)_2(CNAr)_2]$  and related complexes.

## Acknowledgements

I like to begin by expressing my gratitude to my graduate adviser and mentor, Misha Barybin. Misha it has been an honor to have been part of your research group at the University of Kansas for the last several years. You are an outstanding teacher and I have learned so much from you. Your dedication to your profession and family is inspirational. I will forever be indebted to you for your friendship and support over the last few months.

I have been blessed to have had such knowledgeable and dedicated professors for all of the courses I took at KU. In particular I would like to thank Dr. Jackson. I will always appreciate the extra help I received during my first semester at KU when I took my first course in inorganic chemistry. I would like to thank my undergraduate advisor Dr. Beard, who was instrumental getting me to pursue a degree in chemistry and for encouraging me to consider graduate school.

To all the current and former members of the Barybin group, I appreciate all of hard work that each of you has done. I feel privileged to have worked besides Tiffany Maher, David McGinnis, Alexander Vorushilov, Brad Neal, John Meyers, Andrew Spaeth, and Mason. All of you have contributed to ensure that there has never been a dull moment and helped make it a joy to come into lab every day.

I would like to thank the Chemistry Department at KU. Justin Douglas and Sarah Neuenswander, your help with my NMR experiments is greatly appreciated and in particular your assistance in the low temperature NMR studies. Bob Drake your assistance with my mass spec. experiments was invaluable. In particular I would like to give a special thanks to my committee members Dr. Helena Malinakova, Dr. David Benson, and Dr. Judy Wu.

Mom and Dad I appreciate all of the work and sacrifices you made over the years to ensure that I would have the opportunity to obtain a quality education. Your selfless love and support has meant more to me than I can express. To my wife Rachel, you have been a wonderful source of support and encouragement. You are one of the strongest women I have met. You are a wonderful mother to our beautiful daughter, Elizabeth “Liza”, and I can’t imagine life without you.

## **Table of Contents**

<b>Chapter I</b> The 2,6-dimercaptoazulene motif: efficient synthesis and completely regioselective metallation of its 6-mercapto terminus.....	1
I.1 Historical Perspective .....	2
I.2 Introduction .....	4
I.3 Work Described in Chapter 1 .....	7
I.4 Experimental Section.....	7
I.4.1 General Procedures .....	3
I.4.2 Synthesis of 2,6-dichloro-1,3-diethoxycarbonylazulene (I.1). ....	9
I.4.3 Synthesis of 2-chloro-6-mercapto-1,3-diethoxycarbonylazulene (I.2) .....	10
I.4.4 Synthesis of 2,6-di(2-methoxycarbonylethylthio)-1,3-diethoxycarbonylazulene (I.3) from I.1 .....	10
I.4.5 Synthesis of 6-bromo-2-(trifluoromethylsulfonyl)oxy-1,3-diethoxycarbonylazulene (I.4). ....	11
I.4.6 Synthesis of I.3 from I.4.....	12
I.4.7 Synthesis of 2,6-dimercapto-1,3-diethoxycarbonylazulene (I.5) .....	12
I.4.8 Synthesis of [Ph <sub>3</sub> PAu](1,3-diethoxycarbonyl-2-mercapto-6-azulenethiolate) (I.6) ....	14
I.4.9 Synthesis of [Ph <sub>3</sub> PAu] <sub>2</sub> ( $\eta^1:\eta^1$ -1,3-diethoxycarbonyl-2,6-azulenedithiolate) (I.7) .....	15
I.4.10 Synthesis of 2,6-dibromo-1,3-diethoxycarbonylazulene (I.8) .....	16
I.4.11 X-ray structure determination for I.1 and I.6 .....	16
I.4.12 Computational work.....	22
I.4 Results and Discussion .....	23
I.6 Conclusions and Outlook .....	41
I.7 References .....	42
<b>Chapter II</b> Synthesis of 6-cyano-2-mercaptoazulene and efforts toward preparation of 2-cyano-6-mercaptoazulene: a pair of isomeric derivatives for probing charge transport along azulene's molecular axis .....	46
II.1. Introduction .....	47
II.2. Work Described in Chapter II .....	58
II.3 Experimental Section .....	58
II.3.2 Synthesis of 6-bromo-2-hydroxyazulene (II.1).....	59
II.3.3 Synthesis of 6-cyano-2-hydroxyazulene (II.2).....	60
II.3.4 Synthesis of 6-cyano-2-(trifluoromethylsulfonyl)oxyazulene (II.3) .....	60
II.3.5 Synthesis of 6-cyano-2-mercaptoazulene (II.4) .....	61
II.3.6 Synthesis of 6-cyano-2-N,N-dimethylamino-1,3-diethoxycarbonylazulene (II.5) .....	62
II.3.7 Synthesis of 2-amino-6-cyano-1,3-diethoxycarbonylazulene (II.6).....	63
II.3.8 Synthesis of 6-amino-2-cyanoazulene (II.7).....	63
II.3.9 Synthesis of 2-cyano-1,3-diethoxycarbonylazulene (II.8).....	64
II.3.10 Synthesis of 2-chloro-6-hydroxy-1,3-diethoxycarbonylazulene (II.9).....	65
II.3.10 Synthesis of 2-chloro-6-hydroxy-1,3-diethoxycarbonylazulene (II.9).....	65
II.4 Results and Discussion .....	66
II.5 Conclusions and Outlook .....	75

II.6 References.....	78
<b>Chapter III</b> Coordination Chemistry of Nonbenzenoid Isocyanoarenes with Low Valent Molybdenum and Tungsten .....	81
III.1 Historical Perspective .....	82
III.2 Introduction .....	86
III.3 Work Described in Chapter 3 .....	85
III.4 Experimental Section .....	89
III.4.1 General Procedures .....	86
III.4.2 Synthesis of <i>trans</i> -[W(dppe) <sub>2</sub> (CN <sup>2</sup> CO <sub>2</sub> Et <sup>1,3</sup> Az) <sub>2</sub> ] (III.1).....	86
III.4.3 Synthesis of <i>trans</i> -[W(dppe) <sub>2</sub> (CN <sup>1</sup> Az) <sub>2</sub> ] (III.2) .....	87
III.4.4 Synthesis of [W(dppe) <sub>2</sub> (CNFc) <sub>2</sub> ] (III.3) .....	87
III.4.5 Synthesis of [Mo(CO)(dppe) <sub>2</sub> (CN <sup>2</sup> CO <sub>2</sub> Et <sup>1,3</sup> Az)] (III.4).....	88
III.4.6 Synthesis of [Mo(CO)(dppe) <sub>2</sub> (CN <sup>2</sup> AzNC <sup>6</sup> )Mo(CO)(dppe) <sub>2</sub> ] (III.5).....	88
III.5 Results and Discussion.....	89
III.6 Conclusions and Outlook .....	96
III.7 References .....	98
<b>Appendix 1</b> Crystallographic Data for Compound I.1 .....	100
<b>Appendix 2</b> Crystallographic Data for Compound I.6 .....	111
<b>Appendix 3</b> NMR Spectra of Selected Compounds from Chapter I .....	135
<b>Appendix 4</b> NMR Spectra of Selected Compounds from Chapter II.....	151
<b>Appendix 5</b> FTIR Spectra of Selected Compounds .....	160



## List of Tables

<b>Table I.1</b> Crystal data and structure refinement for <b>I.1</b> .....	18
<b>Table I.2</b> Crystal data and structure refinement for <b>I.6</b> .....	20
<b>Table I.3</b> DFT-calculated energy differences ( $\Delta E = E_B - E_A$ ) in kcal/mol between isomeric structures B and A in the gas phase and in THF .....	24
<b>Table 1.2</b> FTIR (KBr) and $^1\text{H}$ NMR ( $\text{CDCl}_3$ ) spectroscopic signatures of the mercapto functionalities in <b>1a</b> , <b>1b</b> , <b>3b</b> , <b>I.5</b> and <b>I.6</b> .....	33
<b>Table III.1</b> Stereochemistry of the $(p\text{-R-C}_6\text{H}_4\text{-NC})_2\text{W}(\text{dppe})_2$ complexes and the corresponding $\nu_{\text{CN}}$ data adapted from reference 16. ....	86
<b>Table III.2</b> FTIR $\nu_{\text{CN}}$ stretches of free and bound isocyanides .....	95
<b>Table III.3</b> FTIR $\nu_{\text{CN}}$ and $\nu_{\text{CO}}$ stretches of complexes <b>III.4</b> and <b>III.5</b> .....	96

## List of Figures

<b>Figure I.1</b> Examples of 3- and 4-coordinate Au(I) complexes. ....	3
<b>Figure I.2</b> Atom numbering schemes for 1,4-dimercaptobenzene (left), 2,6-dimercaptonaphthalene (center), and unknown 2,6-dimercaptoazulene (right). ....	4
<b>Figure I.3</b> Currently known mercaptoazulenes .....	5
<b>Figure I.4</b> Resonance stabilization of 2-mercapto-6-azulenylthiolate .....	25
<b>Figure I.5</b> DFT-optimized structures of [Ph <sub>3</sub> PAu](2-mercapto-1,3-di-ethoxycarbonyl-6-azulenethiolate) and [Ph <sub>3</sub> PAu](6-mercapto-1,3-di-ethoxycarbonyl-2-azulenethiolate). The $\Delta E$ values in the gas phase and in THF are given in kcal/mol .....	26
<b>Figure I.6</b> Left: molecular structure of <b>1b</b> . <sup>27</sup> Selected interatomic distances (Å) and angles (°) for <b>1b</b> : S(1)-C(2) 1.739(2), C(11)-O(3) 1.215(2), C(14)-O(4) 1.216(2), S1...O4 3.034(1), S1-H...O4 121.0. Right: molecular structure of one of two crystallographically independent molecules of <b>3b</b> . <sup>26</sup> Selected bond distances (Å) for <b>3b</b> : S(1)-C(6) 1.765(3), C(11)-O(3) 1.217(3), C(14)-O(4) 1.217(3) .....	27
<b>Figure I.7</b> Deprotonation study of 6-mercapto-1,3-diethoxycarbonylazulene ( <b>3b</b> ) in CH <sub>2</sub> Cl <sub>2</sub> at 25 °C with NEt <sub>3</sub> .....	28
<b>Figure I.8</b> Deprotonation study of 2-mercapto-1,3-diethoxycarbonylazulene ( <b>1b</b> ) in CH <sub>2</sub> Cl <sub>2</sub> at 25 °C with NEt <sub>3</sub> .....	28
<b>Figure I.9</b> Deprotonation study of 2-mercapto-1,3-diethoxycarbonylazulene ( <b>1b</b> ) in CH <sub>2</sub> Cl <sub>2</sub> at 25 °C with DBU .....	29
<b>Figure I.10</b> Molecular structure of <b>I.1</b> . Selected bond distances (Å): Cl(1)-C(2) and angles (°): C(2)-Cl(1) 1.714(4), C(6)-Cl(2) 1.759(4) .....	30
<b>Figure I.11</b> Resonance contribution to the deactivation of the halogen at the 2- position of azulene toward nucleophilic substitution .....	31
<b>Figure I.12</b> FTIR spectrum (KBr) of <b>I.5</b> in the $\nu$ (S-H) region .....	34
<b>Figure I.13</b> Molecular structure of <b>I.6</b> . One of two crystallographically independent molecules is shown. Selected interatomic distances (Å) and angles (°): Au <sup>a</sup> -P <sup>a</sup> 2.266(2), Au <sup>a</sup> -S2 <sup>a</sup> 2.319, S2 <sup>a</sup> -C6 <sup>a</sup> 1.772(7), S1 <sup>a</sup> -C2 <sup>a</sup> 1.755(7), S1 <sup>a</sup> ...O1 <sup>a</sup> 3.030(7), P <sup>a</sup> -Au <sup>a</sup> -S <sup>a</sup> 178.56(6), Au <sup>a</sup> -S2 <sup>a</sup> -C6 <sup>a</sup> 104.5, S1 <sup>a</sup> -H---O1 <sup>a</sup> 139.4. ....	35
<b>Figure I.14</b> Frontier molecular orbitals of <b>I.6</b> .....	36
<b>Figure I.15</b> UV-vis spectra of <b>I.6</b> before and after treatment with excess DBU in CH <sub>2</sub> Cl <sub>2</sub> .....	37

<b>Figure I.16</b> UV-Vis spectra of <b>I.6</b> (blue) and <b>I.7</b> (green) in CH <sub>2</sub> Cl <sub>2</sub> at 25 °C .....	38
<b>Figure I.17</b> Variable temperature <sup>31</sup> P{ <sup>1</sup> H} NMR spectra of <b>I.7</b> in CD <sub>2</sub> Cl <sub>2</sub> .....	39
<b>Figure II.1</b> Atom numbering scheme of azulene showing resonance forms and its polar nature .....	47
<b>Figure II.2</b> Molecular diode composed of extended π-systems .....	48
<b>Figure II.3</b> Schematic of azulene connected at the 2- and 6- to electron reservoirs (Ref 15). ....	49
<b>Figure II.4</b> 2,2'-disocyano-1,1',3,3'-tetraethoxycarbonyl-6,6'-biazulenylacetylene (Ref 19) ....	49
<b>Figure II.5</b> Targeted isomeric 2-cyano-6-mercaptoazulene and 6-cyano-2-mercaptoazulene ....	51
<b>Figure II.6</b> Selected examples of 2- and 6-mercaptoazulenes A (Ref 30a), B (Ref 30a, 30b), C (Ref 25), D (Ref 30a) .....	51
<b>Figure II.7</b> 2- and 6-cyanoazulenes A (Ref 31a) B and C (Ref 31b).....	52
<b>Figure II.8</b> Frontier Molecular Orbitals of Azulene (Extended Huckel Calculation) .....	53
<b>Figure II.9</b> Selected mono- and di-functionalized azulene derivatives that have been prepared through EAS reactions (Ref 33).....	54
<b>Figure II.10</b> FTIR spectrum of 6-cyano-2-hydroxyazulene in a KBr pellet .....	67
<b>Figure II.11</b> Solid state FTIR spectrum of 6-cyano-2-(trifluoromethylsulfonyl)oxyazulene in KBr .....	69
<b>Figure II.12</b> FTIR spectrum of 6-cyano-2-mercaptoazulene in KBr .....	70
<b>Figure III.1</b> Isocyanides as σ-donors and π-acceptors .....	84
<b>Figure III.3</b> Local symmetry around the metal center in bis-isocyano octahedral coordination complexes. ....	93
<b>Figure III.3</b> Local symmetry around the metal center in bis-isocyano octahedral coordination complexes .....	94
<b>Figure III.4</b> IR spectra of free ligand (grey) and <b>III.3</b> (black) in THF.....	95
<b>Figure III.5</b> Diisocyanoarenes that may be suitable for the construction of 1-D organometallic materials .....	96

## List Schemes

<b>Scheme I.1</b> Synthesis of the 2,6-dimercapto-1,3-diethoxycarbonylazulene .....	32
<b>Scheme I.2</b> Regioselective metallation of <b>I.5</b> and the formation of <b>I.6</b> and <b>I.7</b> .....	38
<b>Scheme II.1</b> Nozoe's synthesis of substituted azulenes from tropolone (Ref 45). .....	55
<b>Scheme II.2</b> Diazotization of 2-amino-1-cyano-3-methylcarboxylateazulene (Ref 46) .....	56
<b>Scheme II.3</b> Oxidation of 6-methyl during diazotization of 2-amino (Ref 47) .....	56
<b>Scheme II.4</b> Synthesis of 2-bromoazulene (Ref 48) .....	56
<b>Scheme II.5</b> Synthesis of dichloroazulenes (Ref 49) .....	57
<b>Scheme II.6</b> Synthesis of 6-cyano-2-mercaptoazulene .....	66
<b>Scheme II.7</b> Synthesis of 2-mercaptoazulene (Ref 30a) .....	68
<b>Scheme II.9</b> Proposed synthesis of 2-cyano-6-mercaptoazulene .....	71
<b>Scheme II.10</b> Synthesis of 1-(azulen-6-ylazo)-azulen-6-yl-amine (Ref 37) .....	73
<b>Scheme II.11</b> Proposed synthesis of 2-cyano-6-mercaptoazulene .....	74
<b>Scheme II.12</b> Proposed synthesis of 2-cyano-6-mercaptoazulene .....	76
<b>Scheme III.1</b> Synthesis of $[\text{Mo}(\text{N}_2)_2(\text{dppe})_2]$ and $[\text{W}(\text{N}_2)_2(\text{dppe})_2]$ (Ref 4) .....	82
<b>Scheme III.2</b> Synthesis of W and Mo $[\text{M}(\text{CO})(\text{DMF})(\text{dppe})_2]$ .....	83
<b>Scheme III.3</b> Synthesis of $[\text{Mo}(\text{CNR})(\text{N}_2)(\text{dppe})_2]$ .....	83
<b>Scheme III.4</b> Synthesis of <i>trans</i> - $[\text{M}(\text{CNR})_2(\text{dppe})_2]$ .....	85
<b>Scheme III.5</b> Proposed method for the formation of uniform 1-D organometallic materials by the systematic addition of metal centers .....	87
<b>Scheme III.6</b> Controlled Mono- and Heterobimetallic Complexation of 2,6-diisocyano-1,3-diethoxycarbonylazulene (Ref 19) .....	88

## Chapter I

The 2,6-dimercaptoazulene motif: efficient synthesis and completely regioselective metallation  
of its 6-mercapto terminus

Portions of this work have been reproduced from:

Scheetz, K. J.; Spaeth, A. D.; Vorushilov, A. S.; Powell, D. R.; Day, V. W.; Barybin, M. B. “The 2,6-dimercaptoazulene motif: efficient synthesis and completely regioselective metallation of its 6-mercapto terminus,” submitted to *Chemical Science*

## I.1 Historical Perspective

### Chemistry of Gold and Gold(I) complexes

The rich history of gold expands to more than just usage in coinage and jewelry. Even 3500 years ago in China and Arabia gold was used in the treatment of numerous ailments.<sup>1</sup> The discovery of Robert Koch that  $K[Au(CN)_2]$  inhibited the growth *Tubercle bacilli*<sup>2</sup> sparked the renewed pursuit of pharmaceuticals containing gold. In modern times, drugs with gold(I) thiolates are a common treatment for rheumatoid arthritis.<sup>3</sup> The drug auranfin, which was first developed for the treatment of rheumatoid arthritis,<sup>4</sup> is currently being investigated as a future candidate for treating HIV.<sup>5</sup> Beyond pharmaceutical applications, gold has many other intriguing applications. A recent review highlights some of the catalytic activity of gold complexes.<sup>6</sup>

Gold(I) complexes have an electron configuration of  $5d^{10}$  and are diamagnetic. The most common gold(I) complexes feature two ligands bound in a linear fashion but complexes with three or four ligands are also known.<sup>7</sup> The majority of gold(I) complexes with more than two ligands contain at least one phosphine.<sup>7</sup> If the number of ligands coordinating to a gold(I) complexes is not readily discernible, x-ray crystallography may be employed to enable such a determination.<sup>7</sup> Figure 1.1 shows examples of both three and four coordinate gold(I) complexes.

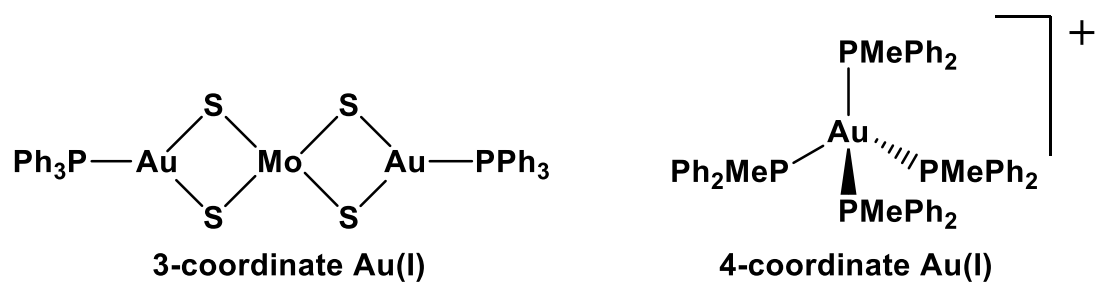


**Figure 1.1** Examples of 3- and 4-coordinate Au(I) complexes.<sup>8,9</sup>

Similar to other late third row transition metals, gold(I) complexes are subject to the trans effect.<sup>10</sup>

## I.2 Introduction

Linear dimercaptoarenes, such as 1,4-dimercaptobenzene (Figure I.2 left), have recently sparked renewed theoretical and experimental interest in the quest for deeper understanding of the fundamental principles that govern the design of molecular conductors and rectifiers.<sup>11</sup>

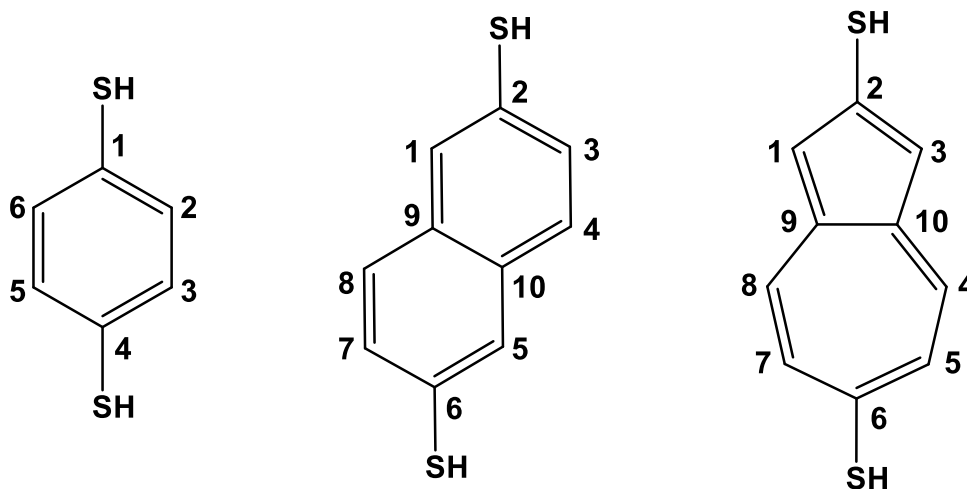


**Figure I.2** Atom numbering schemes for 1,4-dimercaptobenzene (left), 2,6-dimercaptanaphthalene (center), and unknown 2,6-dimercaptoazulene (right).

A single-molecule wire generally features a conjugated planar  $\pi$ -bridge to ensure facile charge transfer between the donor and acceptor sites.<sup>12</sup> While many such systems studied to date involve aromatic benzenoid platforms, it has been suggested that a framework composed solely of  $sp^2$ -carbon pentagons and heptagons could exhibit metallic-like behavior.<sup>13</sup> The simplest model in this regard is based on the scaffold of azulene, a nonbenzenoid bicyclic aromatic hydrocarbon featuring fused five- and seven-membered  $sp^2$ -carbon rings. Given that the azulenenic scaffold itself carries a dipole of about 1.1 Debye,<sup>14</sup> the linear 2,6-azulene motif can, in principle, behave as a molecular diode even without incorporation of any donor/acceptor substituents.

In 1998, a theoretical study by Treboux *et al.* suggested that a discrete bridging 2,6-



azulenic moiety would have intriguing charge transport characteristics.<sup>15</sup> A decade later, computational work by Pati and co-workers indicated that the hypothetical 2,6-dimercaptoazulene framework should exhibit lower resistance compared to 2,6-dimercaptonaphthalene (Figure I.1).<sup>16</sup> In 2011, yet another theoretical study by Zhang *et al.* concluded that 2,6-dimercaptoazulene and related, currently unknown “azulene-like” molecules could function as highly conductive molecular rectifiers.<sup>17</sup> While the conductivity of 2,6-dimercaptonaphthalene has finally been assessed experimentally by Frisbie *et al.*<sup>18</sup> and Taniguchi, *et al.*,<sup>19</sup> 2,6-mercaptoazulene or any derivatives thereof remain unknown. To date there have been no reports of the preparation of any dimercaptoazulenes. Anderson, *et al.*, attempted to form a 1,3-dimercaptoazulene through reduction of 1,3-dithiocynoazulene but was unsuccessful.<sup>20</sup> All isoluble mercaptoazulenes are shown in Figure I.3.

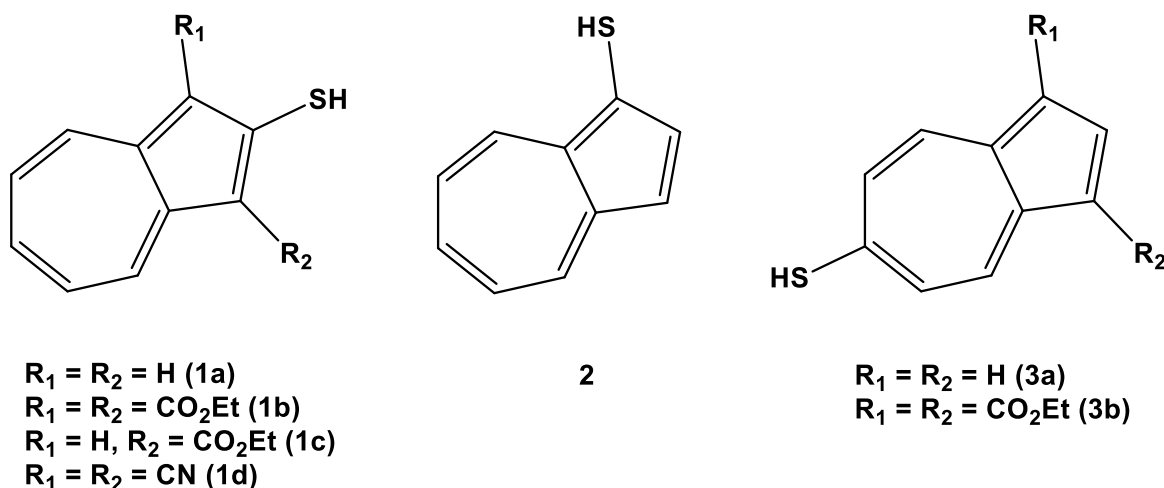


**Figure I.3** Currently known mercaptoazulenes.

Since the original syntheses of **1a**, **1b**, **1c**, **2**, **3a**, and **3b** by Fujimori,<sup>21</sup> Nozoe<sup>22</sup>, and Asao<sup>23, 24</sup> decades ago, their chemistry had remained completely dormant. The lack of literature on the use

of these functionalized azulenes as ligands in coordination and surface chemistry was particularly surprising. Initial investigations of the coordination chemistry of **1b** and **3b** were conducted to and yielded dinuclear gold complexes.<sup>25</sup> More recently in 2011, the surface chemistry of **1a**, **1b**, and **1d** was reported.<sup>26</sup> In addition to a simple synthetic route to a family of 2-mercaptoazulenes (compounds **1a**, **1b**, and **1d** in Figure I.3) use of thiolate junctions in self-assembly of azulenic thin films on metallic gold surfaces was also demonstrated.<sup>26</sup> The adsorbed molecules of **1a**, **1b**, and **1d** orient approximately upright (i.e., linear Au-S-C units) with respect to the metal surface.<sup>26</sup>

### **I.3 Work Described in Chapter 1**

This chapter highlights two efficient synthetic routes to the first 2,6-dimercaptoazulene derivative and describes the initial efforts in developing its coordination chemistry, including exclusively regioselective metallation of the 6-SH terminus.

## I.4 Experimental Section

**I.4.1 General procedures, starting materials and equipment.** Unless specified otherwise, all operations were performed under an atmosphere of 99.5% argon further purified by passage through columns of activated BASF catalyst and molecular sieves. All connections involving the gas purification systems were made of glass, metal, or other materials impermeable to air. Solutions were transferred via stainless steel needles (cannulas) whenever possible. Standard Schlenk techniques were employed with a double manifold vacuum line. Both  $\text{CH}_2\text{Cl}_2$  and  $\text{CD}_2\text{Cl}_2$  were distilled over  $\text{CaH}_2$ . Deuterated chloroform was distilled over  $\text{P}_2\text{O}_5$ . Tetrahydrofuran (THF) was distilled from Na/benzophenone. Pentane was distilled from Na/benzophenone dissolved in a minimum amount of diglyme. Benzene was dried over molecular sieves and then distilled over freshly cut potassium metal. Methanol was distilled over Mg turnings. Other solvents were used as received from commercial sources.

Infrared spectra were recorded on a PerkinElmer Spectrum 100 FTIR spectrometer with liquid samples sealed in 0.1 mm NaCl cells or solid samples embedded in KBr pellets. NMR samples were analyzed on Bruker Avance 400 or 500 spectrometers.  $^1\text{H}$  and  $^{13}\text{C}$  NMR chemical shifts are given with reference to residual solvent resonances relative to  $\text{SiMe}_4$ .  $^{31}\text{P}$  NMR chemical shifts are referenced externally to 85% aqueous  $\text{H}_3\text{PO}_4$  (a sealed capillary tube containing 85% aqueous  $\text{H}_3\text{PO}_4$  was inserted into each sample tube subject to  $^{31}\text{P}$  NMR analysis). UV-Vis spectra were recorded at 24 °C using a CARY 100 spectrophotometer.

Melting points are uncorrected and were determined for samples in capillary tubes sealed under argon. Elemental analyses were carried out by ALS Environmental (formerly Columbia Analytical Services), Tucson, Arizona and by Micro-Analysis, Inc., Wilmington, Delaware. Mass-spectral data were obtained in the Mass-spectrometry facility at the University of Kansas.

2-Amino-6-bromo-1,3-diethoxycarbonylazulene,<sup>27</sup> 2-hydroxy-6-bromo-1,3-diethoxycarbonylazulene,<sup>28</sup> and Au(PPh<sub>3</sub>)Cl<sup>29</sup> were prepared according to literature procedures. Other reagents were obtained from commercial sources and used as received.

**I.4.2 Synthesis of 2,6-dichloro-1,3-diethoxycarbonylazulene (I.1).** Dry HCl(g) was bubbled through a solution of 2-amino-6-bromo-1,3-diethoxycarbonylazulene (1.248 g, 3.408 mmol) in 250 mL of benzene at room temperature. The HCl treatment was stopped after 2 hrs and isoamyl nitrite (0.798 g, 6.812 mmol) was added to the reaction mixture with stirring. The solution darkened from orange to black, then gradually acquired green color and, finally, turned red. After 24 hrs of stirring at room temperature, the reaction mixture was poured into 200 mL of distilled H<sub>2</sub>O. The organic layer was separated, washed vigorously with deionized H<sub>2</sub>O (3×50 mL), dried over anhydrous Na<sub>2</sub>SO<sub>4</sub>, and filtered. All solvent was removed from the filtrate under vacuum to give a red oil. Recrystallization of the product from EtOH provided a red crystalline solid, which was filtered off and dried at 10<sup>-2</sup> torr to afford **I.1** (0.592 g, 1.735 mmol) in a 51% yield. Mp: 162 °C (lit.<sup>7</sup> 160 -161 °C). IR (CH<sub>2</sub>Cl<sub>2</sub>): ν<sub>CO</sub> 1693 cm<sup>-1</sup>. <sup>1</sup>H NMR (CDCl<sub>3</sub>, 500 MHz, 25 °C): δ 1.48 (t, <sup>3</sup>J<sub>HH</sub> = 7.0 Hz, 6H, CH<sub>3</sub>), 4.50 (q, <sup>3</sup>J<sub>HH</sub> = 7.0 Hz, 4H, CH<sub>2</sub>), 7.80 (d, <sup>3</sup>J<sub>HH</sub> = 10.0 Hz, 2H *H*<sup>5,7</sup>), 9.33 (d, <sup>3</sup>J<sub>HH</sub> = 10.0 Hz, 2H, *H*<sup>4,8</sup>) ppm. <sup>13</sup>C{<sup>1</sup>H} NMR (CDCl<sub>3</sub>, 126 MHz, 26 °C): δ 14.35 (CH<sub>3</sub>), 60.88 (CH<sub>2</sub>), 116.70, 131.10, 135.91, 139.80, 143.42, 147.50 (azulenic C), 163.98 (CO<sub>2</sub>Et) ppm.

Note: it is imperative to conduct this reaction under inert atmosphere (e.g., argon) to avoid substantial reduction in the yield of **I.1**. Performing the above reaction without protection from air resulted in a poor yield of **I.1** and the formation of multiple other products which have not been fully characterized.

**I.4.3 Synthesis of 2-chloro-6-mercapto-1,3-diethoxycarbonylazulene (I.2).** Red crystals of **I.1** (0.109 g, 0.319 mmol) and 2.00 g of 68% aqueous sodium hydrosulfide (24.3 mmol) were added to 40 mL of 70% aqueous ethanol. The resulting solution/slurry was brought to reflux and stirred for 1 hr. After cooling to room temperature, the flask contents were poured into 200 mL of deionized water and acidified slowly with aqueous sulfuric acid until a pink precipitate formed. This pink solid was filtered off and extracted with CH<sub>2</sub>Cl<sub>2</sub> (3×15 mL). The organic extracts were combined, washed vigorously with H<sub>2</sub>O (2×25 mL), dried over anhydrous Na<sub>2</sub>SO<sub>4</sub>, and filtered. All solvent was removed from the filtrate under vacuum to leave an orange residue, which was recrystallized by layering its solution in CH<sub>2</sub>Cl<sub>2</sub> with pentane to afford **I.2** (0.088 g, 0.260 mmol) in an 82% yield. Mp: 142-144 °C. HRMS (*m/z*, ES<sup>-</sup>): found for [M-H]<sup>-</sup> 337.0337; calcd for C<sub>16</sub>H<sub>14</sub>ClO<sub>4</sub>S<sup>-</sup> 337.0307. IR (KBr): ν<sub>SH</sub> 2521 w; ν<sub>CO</sub> 1675 s cm<sup>-1</sup>. <sup>1</sup>H NMR (CDCl<sub>3</sub>, 500 MHz, 25 °C): δ 1.46 (t, <sup>3</sup>J<sub>HH</sub> = 7.0 Hz, 6H, CH<sub>3</sub>), 4.23 (s, 1H, SH), 4.47 (q, <sup>3</sup>J<sub>HH</sub> = 7.0 Hz, 4H, CH<sub>2</sub>), 7.54 (d, <sup>3</sup>J<sub>HH</sub> = 11.2 Hz, 2H, H<sup>5,7</sup>), 9.15 (d, <sup>3</sup>J<sub>HH</sub> = 11.2 Hz, 2H, H<sup>4,8</sup>), ppm. <sup>13</sup>C{<sup>1</sup>H} NMR (CDCl<sub>3</sub>, 126 MHz, 25 °C): δ 14.37 (CH<sub>3</sub>), 60.65 (CH<sub>2</sub>), 116.18, 129.33, 136.03, 139.08, 141.41, 151.86 (azulenic C), 164.20 (CO<sub>2</sub>Et) ppm.

**I.4.4 Synthesis of 2,6-di(2-methoxycarbonylethylthio)-1,3-diethoxycarbonylazulene (I.3) from I.1.** Methyl-3-mercaptopropionate (0.130 g, 1.082 mmol) was added to a solution of **I.1** (0.136 g, 0.399 mmol) in 10 mL of pyridine. The mixture was refluxed for 4 hrs with stirring, then cooled to room temperature and poured into 25 mL of CH<sub>2</sub>Cl<sub>2</sub>. The resulting solution was washed with 3M H<sub>2</sub>SO<sub>4</sub> (2×25 mL), then once with 25 mL of deionized H<sub>2</sub>O, dried over anhydrous Na<sub>2</sub>SO<sub>4</sub>, and concentrated under vacuum to give a red oil. The red oil was dissolved in a minimum amount of CH<sub>2</sub>Cl<sub>2</sub> and layered with pentane to form orange crystals upon solvent

diffusion at room temperature. The crystals were filtered off and dried at  $10^{-2}$  torr to afford **I.3** (0.163 g, 0.320 mmol) in an 80% yield. Mp: 94 °C. HRMS ( $m/z$ , ES<sup>+</sup>): found for [M+H]<sup>+</sup> 509.1300; calcd for C<sub>24</sub>H<sub>29</sub>O<sub>8</sub>S<sub>2</sub><sup>+</sup> 509.1298. IR (CH<sub>2</sub>Cl<sub>2</sub>):  $\nu_{\text{CO}}$  1737 s, 1690 s cm<sup>-1</sup>. <sup>1</sup>H NMR (CDCl<sub>3</sub>, 400 MHz, 20 °C):  $\delta$  1.47 (t, <sup>3</sup>J<sub>HH</sub> = 7.2 Hz, 6H, CH<sub>2</sub>CH<sub>3</sub>), 2.59 (t, <sup>3</sup>J<sub>HH</sub> = 7.6 Hz, 2H, CH<sub>2</sub>), 2.79 (t, <sup>3</sup>J<sub>HH</sub> = 7.4 Hz, 2H, CH<sub>2</sub>), 3.30 (t, <sup>3</sup>J<sub>HH</sub> = 7.6 Hz, 2H, CH<sub>2</sub>), 3.40 (t, <sup>3</sup>J<sub>HH</sub> = 7.4 Hz, 2H, CH<sub>2</sub>), 3.64 (s, 3H, CO<sub>2</sub>CH<sub>3</sub>), 3.74 (s, 3H, CO<sub>2</sub>CH<sub>3</sub>), 4.49 (q, <sup>3</sup>J<sub>HH</sub> = 7.2 Hz, 4H, CH<sub>2</sub>CH<sub>3</sub>), 7.45 (d, <sup>3</sup>J<sub>HH</sub> = 11.3 Hz, 2H, H<sup>5,7</sup>), 8.94 (d, <sup>3</sup>J<sub>HH</sub> = 11.3 Hz, 2H, H<sup>4,8</sup>) ppm. <sup>13</sup>C{<sup>1</sup>H} NMR (CDCl<sub>3</sub>, 126 MHz, 25 °C):  $\delta$  14.43 (CH<sub>2</sub>CH<sub>3</sub>), 28.13 (CH<sub>2</sub>), 30.70 (CH<sub>2</sub>), 33.01 (CH<sub>2</sub>), 34.41 (CH<sub>2</sub>), 51.74 (CO<sub>2</sub>CH<sub>3</sub>), 52.15 (CO<sub>2</sub>CH<sub>3</sub>), 60.90 (CH<sub>2</sub>CH<sub>3</sub>), 119.85, 126.86, 134.09, 139.08, 147.80, 153.33 (azulenic C), 162.29 (CO<sub>2</sub>Et), 171.49 (CO<sub>2</sub>Me), 171.99 (CO<sub>2</sub>Me) ppm.

#### **I.4.5 Synthesis of 6-bromo-2-(trifluoromethylsulfonyl)oxy-1,3-diethoxycarbonyl-azulene**

**(I.4).** Triethylamine (0.20 mL, 1.43 mmol) was added to a solution of 2-hydroxy-6-bromo-1,3-diethoxycarbonylazulene (0.344 g, 0.937 mmol) in 25 mL of CH<sub>2</sub>Cl<sub>2</sub> at room temperature with stirring. The reaction mixture darkened. To the resulting solution, triflic anhydride (0.530 g, 1.879 mmol) dissolved in 10 mL of CH<sub>2</sub>Cl<sub>2</sub> was added dropwise. Upon the addition of Tf<sub>2</sub>O, the mixture turned red and was stirred at room temperature for a period of one hour. Then, the reaction flask contents were poured into 100 mL of deionized H<sub>2</sub>O. The organic layer was separated, washed sequentially with 25 mL of H<sub>2</sub>O and 25 mL of brine, and dried over anhydrous Na<sub>2</sub>SO<sub>4</sub>. Following filtration, all solvent was removed from the filtrate under vacuum to afford red microcrystals of **I.4**. While the product can be used in the next step without further purification, it can be recrystallized by layering its CH<sub>2</sub>Cl<sub>2</sub> solution with pentane to provide spectroscopically pure **I.4** (0.450 g, 0.900 mmol) in a 96% yield. HRMS ( $m/z$ , ES<sup>+</sup>): found for

$[M+Na]^+$  520.9473 and 522.9448; calcd for  $C_{17}H_{14}^{79}BrF_3NaO_7S^+$  520.9488, calcd for  $C_{17}H_{14}^{81}BrF_3NaO_7S^+$  522.9467.  $^1H$  NMR ( $CDCl_3$ , 400 MHz, 20 °C):  $\delta$  1.46 (t,  $^3J_{HH} = 7.1$  Hz, 6H,  $CH_3$ ), 4.49 (q,  $^3J_{HH} = 7.1$  Hz, 4H,  $CH_2$ ), 8.15 (d,  $^3J_{HH} = 11.4$  Hz, 2H,  $H^{5,7}$ ), 9.54 (d,  $^3J_{HH} = 11.4$  Hz, 2H,  $H^{4,8}$ ) ppm.  $^{13}C\{^1H\}$  NMR ( $CDCl_3$ , 126 MHz, 25 °C):  $\delta$  14.10 ( $CH_3$ ), 61.23 ( $CH_2$ ), 109.40 (azulenic C), 118.70 (q,  $^1J_{CF} = 320.0$  Hz,  $CF_3$ ), 135.28, 138.66, 138.78, 140.34, 152.37 (azulenic C), 162.80 ( $CO_2Et$ ) ppm.

**I.4.6 Synthesis of I.3 from I.4.** Methyl-3-mercaptopropionate (0.03 mL, 0.27 mmol) was added, with stirring, to a solution of **I.4** (0.054 g, 0.108 mmol) in 3 mL of pyridine. The reaction mixture was heated to 90 °C and stirred at this temperature for 4 hrs. After cooling to room temperature, the contents of the reaction flask were poured into 25 mL of 3M  $H_2SO_4$ . The resulting mixture was extracted with  $CH_2Cl_2$  (3×10mL). The organic extracts were combined, washed sequentially with 10 mL of 3M  $H_2SO_4$ , 10mL of  $H_2O$ , and 10 mL of brine, and dried over anhydrous  $Na_2SO_4$ . Filtration followed by solvent removal from the filtrate on a rotary evaporator provided a red oil. This red oil was crystallized by layering its solution in a minimum amount of  $CH_2Cl_2$  with pentane to afford **I.3** (0.041 g, 0.081 mmol) in a 75% yield. The product was spectroscopically identical to the sample of **I.3** obtained through the procedure I.4.5 described above.

**I.4.7 Synthesis of 2,6-dimercapto-1,3-diethoxycarbonylazulene (I.5).** Absolute ethanol, deionized  $H_2O$ , and 3M  $H_2SO_4$  were all purged with argon for 30 minutes prior to their use in the following procedure. A solution of sodium ethoxide prepared by *carefully* dissolving sodium metal (0.030 g, 1.305 mmol) in 20 mL of EtOH was transferred into a flask containing a



suspension of **I.3** (0.150 g, 0.295 mmol) in 10 mL of EtOH. Following the addition of the sodium ethoxide solution, the reaction mixture was stirred for 4 hrs at room temperature while acquiring red color. Then, the mixture was diluted with 300 mL of H<sub>2</sub>O and slowly acidified with 3M H<sub>2</sub>SO<sub>4</sub> until formation of a yellow precipitate. At this point, the reaction flask was opened to the air atmosphere. The precipitate was filtered off, washed extensively with water and dried at 10<sup>-2</sup> torr. The yellow solid was dissolved in a minimum amount of CH<sub>2</sub>Cl<sub>2</sub> and the resulting solution was layered with pentane. Upon solvent diffusion, small, yellow, needlelike crystals formed. These crystals were filtered off and dried at 10<sup>-2</sup> torr to afford **I.5** (0.084 g, 0.250 mmol) in an 85% yield. Mp: 112-114 °C (dec). Anal. calcd for C<sub>16</sub>H<sub>16</sub>O<sub>4</sub>S<sub>2</sub>: C, 57.12; H, 4.79. Found C, 56.66; H, 4.31. HRMS (*m/z*, ES<sup>-</sup>): found for [M-H]<sup>-</sup> 335.0414; calcd for C<sub>16</sub>H<sub>15</sub>O<sub>4</sub>S<sub>2</sub><sup>-</sup>, 335.0417. <sup>1</sup>H NMR (CDCl<sub>3</sub>, 400 MHz, 25 °C): δ 1.50 (t, <sup>3</sup>J<sub>HH</sub> = 7.2 Hz, 6H, CH<sub>3</sub>), 4.12 (s, 1H, SH), 4.50 (q, <sup>3</sup>J<sub>HH</sub> = 7.2 Hz, 4H, CH<sub>2</sub>), 7.56 (d, <sup>3</sup>J<sub>HH</sub> = 11.4 Hz, 2H, H<sup>5,7</sup>), 7.58 (s, 1H, SH), 9.18 (d, <sup>3</sup>J<sub>HH</sub> = 11.4 Hz, 2H, H<sup>4,8</sup>) ppm. <sup>13</sup>C{<sup>1</sup>H} NMR (CDCl<sub>3</sub>, 126 MHz, 25 °C): δ 14.50 (CH<sub>3</sub>), 60.64 (CH<sub>2</sub>), 114.50, 130.12, 133.88, 141.44, 148.07, 153.53 (azulenic C), 165.79 (CO<sub>2</sub>) ppm. IR (KBr): ν<sub>SH</sub> 2540 m, 2450 w br; ν<sub>CO</sub> 1683 s sh, 1666 s cm<sup>-1</sup>. UV-Vis (CH<sub>2</sub>Cl<sub>2</sub>, λ<sub>max</sub> (ε×10<sup>-3</sup> M<sup>-1</sup> cm<sup>-1</sup>), 24 °C): 230 (9.3), 250 (13.8), 270 (14.3), 275 (14.1) ~335 (47.3) sh, 340 (53.5), ~405 (10.9) sh, 420 (15.0) nm.

Note: if the acidification is performed without rigorous protection from air, only minute amounts of the desired compound **I.5** can be isolated. Indeed, upon acidification of the reaction mixture under normal atmospheric conditions, the solution turns red and little to no yellow precipitate forms. Following extraction and work up, the major product gives the following <sup>1</sup>H NMR (C<sub>6</sub>D<sub>6</sub>, 400 MHz, 21 °C) spectrum: δ 1.10 (t, <sup>3</sup>J<sub>HH</sub> = 8 Hz, 6H, CH<sub>3</sub>), 4.21 (q, <sup>3</sup>J<sub>HH</sub> = 8 Hz, 4H, CH<sub>2</sub>), 7.34 (d, 12 Hz, 2H, H<sup>5,7</sup>), 8.26 (s, 1H, SH), 9.29 (d, <sup>3</sup>J<sub>HH</sub> = 8 Hz, 2H, H<sup>4,8</sup>) ppm, which

does not feature a characteristic resonance for the 6-*SH* mercapto hydrogen nucleus and could correspond to the disulfide species.

**I.4.8 Synthesis of [Ph<sub>3</sub>PAu](1,3-diethoxycarbonyl-2-mercapto-6-azulenethiolate) (I.6).** A solution of Ph<sub>3</sub>AuCl (0.177 g, 0.382 mmol) and **I.5** (0.120 g, 0.357 mmol) in 10 mL of THF was treated with triethylamine (0.054 mL, 0.389 mmol) with stirring at room temperature. The color of the reaction mixture changed from orange to red-orange upon the addition of the base. After stirring for 5 hrs, the mixture was concentrated under vacuum to about 5 mL and *ca.* ~5 mL of pentane was added to the reaction flask to precipitate the crude product as an orange powder. This solid was filtered off and re-dissolved in a minimum amount of CH<sub>2</sub>Cl<sub>2</sub>. The resulting solution was carefully layered with pentane. After slow diffusion of pentane into the CH<sub>2</sub>Cl<sub>2</sub> layer at room temperature, orange crystals formed. These crystals were filtered off, washed with pentane, and dried at 10<sup>-2</sup> torr to afford **I.6** (0.282 g, 0.355 mmol) in a 99.4% yield. Mp: 179-181 °C. Anal. calcd for C<sub>34</sub>H<sub>30</sub>AuO<sub>4</sub>PS<sub>2</sub>: C, 51.39; H, 3.81. Found: C, 51.53; H, 4.02. IR (KBr):  $\nu_{SH}$  2438 w br;  $\nu_{CO}$  1680 s, 1657 s cm<sup>-1</sup>. <sup>1</sup>H NMR (CDCl<sub>3</sub>, 400 MHz, 25 °C):  $\delta$  1.48 (t, <sup>3</sup>J<sub>HH</sub> = 8 Hz, 6H, CH<sub>3</sub>), 4.47 (q, <sup>3</sup>J<sub>HH</sub> = 8 Hz, 4H, CH<sub>2</sub>), 7.49 (s, 1H, SH) 7.55 (m, 15 H, PPh<sub>3</sub>), 8.20 (d, <sup>3</sup>J<sub>HH</sub> = 12 Hz, 2H, H<sup>5,7</sup>), 8.97 (d, <sup>3</sup>J<sub>HH</sub> = 12 Hz, 2H, H<sup>4,8</sup>) ppm. <sup>13</sup>C{<sup>1</sup>H} NMR (CDCl<sub>3</sub>, 126 MHz, 25 °C):  $\delta$  14.5 (CH<sub>3</sub>), 60.2 (CH<sub>2</sub>), 113.2, 128.6, 129.0, 129.4 (d, <sup>2</sup>J<sub>CP</sub> = 11.3 Hz), 132.0 (d, <sup>3</sup>J<sub>CP</sub> = 2.5 Hz), 132.4, 134.1 (d, <sup>1</sup>J<sub>CP</sub> = 13.8 Hz), 135.6, 141.1, 149.9, 165.3 (CO<sub>2</sub>Et), 166.2 (CO<sub>2</sub>Et) ppm. <sup>31</sup>P{<sup>1</sup>H} NMR (162 MHz, CDCl<sub>3</sub>, 25 °C): 37.54 ppm. <sup>31</sup>P{<sup>1</sup>H} NMR (202 MHz, CD<sub>2</sub>Cl<sub>2</sub>, 25 °C): 37.89 ppm. UV-Vis (CH<sub>2</sub>Cl<sub>2</sub>,  $\lambda_{max}$  ( $\epsilon \times 10^{-3}$  M<sup>-1</sup> cm<sup>-1</sup>), 24 °C): 235 (35.4), 245 (32.8), 275 (26.2), ~295 (15.1) sh, 325 (21.0), 365 (41.6), ~425 (25.2) sh, 445 (39.1) nm.

**I.4.9 Synthesis of [Ph<sub>3</sub>PAu]<sub>2</sub>( $\eta^1$ : $\eta^1$ -1,3-diethoxycarbonyl-2,6-azulenedithiolate) (**I.7**).** All manipulations in the following procedure were conducted with protection from ambient laboratory lighting. A solution prepared by dissolving NaOH (0.0115 g, 0.2875 mmol) in 7 mL of dry methanol was transferred via cannula to a flask containing a solid mixture of **I.6** (0.0459 g, 0.0578 mmol) and Ph<sub>3</sub>PAuCl (0.0286 g, 0.0578 mmol). The resulting suspension was stirred for 30 minutes at room temperature and then diluted with 7 mL of CH<sub>2</sub>Cl<sub>2</sub>. After stirring for *ca.* 24 hrs in the dark, all solvent was removed under vacuum to leave an orange-red residue. This solid was extracted with CH<sub>2</sub>Cl<sub>2</sub> (2×15 mL). The extracts were combined, concentrated under reduced pressure and passed through a 1.5 cm plug of basic alumina using a 1:10 MeOH/CH<sub>2</sub>Cl<sub>2</sub> eluent to remove any trace of **I.6** from the product. Solvent removal from the red band and drying of the resulting product at 10<sup>-2</sup> torr provided **I.7** (0.0660 g, 0.0527 mmol), which can be recrystallized at -30 °C by layering its solution in CH<sub>2</sub>Cl<sub>2</sub> with pentane, in a 92% yield. Anal. calcd for C<sub>52</sub>H<sub>44</sub>Au<sub>2</sub>O<sub>4</sub>P<sub>2</sub>S<sub>2</sub>: C, 49.85; H, 3.54. Found: C, 49.72; H, 3.28. HRMS (*m/z*, ES<sup>+</sup>): found for [M+H]<sup>+</sup> 1253.1685; calcd for C<sub>52</sub>H<sub>45</sub>Au<sub>2</sub>O<sub>4</sub>P<sub>2</sub>S<sub>2</sub><sup>+</sup> 1253.1566. IR (KBr):  $\nu_{\text{CO}}$  1681 s cm<sup>-1</sup>. <sup>1</sup>H NMR (CDCl<sub>3</sub>, 400 MHz, 20 °C):  $\delta$  1.32 (t, <sup>3</sup>J<sub>HH</sub> = 7 Hz, 6H, CH<sub>3</sub>), 4.23 (q, <sup>3</sup>J<sub>HH</sub> = 7 Hz, 4H, CH<sub>2</sub>), 7.53 (m, 30 H, PPh<sub>3</sub>) 8.01 (d, <sup>3</sup>J<sub>HH</sub> = 11.0 Hz, 2H, H<sup>5,7</sup>) 8.42 (d, <sup>3</sup>J<sub>HH</sub> = 11.0 Hz, 2H, H<sup>4,8</sup>) ppm. <sup>31</sup>P{<sup>1</sup>H} NMR (202 MHz, CD<sub>2</sub>Cl<sub>2</sub>, 22 °C): 37.19 (broad singlet) ppm. <sup>31</sup>P NMR (202 MHz, CD<sub>2</sub>Cl<sub>2</sub>, -40 °C): 37.95, 36.19 ppm. UV-Vis (CH<sub>2</sub>Cl<sub>2</sub>,  $\lambda_{\text{max}}$  ( $\epsilon \times 10^{-3} \text{ M}^{-1} \text{ cm}^{-1}$ ), 24 °C): 290 (17.0), ~320 (24.0) sh, ~340 (32.2), 365 (40.3), ~450 (28.9) sh, 475 (38.8) nm.

**I.4.10 Synthesis of 2,6-dibromo-1,3-diethoxycarbonylazulene (I.8).** This synthesis constitutes a modified procedure originally reported by Morita *et al.*<sup>30</sup> To a suspension of 2-amino-6-bromo-1,3-diethoxycarbonylazulene (0.252 g, 0.688 mmol) in 20 mL of benzene 5 drops of concentrated H<sub>2</sub>SO<sub>4</sub> and then isoamyl nitrite (0.20 mL, 1.5 mmol) were added. The reaction was stirred for 5 minutes at room temperature. Then CuBr (0.263 g, 1.833 mmol) and 6 mL of acetonitrile were added to the mixture. Following this addition, the reaction was left stirring at room temperature for 12 hours. The mixture was carefully decanted into 50 mL of H<sub>2</sub>O making sure to leave solid CuBr in the reaction flask. The organic layer was separated from the aqueous layer and the organic fraction was washed with 3 × 20 mL of H<sub>2</sub>O, dried over anhydrous Na<sub>2</sub>SO<sub>4</sub>, and concentrated to dryness under vacuum. The resulting violet residue was redissolved in benzene and then subjected to column chromatography on silica gel using neat benzene as the eluent. Two red bands were observed traveling extremely close to one another. The second band was the collected and its solution was evaporated and dried under vacuum to give **I.8** (0.055 g, 0.128 mmol) in an 18.5% yield. <sup>1</sup>H NMR (CDCl<sub>3</sub>, 500 MHz, 25 °C): δ 1.49 (t, <sup>3</sup>J<sub>HH</sub> = 7 Hz, 6H, CH<sub>3</sub>), 4.50 (q, <sup>3</sup>J<sub>HH</sub> = 7 Hz, 4H, CH<sub>2</sub>), 7.97 (d, <sup>3</sup>J<sub>HH</sub> = 11 Hz, 2H, H<sup>5,7</sup>), 9.14 (d, <sup>3</sup>J<sub>HH</sub> = 11 Hz, 2H, H<sup>4,8</sup>), ppm-. <sup>13</sup>C{<sup>1</sup>H} NMR (CDCl<sub>3</sub>, 126 MHz, 25°C) δ 14.36 (CH<sub>3</sub>), 61.01 (CH<sub>2</sub>), 119.44, 131.71, 133.92, 135.96, 138.11, 140.07, (aromatic C), 164.12 (CO<sub>2</sub>Et) ppm.

#### **I.4.11 X-ray structure determination for I.1 and I.6.**

X-ray quality red needle-shaped crystals of **I.1**, and red block-shaped crystals of **I.6** were grown by carefully layering pentane over relatively dilute solutions of these compounds in CH<sub>2</sub>Cl<sub>2</sub> at room temperature and then cooling the samples to -30 °C for a period of 1-2 weeks. Intensity data for all samples were collected using diffractometers with a Bruker SMART APEX CCD area detector and graphite-monochromated MoKα radiation (λ= 0.71073 Å).<sup>31</sup> Lattice

constants were determined with the Bruker SAINT software package.<sup>32</sup> The data were corrected empirically for variable absorption effects using equivalent reflections.<sup>33</sup> The space groups for **I.1** and **I.6** were determined by statistical tests and verified by subsequent refinements. The Bruker software package SHELXTL was used to solve the structure using “direct methods” techniques.<sup>34</sup> All stages of weighted full-matrix least-squares refinement were conducted using  $F_o^2$  data.<sup>35</sup>

The positions of hydrogen atoms bonded to carbons were initially determined by geometry and refined by a riding model. For **I.6** the hydrogen atoms bonded to sulfur atoms were located on a difference map, and their positions were refined independently. Hydrogen atom displacement parameters were set to 1.2 (1.5 for methyl) times the isotropic equivalent displacement parameters of the bonded atoms. Non-hydrogen atoms were refined with anisotropic displacement parameters. All displacement ellipsoids are drawn at the 50% probability level.

The asymmetric unit of **I.1** contains one  $C_{16}H_{14}Cl_2O_4$  molecule. For **I.1**, the final difference map shows two peaks  $> 2 \text{ e}^-/\text{\AA}^3$ . These peaks were located *ca.* 0.9 Å from the two chlorine atoms. The vector between the two chlorine atoms and the two large peaks in the difference map are approximately the same. Therefore, it is likely that these extra peaks represent an example of whole molecule disorder.

There are two molecules  $C_{34}H_{30}AuO_4PS_2$  per asymmetric unit of **I.6**. The selected crystal of **I.6** exhibited racemic twinning as was shown by the refined value of the Flack parameter.<sup>36</sup> The polar axis restraints were taken from Flack and Schwarzenbach.<sup>37</sup>

**Table I.1** Crystal data and structure refinement for **I.1**.

---

Empirical formula	$\text{C}_{16}\text{H}_{14}\text{Cl}_2\text{O}_4$	
Formula weight	341.17	
Crystal system	triclinic	
Space group	$P\bar{1}$	
Unit cell dimensions	$a = 3.9099(11) \text{ \AA}$	$\alpha = 82.606(5)^\circ$
	$b = 13.413(4) \text{ \AA}$	$\beta = 86.888(6)^\circ$
	$c = 14.207(4) \text{ \AA}$	$\gamma = 82.453(6)^\circ$
Volume	$731.9(4) \text{ \AA}^3$	
Z, Z'	2, 1	
Density (calculated)	$1.548 \text{ Mg/m}^3$	
Wavelength	$0.71073 \text{ \AA}$	
Temperature	$100(2) \text{ K}$	
$F(000)$	352	
Crystal size	$0.46 \times 0.18 \times 0.07 \text{ mm}^3$	
Absorption coefficient	$0.459 \text{ mm}^{-1}$	
Absorption correction	Semi-empirical	
Max. and min. transmission	0.9686 and 0.8167	
Theta range for data collection	$1.54$ to $25.25^\circ$	
Reflections collected	7409	
Independent reflections	2654 [ $R(\text{int}) = 0.0499$ ]	
Data / restraints / parameters	2654 / 0 / 201	

$wR(F^2 \text{ all data})$	$wR2 = 0.1876$
$R(F \text{ obsd data})$	$R1 = 0.0700$
Goodness-of-fit on $F^2$	1.017
Observed data [ $I > 2\sigma(I)$ ]	1994
Largest and mean shift / s.u.	0.000 and 0.000
Largest diff. peak and hole	2.253 and -0.309 e/Å <sup>3</sup>

---


$$R_1 = \Sigma ||F_O| - |F_C|| / \Sigma |F_O|$$

$$wR_2 = \{ \Sigma [w(F_O^2 - F_C^2)^2] / \Sigma [w(F_O^2)^2] \}^{1/2}$$

**Table I.2** Crystal data and structure refinement for **I.6**.

---

Empirical formula	$\text{C}_{34}\text{H}_{30}\text{AuO}_4\text{PS}_2$	
Formula weight	794.64	
Crystal system	Orthorhombic	
Space group	$Pca2_1$	
Unit cell dimensions	$a = 23.574(2) \text{ \AA}$	$\alpha = 90^\circ$
	$b = 11.1504(10) \text{ \AA}$	$\beta = 90^\circ$
	$c = 23.342(2) \text{ \AA}$	$\gamma = 90^\circ$
Volume	$6135.7(9) \text{ \AA}^3$	
Z, Z'	8, 2	
Density (calculated)	$1.720 \text{ Mg/m}^3$	
Wavelength	$0.71073 \text{ \AA}$	
Temperature	$100(2) \text{ K}$	
$F(000)$	3136	
Crystal size	$0.32 \times 0.30 \times 0.12 \text{ mm}^3$	
Absorption coefficient	$5.022 \text{ mm}^{-1}$	
Absorption correction	Semi-empirical from equivalents	
Max. and min. transmission	0.5840 and 0.2964	
Theta range for data collection	$1.73$ to $25.50^\circ$	
Reflections collected	37712	
Independent reflections	10050 [ $R(\text{int}) = 0.0404$ ]	
Data / restraints / parameters	10050 / 1 / 768	
	20	



$wR(F^2 \text{ all data})$	$wR2 = 0.0721$
$R(F \text{ obsd data})$	$R1 = 0.0294$
Goodness-of-fit on $F^2$	0.998
Observed data [ $I > 2\sigma(I)$ ]	9157
Absolute structure parameter	0.240(6)
Largest and mean shift / s.u.	0.030 and 0.001
Largest diff. peak and hole	1.203 and -0.548 e/Å <sup>3</sup>

---


$$R_1 = \Sigma ||F_O| - |F_C|| / \Sigma |F_O|$$

$$wR_2 = \{ \Sigma [w(F_O^2 - F_C^2)^2] / \Sigma [w(F_O^2)^2] \}^{1/2}$$

### **I.4.12 Computational work**

All computational work was done by Andrew D. Spaeth. All Density Functional Theory (DFT) calculations were performed using the ORCA (v.2.9.1) program.<sup>38</sup> Geometric optimizations for the gold complexes were performed spin-restricted using the BP86 functional<sup>39</sup> with a TZVP basis set.<sup>40</sup> The resolution of identity approximation (RI) was used along with the SV/J auxiliary basis set,<sup>41</sup> and the Zero-Order Regular Approximation (ZORA).<sup>42</sup> Single point energy and time-dependent DFT (TD-DFT) calculations were then performed using the B3LYP functional<sup>43</sup> with ZORA, a TZVP basis set, and a TZV/J auxiliary basis set.<sup>42</sup>

## I.5 Results and Discussion

All transition metal complexes of dimercaptoarenes known to date involve coordination of both of their S-termini through the formation of the thiolate junctions between the metal centers and the aromatic linker. Given the currently accessible substitution patterns in 2- and 6-mercaptoazulenes (Figure I.3), we considered several hypothetical isomeric pairs of functionalized 2,6-dimercaptoazulenic conjugate bases by Density Functional Theory (DFT), see Table I.3.

**Table I.3** DFT-calculated energy differences ( $\Delta E = E_B - E_A$ ) in kcal/mol between isomeric structures B and A in the gas phase and in THF <sup>a</sup>

A	B	$\Delta E_{\text{gas}}^a$	$\Delta E_{\text{THF}}^a$
		4.8	3.2
		11.9	9.8
		16.1	14.4
		7.17	3.31
		0.3	0.5
		4.7	2.8
		9.9	8.9
		9.7	9.4

<sup>a</sup> ORCA (v.2.9.1) SP: B3LYP/TZVP.

The relative energies of these anions may be related to the acidity strengths of the SH groups being deprotonated. In the case of the simplest pair, 2-mercapto-6-azulenethiolate appears to be slightly more stable than its 6-mercapto-2-azulenethiolate congener. This may be explained by the direction the azulenic dipole ( $e^-$ -rich 5-membered ring /  $e^-$ -poor 7-membered ring) and the

possibility of resonance stabilization of the former anion to give the aromatic cyclopentadienide-like structure (Figure I.4).

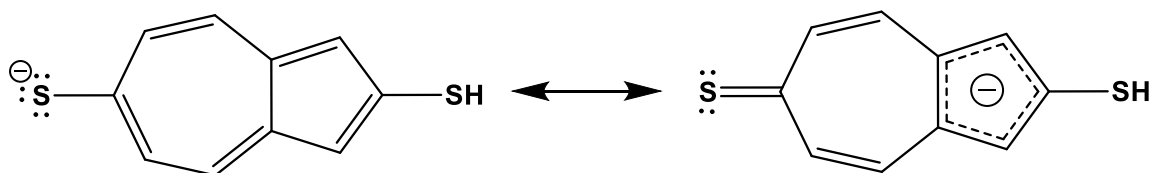


**Figure I.4** Resonance stabilization of 2-mercapto-6-azulenylthiolate.

Introduction of cyano substituents at the 1,3-positions of the azulenic nucleus results in little change in the stabilities of these isomeric mercaptoazulene thiolates. On the other hand, the 2-thiolate isomer becomes substantially less stable than the 6-thiolate isomer upon 1,3-diethoxycarbonyl substitution due to unfavourable electrostatic interaction of the 2-thiolate anion with the ethoxycarbonyls.

Interestingly, complexation of the “parent” 2-mercapto-6-azulenethiolate and 6-mercapto-2-azulenethiolate ligands with the  $\text{Ph}_3\text{PAu}^{\text{I}}$  fragment is predicted to yield isoenergetic adducts, whereas the energy difference between the corresponding complexes featuring one ester substituent is marginal at best. However, the isomeric gold(I) triphenylphosphine complexes of the mercaptoazulene thiolates possessing two ester substituents are suggested to have markedly different stabilities. The less favorable isomer involves binding of the  $\text{Au}^{\text{I}}$  unit to the 2-thiolate junction and features substantial steric congestion, which moves the carboxylate groups out of the aromatic plane, thereby disrupting their conjugation with the azulenic ring (Figure I.5).

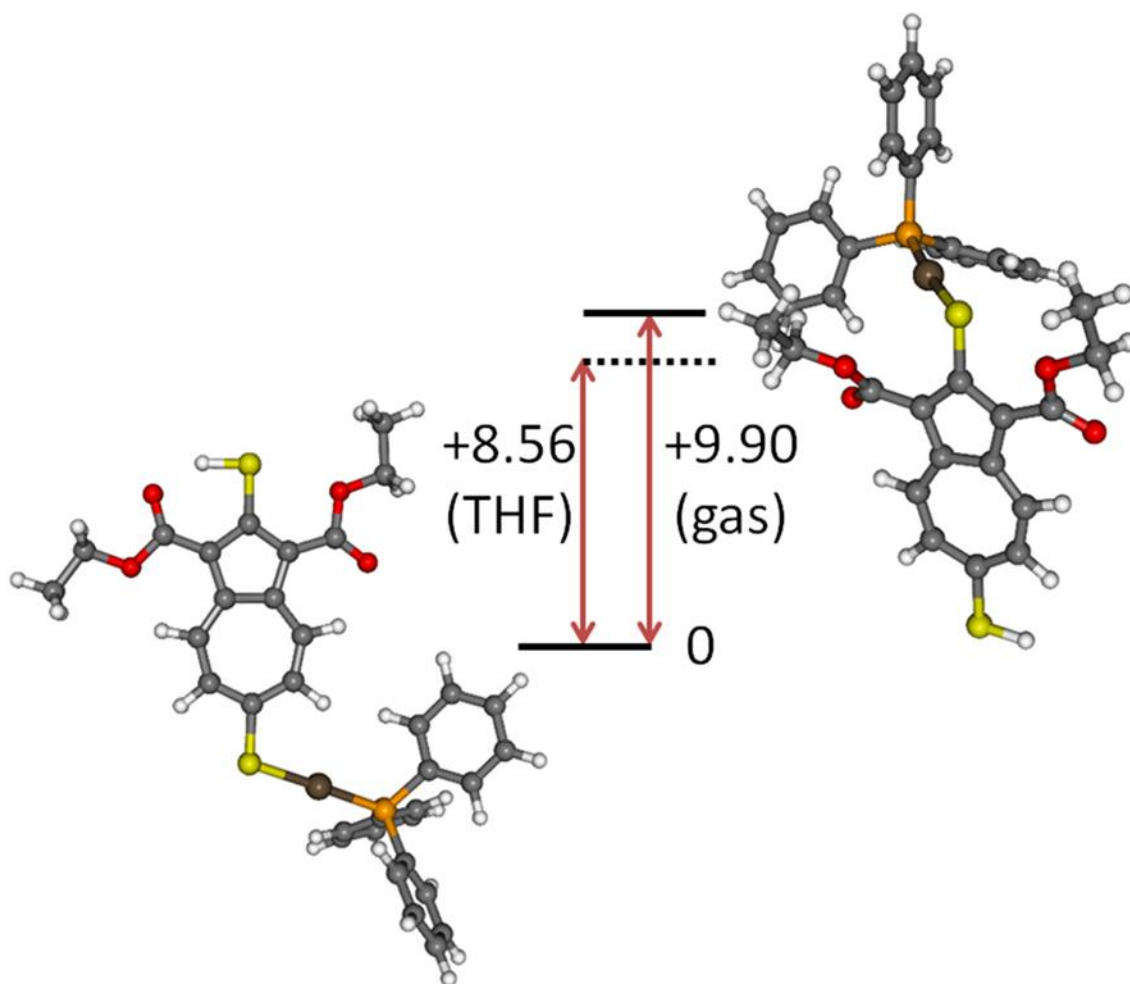


**Figure I.5** DFT-optimized structures of [Ph<sub>3</sub>PAu](2-mercapto-1,3-di-ethoxycarbonyl-6-azulenethiolate) and [Ph<sub>3</sub>PAu](6-mercapto-1,3-di-ethoxycarbonyl-2-azulenethiolate). The  $\Delta E$  values in the gas phase and in THF are given in kcal/mol.

Replacing the PPh<sub>3</sub> ligand with a smaller phosphine (PMe<sub>3</sub>) has no effect on the predicted relative stabilities of these complexes.

The Barybin group has previously reported the X-ray structures of **1b**<sup>26</sup> and **3b**<sup>25</sup>. Figure I.6 nicely captures the most prominent difference in this regard, which is related to the orientation of the ethoxycarbonyl substituents.

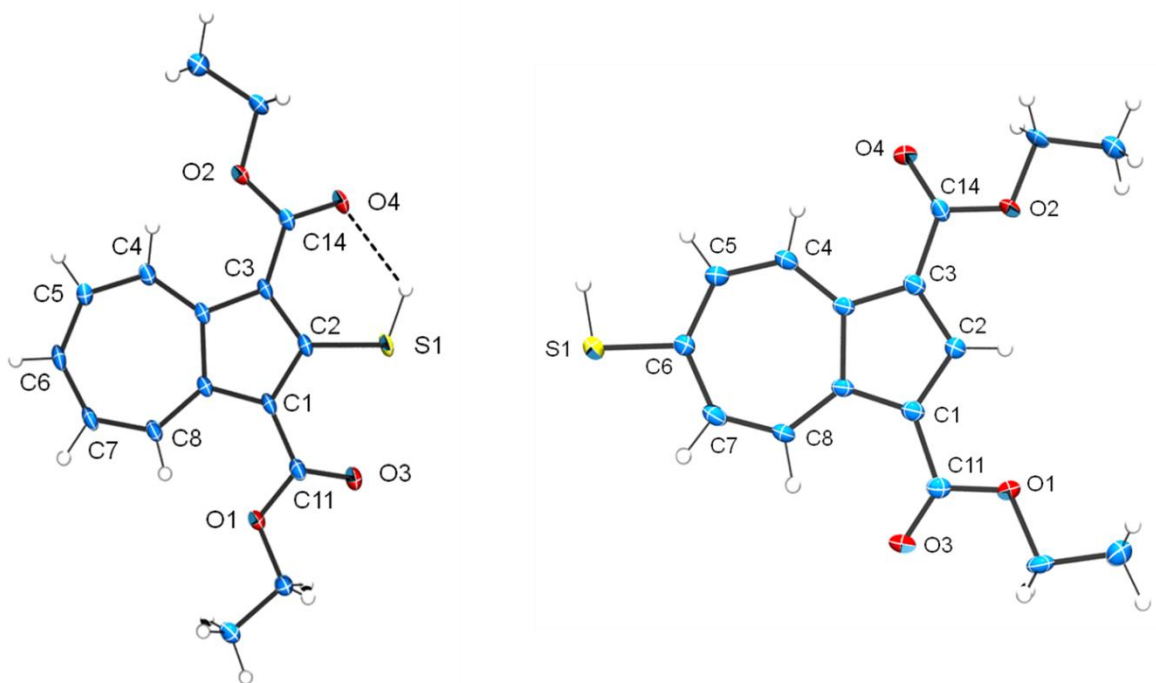


**Figure I.6** Left: molecular structure of **1b**.<sup>27</sup> Selected interatomic distances (Å) and angles (°) for **1b**: S(1)-C(2) 1.739(2), C(11)-O(3) 1.215(2), C(14)-O(4) 1.216(2), S1...O4 3.034(1), S1-H...O4 121.0. Right: molecular structure of one of two crystallographically independent molecules of **3b**.<sup>26</sup> Selected bond distances (Å) for **3b**: S(1)-C(6) 1.765(3), C(11)-O(3) 1.217(3), C(14)-O(4) 1.217(3).

In both **1b** and **3b**, the carboxylate units are coplanar with the azulenic framework. In **1b**, the ester carbonyl groups “embrace” the 2-SH terminus. This conformation supports formation of an internal hydrogen bond by closing the six-membered ring with little, if any, torsional strain (*cf.* H-bonding in *o*-mercaptobenzoates<sup>44</sup>). In contrast, the carbonyl bond vectors in **3b** are pointed toward the 4,8-H atoms of the seven-membered ring. Treatment of **3b** with Et<sub>3</sub>N resulted in deprotonation of its 6-SH group (Figure I.7). In contrast **1b** was unaffected by excess of this amine (Figure I.8).

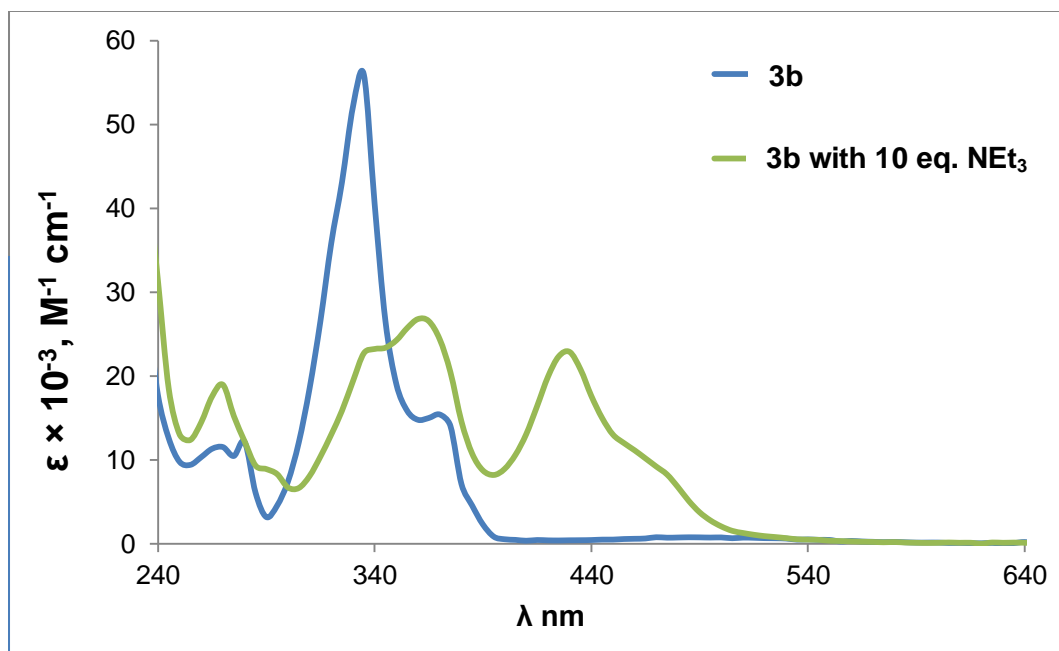


**Figure I.7** Deprotonation study of 6-mercapto-1,3-diethoxycarbonylazulene (**3b**) in  $\text{CH}_2\text{Cl}_2$  at  $25^\circ\text{C}$  with  $\text{NEt}_3$ .

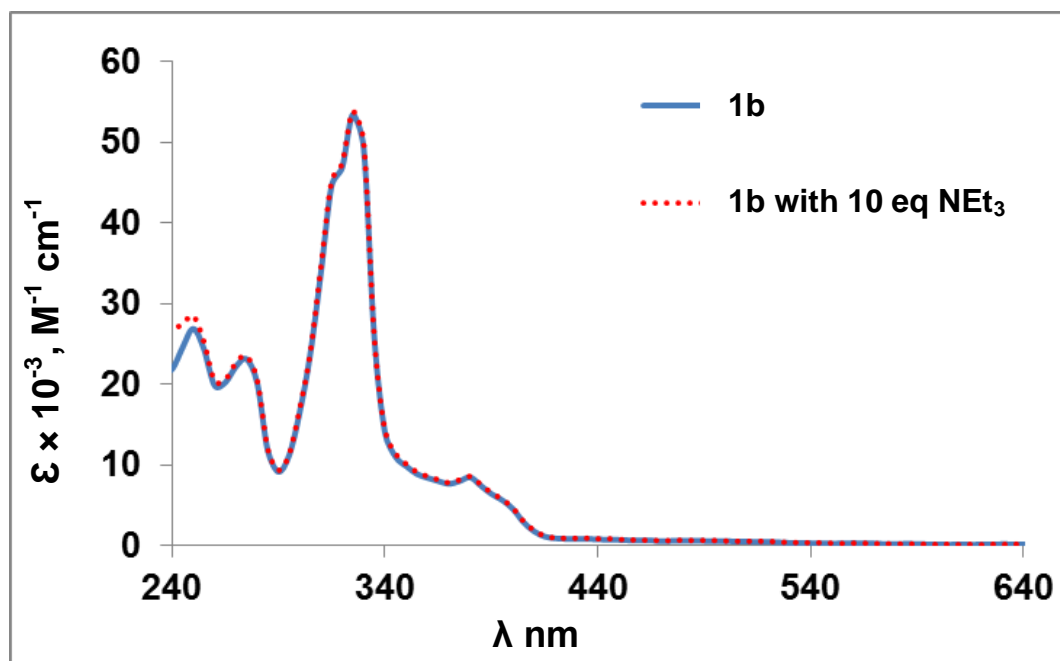


**Figure I.8** Deprotonation study of 2-mercapto-1,3-diethoxycarbonylazulene (**1b**) in  $\text{CH}_2\text{Cl}_2$  at  $25^\circ\text{C}$  with  $\text{NEt}_3$ .



After considering several different bases, it was determined that DBU (diazabicyclo[5.4.0]undec-7-ene), or a more powerful base, was necessary to effect the deprotonation of **1b** (Figure I.9).

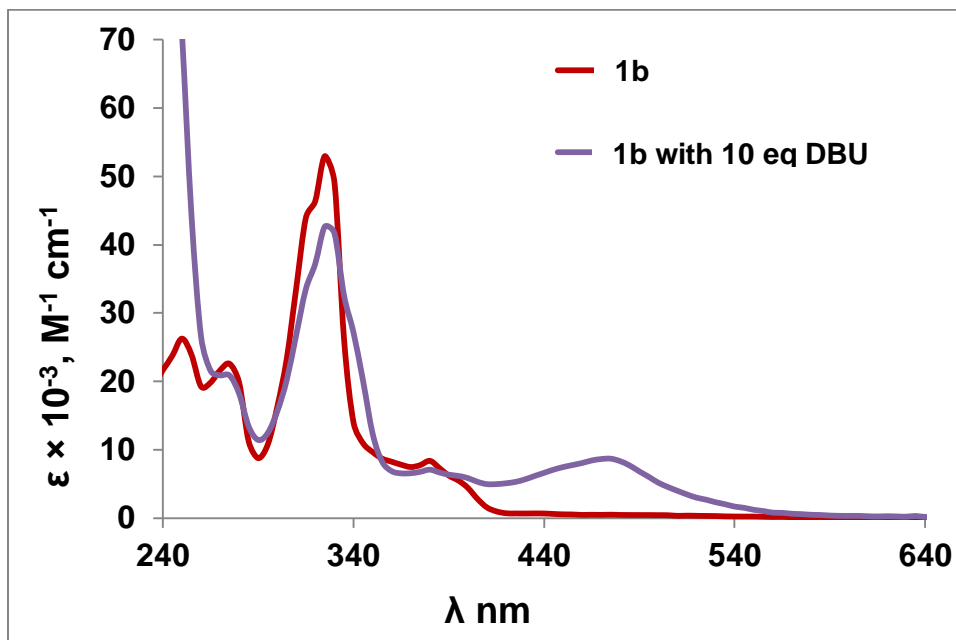


**Figure I.9** Deprotonation study of 2-mercapto-1,3-diethoxycarbonylazulene (**1b**) in  $\text{CH}_2\text{Cl}_2$  at 25 °C with DBU.

Notably, the  $\text{pK}_a$  value of the conjugate acid of DBU is 4.4 - 5.5 units higher than that of  $\text{Et}_3\text{NH}^+$  in organic solvents.<sup>45</sup> Thus, the ester substituents in **1b** considerably mask the  $\text{H}^+$ -donor ability of the 2-SH group, deprotonation of which leads to an unfavourable interaction of the thiolate anion with the ethoxycarbonyls. Given these results, we set out to synthesize the first dimercaptoazulene derivative, namely 2,6-dimercapto-1,3-diethoxycarbonylazulene, which may be viewed as a hybrid of **1b** and **3b**.

Treatment of a solution of 2-amino-6-bromo-1,3-diethoxycarbonylazulene<sup>27</sup> with gaseous HCl followed by the addition of isoamyl nitrite afforded the 2,6-dichloroazulene derivative **I.1** in a *ca.*50% yield. It is imperative to conduct this reaction under rigorously inert atmosphere

conditions to avoid substantial reduction in the yield of **I.1** and formation of multiple other products. The molecular structure of **I.1** is illustrated in Figure I.10.

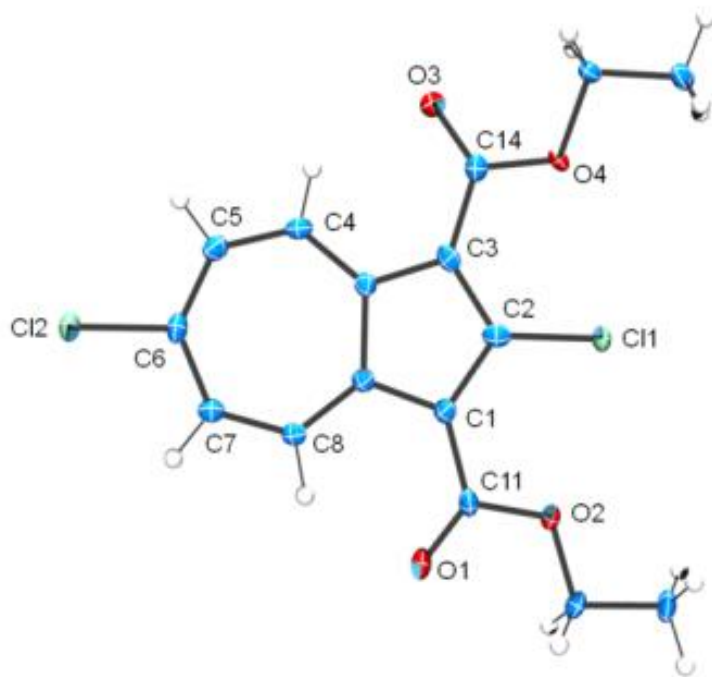


**Figure I.10** Molecular structure of **I.1**. Selected bond distances (Å): Cl(1)-C(2) and angles (°): C(2)-Cl(1) 1.714(4), C(6)-Cl(2) 1.759(4).

The crystal structure of **I.1** shows the C(2)-Cl(1) bond distance of 1.714(4) Å being significantly shorter than the C(6)-Cl(2) bond length of 1.759(4) Å. Notably, the median C-Cl bond distance in a multitude of structurally characterized chlorinated *benzenoid* aromatics containing six-membered  $sp^2$ -carbon rings is 1.74(±0.01) Å,<sup>46</sup> which is right in the middle of the above values. Compound **I.1** is the only structurally characterized “true” 2- or 6-chloroazulene. While the X-ray structure of 1,1,2,3,3,4,5,6,7,8-decachloro-1,2,3,4 -tetrahydroazulene (a precursor to octachloroazulene) has been reported by Lou, Lemal *et al.*,<sup>47</sup> this latter molecule does not have the aromatic  $sp^2$  scaffold of azulene.

The 2,6-dichloroazulene **I.1** appears to be an attractive precursor for accessing other 2,6-substituted azulenes. However, numerous attempts to replace both Cl substituents with mercapto functionalities by reacting **I.1** with excess NaSH invariably led to isolation of the 2-chloro-6-mercapto derivative **I.2** as the terminal product. Similar attempts with the 2,6-dibromoazulene derivative **I.8** afforded 2-bromo-6-mercaptoazulene. Evidently, installation of the first SH group, an electron donating substituent, at the 6-position of the azulenic nucleus deactivates the 2-Cl/Br end of the molecule toward nucleophilic substitution (Figure I.11).

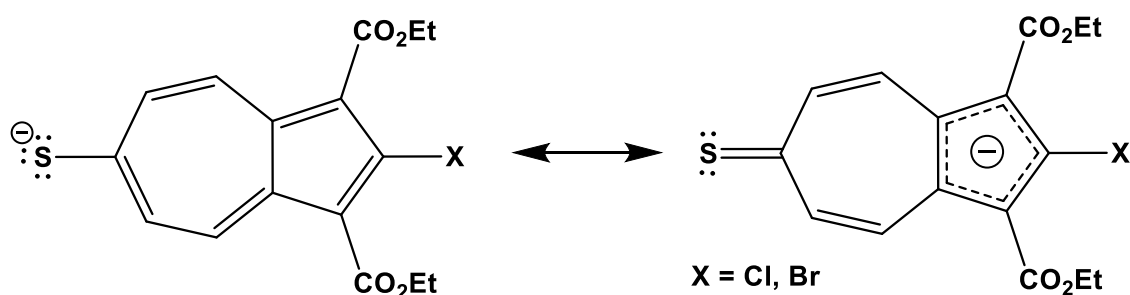
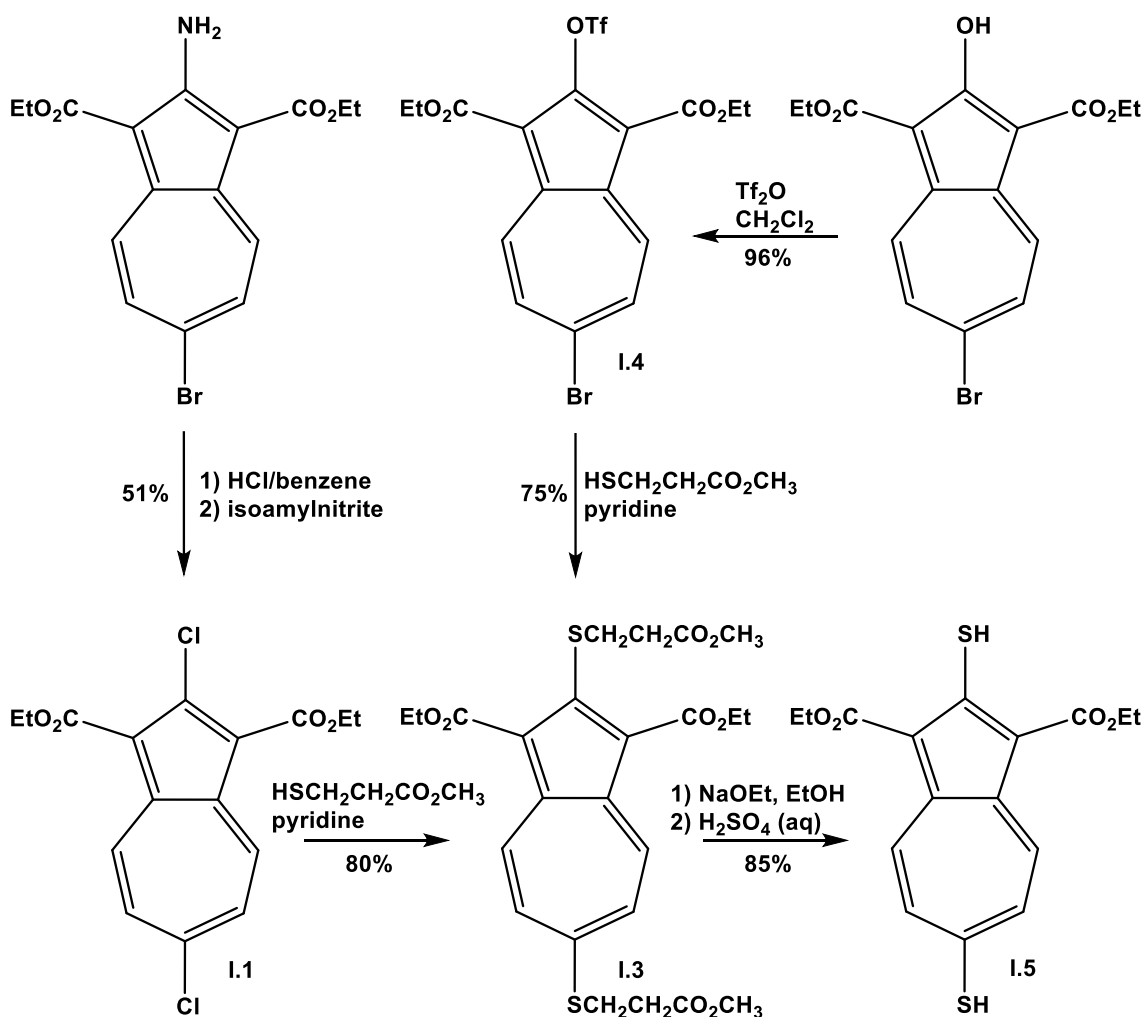


**Figure I.11** Resonance contribution to the deactivation of the halogen at the 2- position of azulene toward nucleophilic substitution.

To circumvent this challenge, **I.1** was subjected to reflux with a slight excess of methyl-3-mercaptopropionate in pyridine. In this reaction, both Cl substituents of **I.1** were cleanly replaced with 2-methoxycarbonylethylthio groups to give the corresponding derivative **I.3**. Compound **I.3** can also be obtained in an even better overall yield from 2-hydroxy-6-bromo-1,3-diethoxycarbonylazulene.<sup>48</sup> Conversion of the 2-OH end of **I.4** into the OTf functionality followed by treatment of the resulting compound **I.4** with methyl-3-mercaptopropionate provided **I.3** in a 72% overall yield.

Abstraction of a proton from an  $\alpha$  carbon followed by the elimination of methyl acrylate released the azulenic di-thiolate and the subsequent acidification of the reaction mixture

generated yellow microcrystals of 2,6-dimercapto-1,3-diethoxycarbonylazulene (**I.5**) in an excellent yield (Scheme I.1).



**Scheme I.1** Synthesis of the 2,6-dimercapto-1,3-diethoxycarbonylazulene.

In this procedure, it is absolutely critical to maintain strictly anaerobic conditions to prevent decomposition of the intermediate, presumably due to formation of disulfide species. Once isolated, the dimercaptan **I.5** is air-stable for practical purposes both in the solid state and in solution. Comparison of the  $^1\text{H}$  NMR and IR signatures of the SH termini of **I.5** with the corresponding parameters documented for **1b** and **3b** indicates that **I.5** can certainly be viewed as

a hybrid of **1b** and **3b** (Table I.4).

**Table 1.4** FTIR (KBr) and  $^1\text{H}$  NMR ( $\text{CDCl}_3$ ) spectroscopic signatures of the mercapto functionalities in **1a**, **1b**, **3b**, **I.5** and **I.6**

	$\nu(\text{S-H}), \text{cm}^{-1}$	$\delta(\text{SH}), \text{ppm}$
<b>1a</b>	2541	3.88
<b>1b</b>	2442 br	7.71
<b>3b</b>	2528	4.23
<b>I.2</b>	2521	4.23
<b>I.5</b>	2540, 2450 br	4.12, 7.58
<b>I.6</b>	2438 br	7.49

Similar to **1b**, for **I.5**, the presence of intramolecular  $\text{S-H}\cdots\text{O}=\text{C}$  hydrogen bonding between its 2-SH terminus and an ester carbonyl is strongly suggested by a substantially deshielded value of  $\delta(2\text{-SH})$ , a relatively low energy and broad nature of the  $\nu(2\text{-SH})$  band (Figure I.12), and the observation of two different  $\nu(\text{C}=\text{O})$  bands at 1683 and 1666  $\text{cm}^{-1}$ .

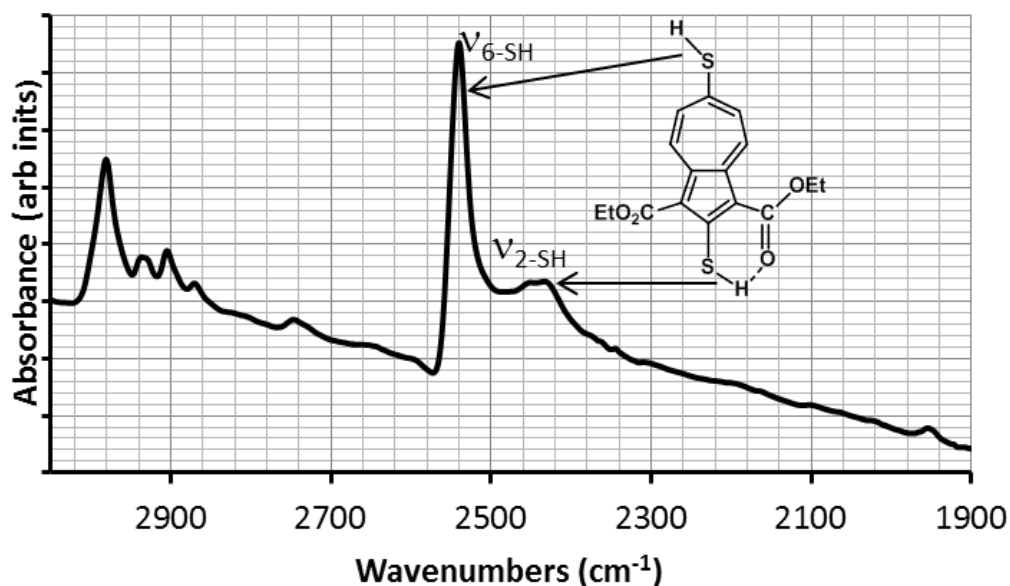


**Figure I.12** FTIR spectrum (KBr) of **I.5** in the  $\nu(\text{S-H})$  region.

On the other hand, the  $^1\text{H}$  NMR and IR characteristics of the 6-SH end in **I.5** are quite close to those observed for **3b**. Compound **I.5** is a very rare example of an asymmetric linear dimercaptoarene.<sup>49</sup>

Addition of 1 equivalent of  $\text{Et}_3\text{N}$  to a 1:1 mixture of **I.5** and  $\text{Ph}_3\text{PAuCl}$  quantitatively produced orange mononuclear complex **I.6**. Employing excess amounts of both  $\text{Et}_3\text{N}$  and  $\text{Ph}_3\text{PAuCl}$  in this reaction still led to **I.6** as the only isolable product. The  $^1\text{H}$  NMR and IR spectra of **I.6** are fully consistent with exclusive metallation of the 6-merapto terminus of its precursor **I.5** (Table 1.2). The single crystal X-ray analysis of **I.6** revealed two independent molecules in the asymmetric unit that have nearly identical metric parameters (Figure I.13).

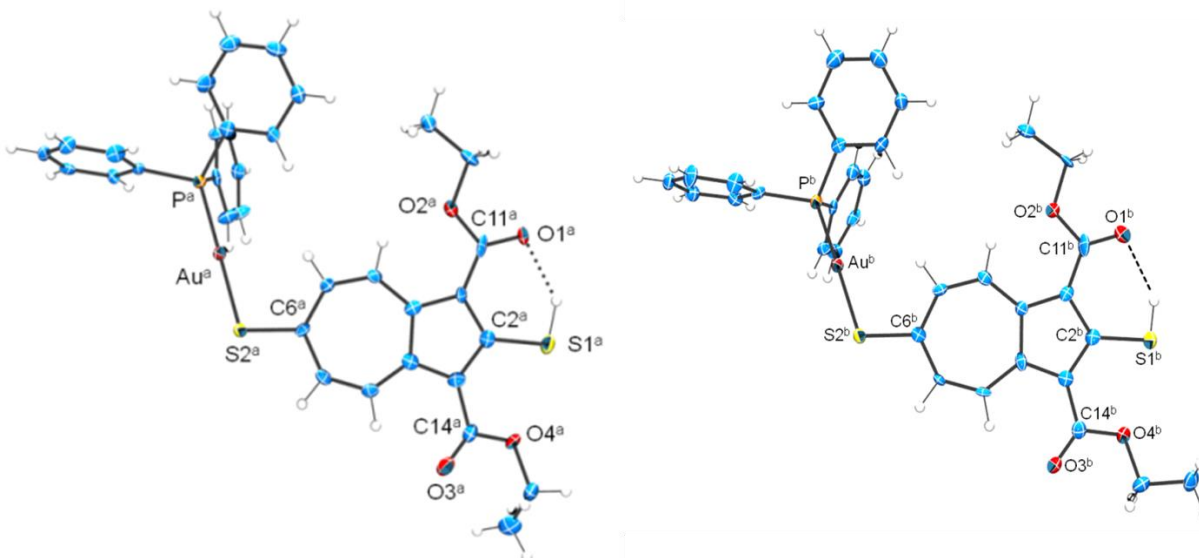


**Figure I.13** Molecular structure of **1.6**. One of two crystallographically independent molecules is shown. Selected interatomic distances (Å) and angles (°): Au<sup>a</sup>-P<sup>a</sup> 2.266(2), Au<sup>a</sup>-S2<sup>a</sup> 2.319, S2<sup>a</sup>-C6<sup>a</sup> 1.772(7), S1<sup>a</sup>-C2<sup>a</sup> 1.755(7), S1<sup>a</sup>...O1<sup>a</sup> 3.030(7), P<sup>a</sup>-Au<sup>a</sup>-S<sup>a</sup> 178.56(6), Au<sup>a</sup>-S2<sup>a</sup>-C6<sup>a</sup> 104.5, S1<sup>a</sup>-H...O1<sup>a</sup> 139.4. Au<sup>b</sup>-P<sup>b</sup> 2.260(2), Au<sup>b</sup>-S2<sup>b</sup> 2.319, S2<sup>b</sup>-C6<sup>b</sup> 1.780(7), S1<sup>b</sup>-C2<sup>b</sup> 1.756(7), P<sup>b</sup>-Au<sup>b</sup>-S<sup>b</sup> 176.20(6), Au<sup>b</sup>-S2<sup>b</sup>-C6<sup>b</sup> 105.4.

Complex **1.6** features the Au-S-C6 angle of *ca.* 105° and a linear geometry about the gold(I) center. The Au-P bond is about 0.05 Å shorter than the Au-S distance. All of the above metric characteristics are well within ranges of the corresponding parameters reported for a number of other complexes of the type Ph<sub>3</sub>PAuSR.<sup>50</sup> While both ethoxycarbonyl units in **1.6** are essentially coplanar with the azulenic moiety, their orientations are quite different from one another. Similar to what we observed for **1b**, the carbonyl oxygen atom of one of the ester groups is engaged in H-bonding interaction with the 2-SH substituent. The other ester group in **1.6** assumes a more common orientation with its carbonyl vector pointed toward the seven-membered ring. To the best of our knowledge, compound **1.6** is the first transition metal adduct of a dimercaptan ligand that features one uncomplexed SH functionality.

The UV-Vis spectrum of **1.6** in CH<sub>2</sub>Cl<sub>2</sub> solution exhibits two intense bands at 445 nm ( $\epsilon = 39.1 \times 10^3 \text{ M}^{-1} \text{ cm}^{-1}$ ), with a shoulder at *ca.* 425 nm, and 365 nm ( $\epsilon = 39.1 \times 10^3 \text{ M}^{-1} \text{ cm}^{-1}$ ).

Time-Dependent DFT calculations (Table S35) indicate that the former band corresponds to the HOMO  $\rightarrow$  LUMO (HOMO = Highest Occupied Molecular Orbital, LUMO = Lowest Unoccupied Molecular Orbital) transition that involves intra-ligand charge transfer within the  $\pi$ -system of the 2-mercapto-6-azulenylthiolate scaffold. Notably, the HOMO includes the entire 2,6-S<sub>2</sub>-azulenic framework whereas the LUMO primarily constitutes the  $\pi^*$ -system of the azulenic moiety with smaller contributions from the two S termini (Figure I.14).

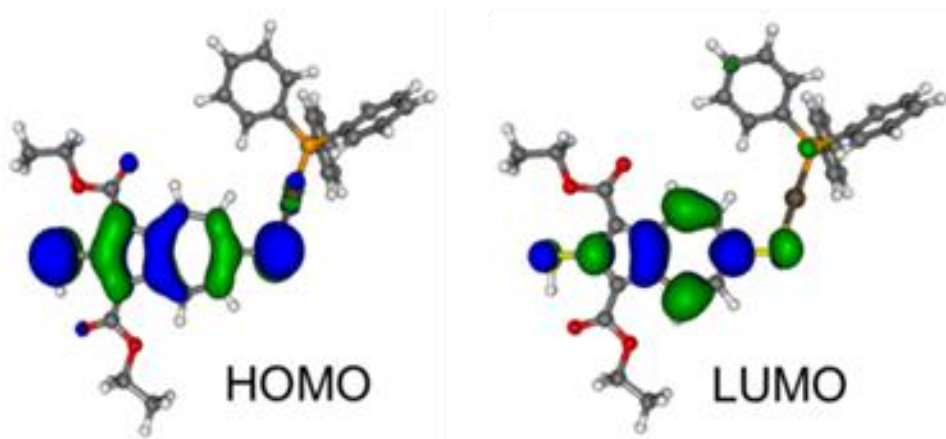


**Figure I.14** Frontier molecular orbitals of **1.6**.

Treatment of **1.6** with a large excess of Et<sub>3</sub>N does not affect its electronic spectrum, which parallels the lack of reactivity of **1b** toward deprotonation with this base. On the contrary, addition of DBU to a solution of **1.6** results in depletion of the band at 445 nm accompanied by growth of a new intense feature with  $\lambda_{\text{max}} = 480$  nm (Figure I.15).



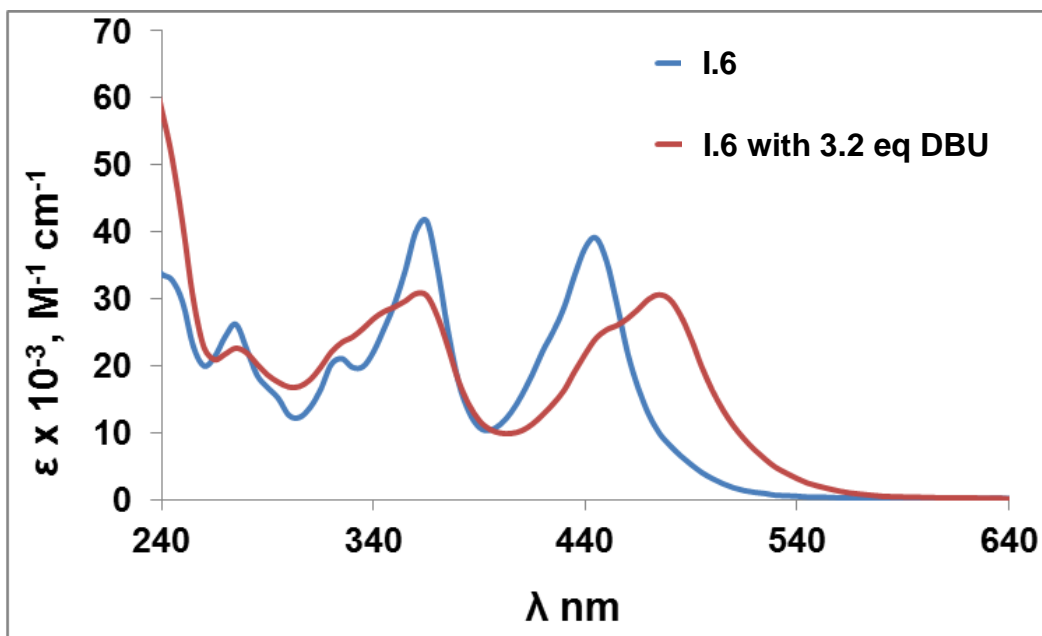
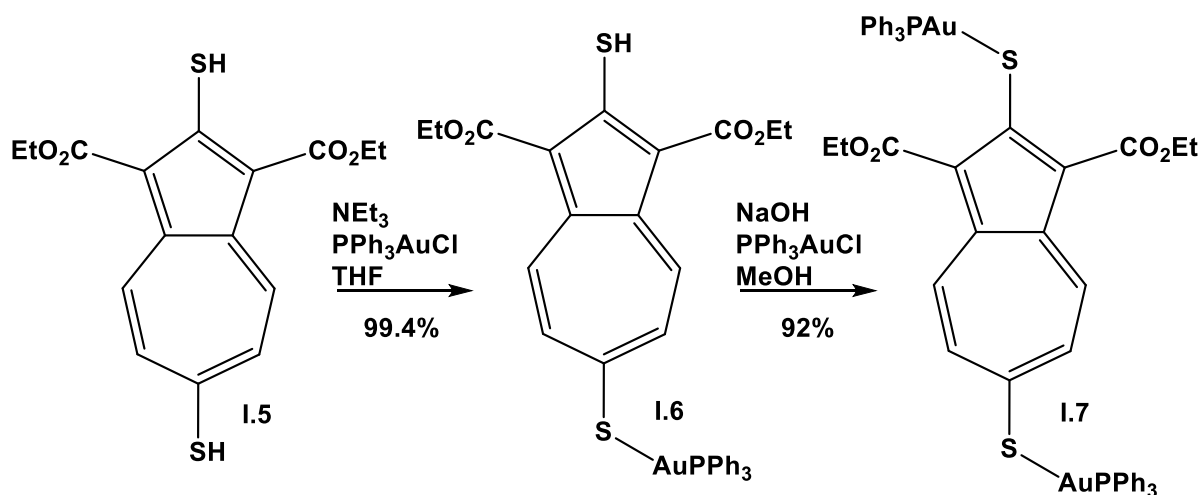


**Figure I.15** UV-vis spectra of **I.6** before and after treatment with excess DBU in  $\text{CH}_2\text{Cl}_2$ .

This is consistent with deprotonation of the SH end of **I.6**, which should raise the energy of the HOMO, thereby shrinking the HOMO-LUMO gap.

Addition of a 5-fold excess of NaOMe (a much stronger base than DBU) to a 1:1 mixture of **I.6** and  $\text{Ph}_3\text{PAuCl}$  afforded pure red dinuclear complex **I.7** in a 92% isolated yield after a simple workup (Scheme I.2).



**Scheme I.2** Regioselective metallation of **I.5** and the formation of **I.6** and **I.7**.

Compound **I.7** can also be obtained in about 70% crude yield by employing excess DBU instead of NaOMe in the above reaction. However, separating DBU and/or its conjugate acid from the product proved tedious at best. Figure I.16 compares the electronic spectra of **I.6** and **I.7**.

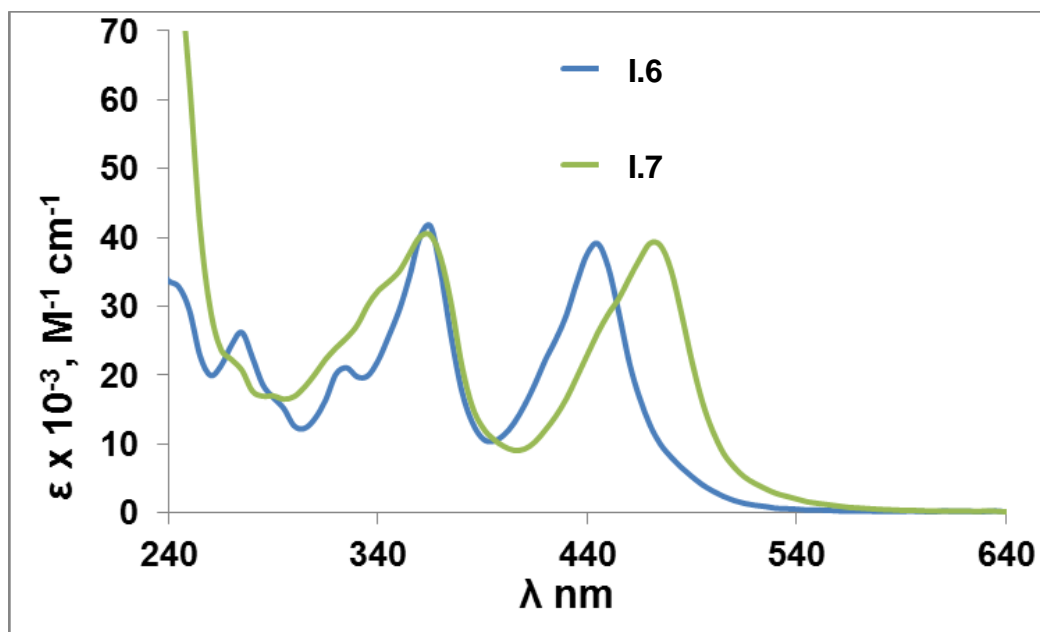


**Figure I.16** UV-Vis spectra of **I.6** (blue) and **I.7** (green) in  $\text{CH}_2\text{Cl}_2$  at 25 °C.

The lowest energy band ( $\lambda_{\text{max}} = 445 \text{ nm}$ ) in the spectrum of **I.6** undergoes a 30 nm red shift upon binucleation of **I.6** to form **I.7**. Notably, addition of 1 equiv. of **I.5** to a solution of **I.7** in  $\text{CH}_2\text{Cl}_2$  cleanly generates **I.6**, as can be conveniently monitored by UV-Vis spectroscopy.

While the  $^{31}\text{P}\{^1\text{H}\}$  NMR spectrum of **I.6** in  $\text{CD}_2\text{Cl}_2$  exhibits a sharp singlet at 37.89 ppm vs. 85% aq.  $\text{H}_3\text{PO}_4$ , it was initially surprising to discover that the  $^{31}\text{P}$  NMR signature of **I.7** at 22 °C consists of a single, albeit broad, resonance at 37.19 ppm. This broad peak gradually splits into two upon cooling the sample to give singlet resonances at  $\delta(^{31}\text{P}) = 37.95$  and 36.19 ppm at -40 °C (Figure I.17).

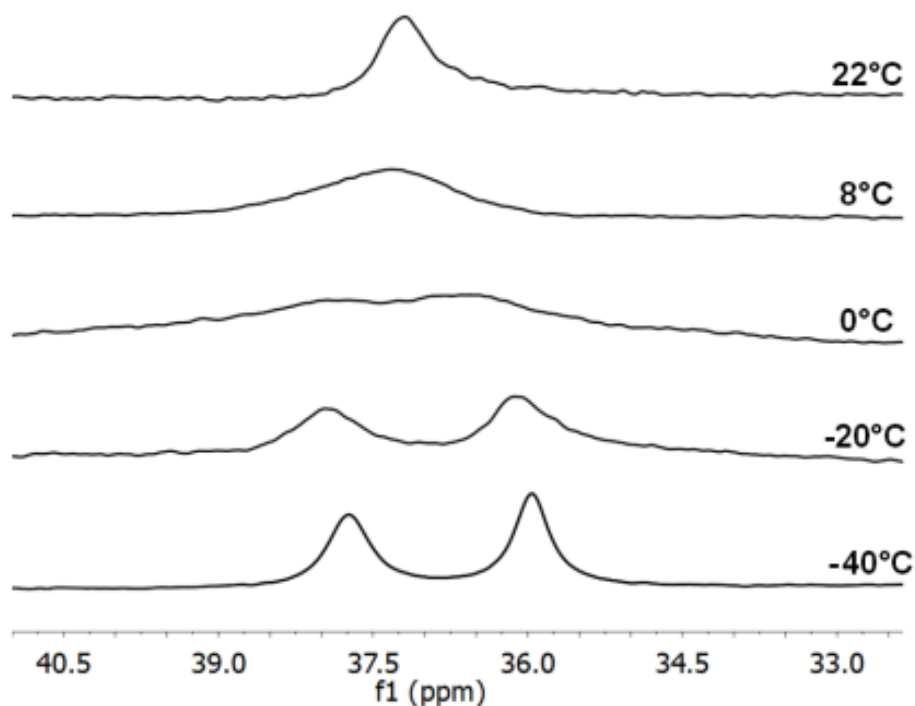


**Figure I.17** Variable temperature  $^{31}\text{P}\{^1\text{H}\}$  NMR spectra of **I.7** in  $\text{CD}_2\text{Cl}_2$ .

The coalescence temperature for this exchange process is about 0°C. The chemical shift of the more downfield peak in the low temperature  $^{31}\text{P}$  NMR spectrum of **I.7** is practically identical to that documented for the  $^{31}\text{P}$  signal of **I.6**. Therefore, this resonance corresponds to the  $\text{AuPPh}_3$

unit bound to the 6-S end of **I.7**. In principle, the exchange of the  $^{31}\text{P}$  environments in solution of **I.7** can be rationalized through either reversible scission of the inequivalent Au-PPh<sub>3</sub> bonds in **I.7**, or heterolytic cleavage of the Au-S bonds to induce scrambling of the  $[\text{AuPPh}_3]^+$  fragments. Previous studies on the ligand exchange involving phosphine-thiolate complexes of Au(I)<sup>51</sup> suggest that the latter possibility is more likely. Interestingly, addition of 2 equiv. of PPh<sub>3</sub> ( $\delta(^{31}\text{P}) = -5.53$  ppm) to a sample of **I.7** ( $\delta(^{31}\text{P}) = -37.19$  ppm) at 25 °C produced a  $^{31}\text{P}$  NMR spectrum (Fig. S12) that features just one broad resonance at 17.94 ppm. Given that the midpoint between the  $^{31}\text{P}$  NMR chemical shifts of **I.7** and PPh<sub>3</sub> is *ca.* 15.8 ppm, it appears that another Au(I)-phosphine species must be present in the equilibrium mixture prepared from **I.7** and 2 equiv. of PPh<sub>3</sub> that reduces the overall presence of free PPh<sub>3</sub> in the mixture. Displacement of the thiolate junctions in **I.7** by PPh<sub>3</sub> to form the well-known  $[\text{Au}(\text{PPh}_3)_2]^+$  cation ( $\delta(^{31}\text{P}) = 33.49$  ppm<sup>52</sup>) may be reasonable to suggest.<sup>54</sup>

## I.6 Conclusions and Outlook

The efficient synthesis of air- and thermally stable 2,6-dimercapto-1,3-diethoxycarbonylazulene **I.5**, a rare example of an asymmetric linear dimercaptoarene has been described. The completely regioselective metallation of its 6-SH terminus with a  $[\text{Ph}_3\text{PAu}^{\text{I}}]$  fragment arises from markedly different acidities of the two SH termini in this dithiol. The mononuclear complex **I.6** can be binucleated with another equivalent of  $[\text{Ph}_3\text{PAu}^{\text{I}}]$  to afford the dinuclear adduct **I.7**. This provides a unique asymmetric platform to consider the exchange of gold-bound thiolates, a topic of significant current interest,<sup>53</sup> using a single compound. The 2,6-dimercaptoazulene linker **I.5** joins the family of 2,6-diisocynoazulene and 2,6-azulenedicarboxylate, whose  $\pi^*$  systems have been shown to be well-suited for supporting charge delocalization between the electron-rich termini.<sup>27,54</sup> With the theoretically appealing 2,6-dimercaptoazulene motif becoming an experimental reality, the door to probing conductivity of the 2,6-dimercaptoazulenic scaffold is now open. It will be interesting to determine if discrimination between the two SH termini of **I.5** occurs upon its adsorption on metallic gold (where the mode of the S-H bond scission may be different from the heterolytic cleavage).

## I.7 References

---

- (1) Orvig, C.; Abrams, M. J. *Chemical Reviews*, **1999**, 99, 2201-2203.
- (2) Fricker, S. P.; *Gold Bulletin*, **1996**, 29, 53-60.
- (3) Shaw III, C. F.; *Chemical Reviews*, **1999**, 99, 2589-2600.
- (4) Suarez-Almazor, M.E. Spooner, C. Belseck, E. Shea, B. *Cochrane Database of Systematic Reviews* **2000**, Issue 2. Art. No.: CD002048.
- (5) Micheva-Viteva, S. Kobayashi, Y. Edelstein, L.C. et al. *J. of Bio. Chem.* **2011**, 286, 21083
- (6) Arcadi, A. *Chemical Reviews*, **2008**, 108, 3266-3325.
- (7) Gimeno, M. C.; Laguna, A. *Chemical Reviews*, **1997**, 97, 511-522.
- (8) Charnock, J. M.; Bristow, S.; Nicholson, J. R. Garner, C. D.; Clegg, W. *Journal of the Chemical Society, Dalton Transactions*, **1987**, 303-306.
- (9) Elder, R. C.; Kelle Zeiher, E. H.; Onady, M.; Whittle, R. R. *Journal of the Chemical Society, Chemical Communications*, **1981**, 900-901.
- (10) Kuz'mina, L. G. *Metalloorganicheskaya*, **1992**, 5, 744-781.
- (11) a) Kim, Y.; Pietsch, T.; Erbe, A.; Belzig, W.; Scheer, E. *Nano Letters*, **2011**, 11, 3734-3738. b) Pontes, R. B.; Rocha, A. R.; Sanvito, S.; Fazzio, A.; da Silva, A. J. R. *Acs Nano*, **2011**, 5, 795 804. c) Bruot, C.; Hihath, J.; Tao N. J. *Nature Nanotechnology*, **2012**, 7, 35-40.
- (12) Functional Supramolecular Architectures: For Organic Electronics and Nanotechnology, Wiley VCH, Weinheim, 2011.
- (13) Crespi, V. H.; Benedict, L. X.; Cohen, M. L.; Louie, S. G. *Physical Review B*, **1996**, 53, R13303-R13305.
- (14) Anderson, A. G., Jr.; Steckler, B. M. *Journal of the American Chemical Society*, **1959**, 81, 4941-4946.
- (15) Treboux, G.; Lapstun, P.; Silverbrook, K. *Journal of Physical Chemistry B*, **1998**, 102, 8978-8980.
- (16) Dutta, S.; Lakshmi, S.; Pati, S. *Bull Mater Sci*, **2008**, 31, 353-358.
- (17) Zhou, K.-G.; Zhang, Y.-H.; Wang, L.-J.; Xie, K.-F.; Xiong, Y.-Q.; Zhang, H.-L.; Wang, C.-W.; *Physical Chemistry Chemical Physics*, **2011**, 13, 15882-15890.

- 
- (18) Kim, B.; Choi, S. H.; Zhu, X. Y.; Frisbie, C. D. *Journal of the American Chemical Society*, **2011**, *133*, 19864-19877.
- (19) Taniguchi, M.; Tsutsui, M.; Mogi, R.; Sugawara, T.; Tsuji, Y.; Yoshizawa, K.; and Kawai, T. *Journal of the American Chemical Society*, **2011**, *133*, 11426-11429.
- (20) Anderson Jr., A. G.; McDonald, R.N. *Journal of the American Chemical Society*, **1959**, *81*, 5669-5674.
- (21) Fujimori, K.; Kitahashi, H.; Koyama, S.; Yamane, K. *Bulletin of the Chemical Society of Japan*, **1986**, *59*, 3320-3322.
- (22) Nozoe, T.; Takase, K.; Tada, M. *Bulletin of the Chemical Society of Japan*, **1965**, *38*, 247-251.
- (23) Asao, T.; Ito, S.; Morita, N. *Tetrahedron Letters*, **1989**, *30*, 6345-6348.
- (24) Asao, T. *Pure Applied Chemistry*, **1990**, *62*, 507-512.
- (25) Vorushilov, A.S. *Regioselective acylation of 2-methoxynaphthalene catalyzed by a C-H superacid and chemistry of mercaptoazulenes*. **2010**, UMI: Ann Arbor.
- (26) Neal, B.; Vorushilov, A. S.; DeLaRosa, A. M.; Robinson, R. E.; Berrie, C. L.; Barybin, M. V. *Chemical Communications*, **2011**, *47*, 10803-10805.
- (27) Holovics, T. C.; Robinson, R. E.; Weintrop, E. C.; Toriyama, M.; Lushington, G. H.; Barybin, M. V. *Journal of the American Chemical Society*, **2006**, *128*, 2300-2309.
- (28) Nozoe, T.; Asao, T.; Oda, M. *Bulletin of the Chemical Society of Japan*, **1974**, *47*, 681-686.
- (29) Mézailles, N.; Richard, L.; Gagosz, F. *Organic Letters*, **2005**, *7*, 4133-4136 (see Supporting Information accompanying this article).
- (30) Huque, F. T. T.; Platts, J. A. *Organic & Biomolecular Chemistry*, **2003**, *1*, 1419-1424.
- (31) Data Collection: SMART Software Reference Manual (2007 and 1998). Bruker-AXS, 5465 E. Cheryl Parkway, Madison, WI 53711-5373 USA
- (32) Data Reduction: SAINT Software Reference Manual (2007 and 1998). Bruker-AXS, 5465 E. Cheryl Parkway, Madison, WI 53711-5373 USA
- (33) G. M. Sheldrick (2001). SADABS. Program for Empirical Absorption Correction of Area Detector Data. University of Göttingen, Germany.
- (34) G. M. Sheldrick (2000). SHELXTL Version 6.10 Reference Manual. Bruker-AXS, 5465 E. Cheryl Parkway, Madison, WI 53711-5373 USA.
- (35) Sheldrick, G. M. *Acta Crystallographica*, **2008**, *A64*, 112-122.

- 
- (36) Flack, H. D. *Acta Crystallographica*, **1983**, A39, 876-881.
- (37) Flack, H. D.; Schwarzenbach, D.; *Acta Crystallographica*, **1988**, A44, 499-506.
- (38) F. Neese, ORCA – an ab initio, Density Functional and Semiempirical Program Package, Version 2.9, University of Bonn, 2012.
- (39) a) A. D. Becke, A. D. *Journal of Chemical Physics*, **1986**, 84, 4524-4529. b) Perdew, J. P. *Physical Review B*, **1986**, 33, 8822-8824.
- (40) a) Schäfer, A.; Horn, H.; Ahlrichs, R. *Journal of Chemical Physics*, **1992**, 97, 2571-2577. b) Schäfer, A.; Horn, H.; Ahlrichs, R. *Journal of Chemical Physics*, **1994**, 100, 5829-5835.
- (41) Neese, F. *Journal of Computational Chemistry*, **2003**, 24, 1740-1747
- (42) Pantazis, D. A.; Chen, X. Y.; Landis, C. R.; Neese, F. *Journal of Chemical Theory and Computation*, **2008**, 4, 908-919.
- (43) a) Becke, A. D. *Journal of Chemical Physics*, **1993**, 98, 5648-5652. b) Becke, A. D. *Journal of Chemical Physics*, **1993**, 98, 1372-1377. c) Lee, C.; Yang, W.; Parr, R. G. *Physical Reviews B*, **1988**, 37, 785-789.
- (44) Schaefer, T.; D. McKinnon, D. M.; Sebastian, R.; Krawchuk, B. *Canadian Journal of Chemistry- Revue Canadienne De Chimie*, **1981**, 59, 566-571.
- (45) Room, E. I.; Kutt, A.; Kaljurand, I.; Leito, I.; Koppel, I. A.; Mishima, M.; Goto, K.; Miyahara, Y. *Chemistry-a European Journal*, **2007**, 13, 7631-7643.
- (46) Allen, F. H.; Kennard, O.; Watson, D. G.; Brammer, L.; Orpen, A. G.; Taylor, R. *Journal of the Chemical Society, Perkins Transactions*, **1987**, S1-S19.
- (47) Lou, Y.; Chang, J.; Jorgensen, J.; Lemal, D. M. *Journal of the American Chemical Society*, **2002**, 124, 15302-15307.
- (48) Ito, S.; Ando, M.; Nomura, A.; Morita, N.; Kabuto, C.; Mukai, H.; Ohta, K.; Kawakami, J.; Yoshizawa, A.; Tajiri, A. *Journal of Organic Chemistry*, **2005**, 70, 3939-3949.
- (49) Koyama, T.; Morishima, M. Jpn. Kokai Tokkyo Koho, 2008, JP2008218327 A20080918.
- (50) a) Tiekink, E. R. T.; and Kang, J. G. *Coordination Chemistry Reviews*, **2009**, 253, 1627-1648. b) Forward, J. M.; Bohmann, D.; Fackler, J. P.; Staples, R. J. *Inorganic Chemistry*, **1995**, 34, 6330-6336. c) Ahmed, L. S.; Clegg, W.; Davies, D. A.; Dilworth, J. R.; Elsegood, M. R. J.; Griffiths, D. V.; Horsburgh, L.; Miller, J. R.; Wheatley, N. *Polyhedron*, **1999**, 18, 593-600.



- 
- (51) Bhabak, K. P.; Mugesh, G. *Inorganic Chemistry*, **2009**, *48*, 2449-2455.
- (52) Basato, M.; Facchin, G.; Michelin, R. A.; Mozzon, M.; Pugliese, S.; Sgarbossa, P.; Tassan, A. *Inorganica Chimica Acta*, **2003**, *356*, 349-356.
- (53) a) Hadley A.; Aikens, C. M. *Journal of Physical Chemistry C*, **2010**, *114*, 18134-18138.  
b) Hakkinen, H. *Nature Chemistry*, **2012**, *4*, 443-455. c) Heinecke, C. L.; Ni, T. W.; Malola, S.; Makinen, V.; Wong, O. A.; Hakkinen, H.; Ackerson, C. J. *Journal of the American Chemical Society*, **2012**, *134*, 13316-13322.
- (54) Barybin, M. V.; Chisholm, M. H.; Dalal, N. S.; Holovics, T. H.; Patmore, N. J.; Robinson, R. E.; Zipse, D. J. *Journal of the American Chemical Society*, **2005**, *127*, 15182-15190.

## **Chapter II**

Synthesis of 6-cyano-2-mercaptoazulene and efforts toward preparation of 2-cyano-6-mercaptoazulene: a pair of isomeric derivatives for probing charge transport along azulene's molecular axis

## II.1. Introduction

Azulene is a planar bi-cyclic aromatic hydrocarbon ( $C_{10}H_8$ ) composed of edge sharing five and seven membered  $sp^2$  hybridized carbon rings. Although isomeric with naphthalene, the asymmetric rings of azulene gives rise to markedly different electronic and physical properties. The aromatic stabilization energy of azulene (4.2 kcal/mol) is much lower than that naphthalene (30.5 kcal/mol).<sup>1</sup> An unequal distribution of electron density between the two rings results in a partial positive charge on the seven membered ring and a partial negative charge on the five membered ring. This partial charge localization in azulene results in a ground state dipole of  $\sim 1.08D$  (Figure II.1).<sup>2</sup>

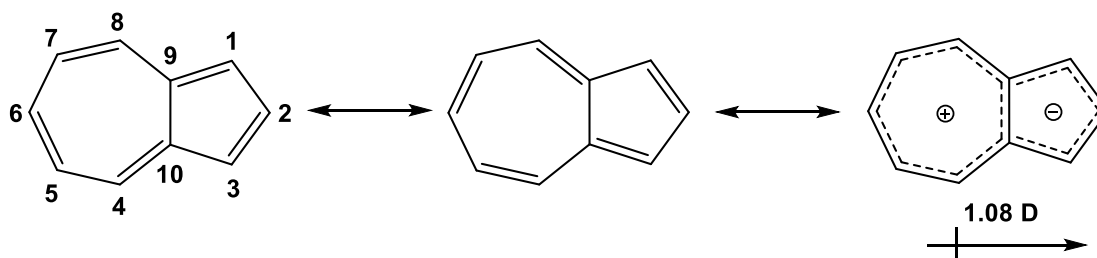


**Figure II.1** Atom numbering scheme of azulene showing resonance forms and its polar nature.

The distinct electronic and physical properties of the azulenetic motif make it attractive for applications in a variety of materials such as non-linear chromophores,<sup>3</sup> liquid crystals,<sup>4</sup> metal-organic frameworks (MOF) for  $H_2$  storage,<sup>5</sup> optical redox switches,<sup>6</sup> conductive polymers,<sup>7</sup> organic light emitting diodes,<sup>8</sup> and organic field-effect transistors.<sup>9</sup>

The quest for the miniaturization of electronics has led to the field of molecular electronics, where individual molecules are envisioned for usage as electronic components. This relatively new field requires more fundamental research to reach its full potential. In this

growing field, organic molecules with conjugated  $\pi$ -systems are of particular interest.<sup>10</sup> In the early 1970's, Aviram and Ratner pioneered the idea of molecular electronics when they proposed that single molecules could function as rectifiers.<sup>11</sup> The concept of molecular rectifiers relies on the production of an asymmetric unit that will have substantially different (I-V) characteristics.<sup>12</sup> One example of such a unit is shown below (Figure II.2).<sup>13</sup> Synthesized in 2005, this benzenoid system features two distinct units conjoined by a single C-C bond. There are an electron poor or accepting unit and an electron donating unit. The methyl groups ortho to the bridging C-C bond provide steric repulsion generating a large torsion angle of  $75.00(8)^\circ$  thereby minimizing the electronic coupling of the extended  $\pi$ -system.

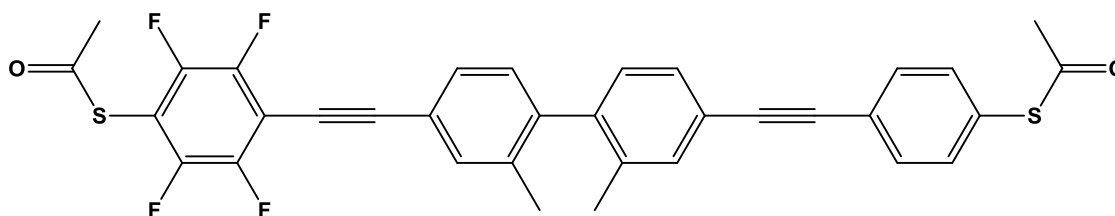


**Figure II.2** Molecular diode composed of extended  $\pi$ -systems

The design of molecular rectifiers features both electron donating (D) and electron accepting (A) units frequently separated by a bridging unit. Recent theoretical studies indicate that azulene and azulene-like molecules, that are not yet known, may act as molecular rectifiers where the seven membered ring functions as the D and the five membered ring as the A.<sup>14</sup>

Charge transport across the asymmetric 2-,6- molecular axis of azulene has been of particular interest since Treboux proposed that such azulenenes connected to electron reservoirs would have intriguing charge transport properties (Figure II.3).<sup>15</sup>

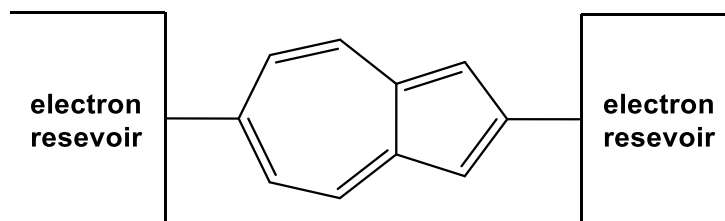


**Figure II.3** Schematic of azulene connected at the 2- and 6- positions to electron reservoirs (Ref 15).

In a simple system the electron reservoirs could be metal centers of coordination complexes. Since azulene tends to form multi hapto coordination complexes,<sup>16</sup> the installation of junction groups was necessary for the controlled coordination of azulenic derivatives.

Previously, the Barybin group has described the syntheses of 2,6-diisocyano-1,3-diethoxycarbonylazulene,<sup>17</sup> 2,6-azenyldicarboxylic acid,<sup>18</sup> and 2,6-dimercapto-1,3-diethoxycarbonylazulene (Chapter 1 of this Thesis). The dicarboxylate and diisocaynoazulene have both been used as  $\pi$ -bridges between the metal centers of organometallic complexes.<sup>17,18</sup> In each case, excellent charge delocalization across the azulenic core was observed.<sup>17,18</sup> Biazulenenic systems such as 2,2'-diisocyano-1,1',3,3'-tetraethoxycarbonyl-6,6'-biazulenylacetylene may also function as an effective  $\pi$ -bridges for charge delocization (Figure II.4) between metal termini.<sup>19</sup>

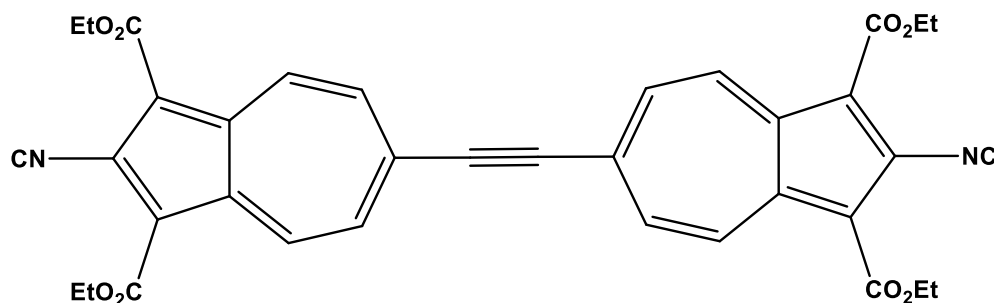


**Figure II.4** 2,2'-disocyano-1,1',3,3'-tetraethoxycarbonyl-6,6'-biazulenylacetylene (Ref 19).

Prior to the implementation of the linear 2,6-azulenic scaffold in electrical components, experimental validation of its theoretical charge transport capabilities is a necessity. Although challenging, there are several methods for probing charge transport in organic molecules including mechanically controlled break junctions (MCB)<sup>20</sup> and conducting atomic force microscopy (C-AFM).<sup>21</sup> These experiments are often done on self-assembled monolayers (SAMs) of the analyte of interest. Both isocyano<sup>22</sup> and thiolate<sup>23</sup> junction groups have been frequently employed for the formation of a variety of different SAMs. The formation of SAMs from isocyanoazulenes<sup>24</sup> and mercaptoazulenes<sup>25</sup> have also been described.

Obtaining high quality experimental measurements of the charge transport dynamics of single molecules is a challenging undertaking since the junction groups and the shape of electrodes can greatly influence the results.<sup>26</sup> Resonant Auger electron spectroscopy (RAES) using the core hole clock (CHC) has proven to be a good method to probe charge transport dynamics at the molecular level.<sup>27</sup> In work done by Zharnikov *et al.* the charge transport dynamics in molecules featuring terminal cyano and mercapto substituents have been successfully measured.<sup>28</sup> The mercapto groups bind the molecule to a gold surface so that when a charge is generated in the cyano group it can delocalize through the molecule and transfer to the gold substrate.<sup>28</sup> A collaboration with Professor Zharnikov affords the opportunity to probe the charge transport dynamics of azulene across its asymmetric 2,6-molecular axis.

However, before such experiments can be conducted both 2-cyano-6-mercaptoazulene and its isomer 6-cyano-2-mercaptoazulene must be synthesized (Figure II.4).



**Figure II.5** Targeted isomeric 2-cyano-6-mercaptoazulene and 6-cyano-2-mercaptoazulene.

In addition to the function of the cyano groups in these RAES experiments, nitriles have also served as good spectroscopic reporters providing additional characterization of SAMs featuring mercapto junction groups in azulenic thin film assembly studies,<sup>25</sup> and for probing the electrostatics at the electrode/SAM/solution interface.<sup>29</sup>

While several mercaptoazulenes have been reported, prior to this work no 2- or 6-mercaptoazulene with an additional functional group at the opposite terminus has been described. Examples of 2- and 6-mercaptoazulenes<sup>25,30</sup> are shown below (Figure II.6).

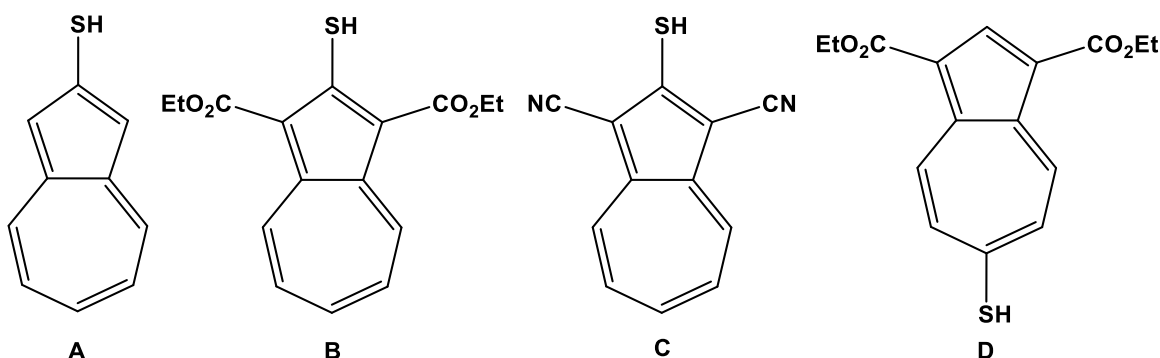


**Figure II.6** Selected examples of 2- and 6-mercaptoazulenes A (Ref 30a), B (Ref 30a, 30b), C (Ref 25), D (Ref 30a).

2- and 6-cyanoazulenes<sup>31</sup> have also been prepared and selected examples are shown in Figure II.7.

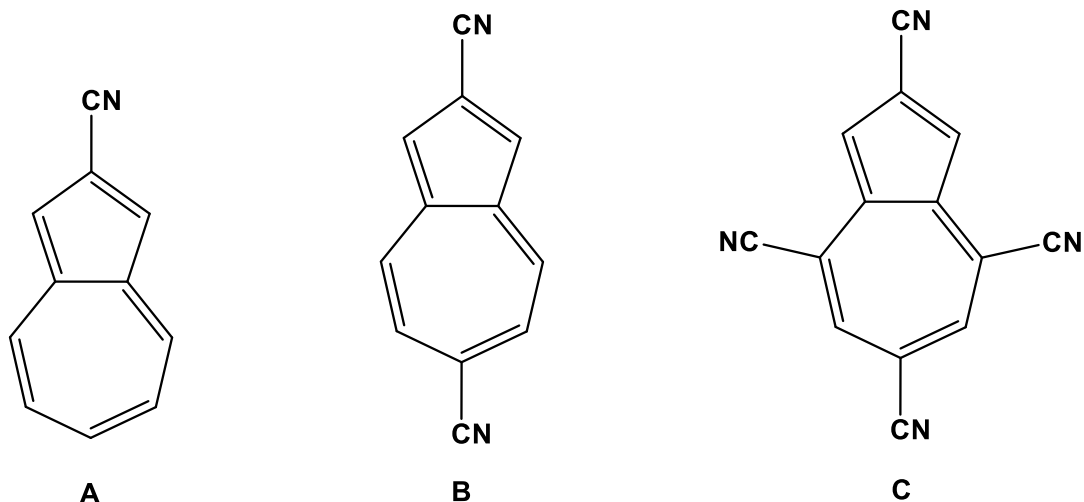


**Figure II.7** 2- and 6-cyanoazulenes A (Ref 31a) B and C (Ref 31b).

Unlike the frontier molecular orbitals of naphthalene and other benzenoid aromatics, the frontier molecular orbitals of azulene feature complementary orbital density contributions (Figure II.8)

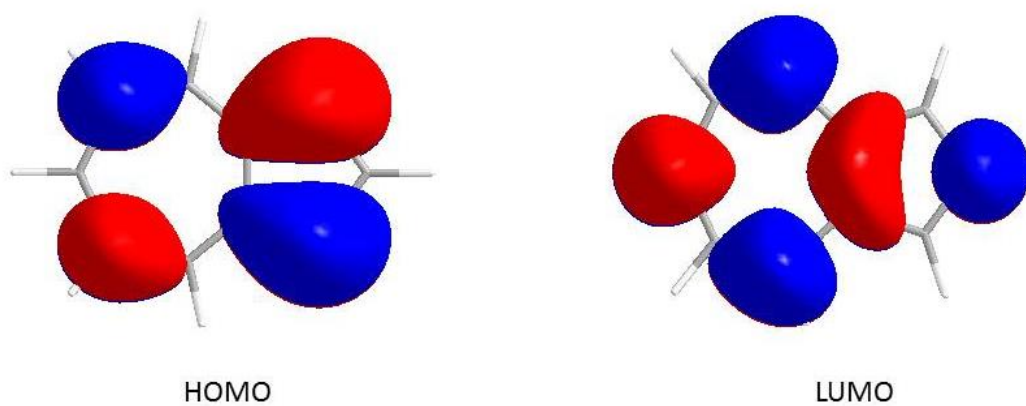


**Figure II.8** Frontier Molecular Orbitals of Azulene (Extended Huckel Calculation)

This complementary orbital density distribution enables the HOMO and LUMO to be tuned independently of one another. Addition of electron donating or withdrawing substituents at the



odd positions 1-, 3-, 5-, and 7- will affect the energy of HOMO while addition of electron donating or withdrawing substituents at the even positions 2-, 4-, 6-, and 8- will affect the energy of the LUMO. The relatively small energy gap between the HOMO and LUMO leads to the absorption of visible light and the intense color of azulene and azulenic derivatives.<sup>32</sup>

The asymmetric bicyclic ring system of azulene has five unique positions that can be functionalized. Direct functionalization of azulene may occur through the addition of either an electrophile or nucleophile. For azulene electrophilic substitution reactions (EAS) preferentially occur at only the 1- and 3- positions of the five membered ring, while nucleophilic additions occur at 4-, 6-, and 8- positions on the seven membered ring. Mono and di-functionalized 1- and 1,3- azulenes with chloro, bromo, and nitro groups have been synthesized through EAS reactions (Figure II.9).<sup>33</sup>

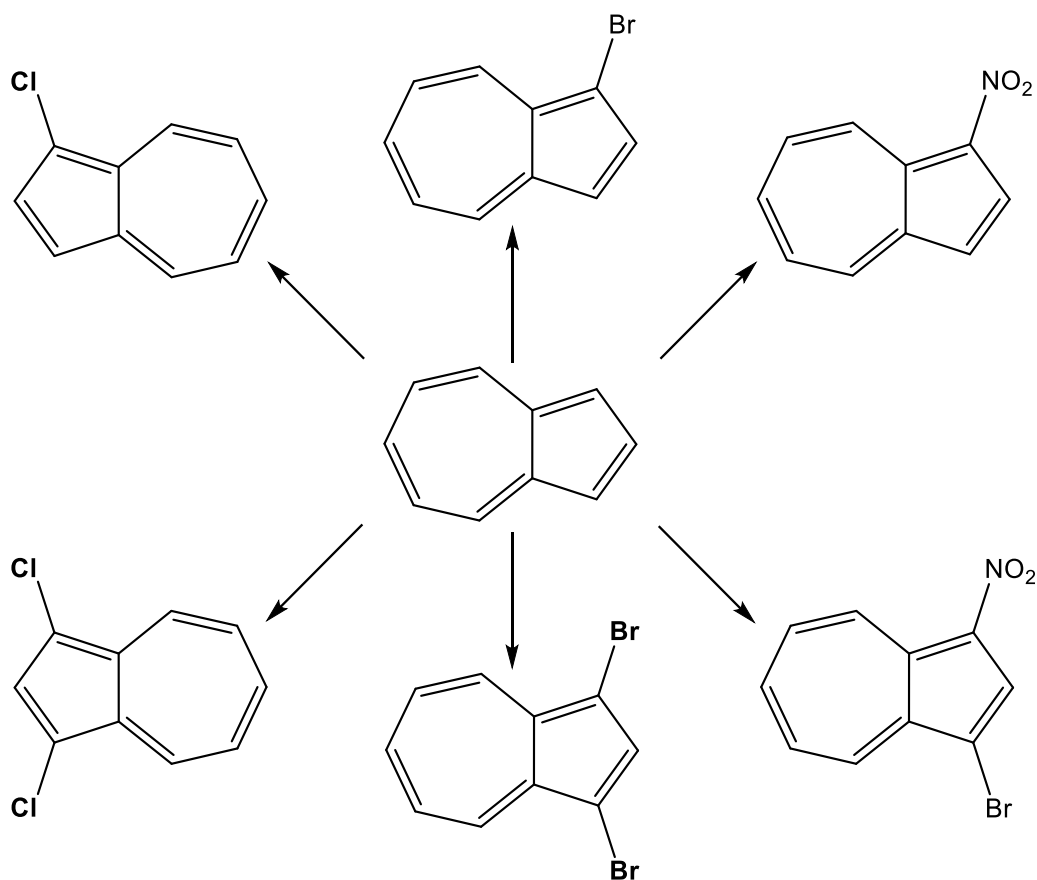
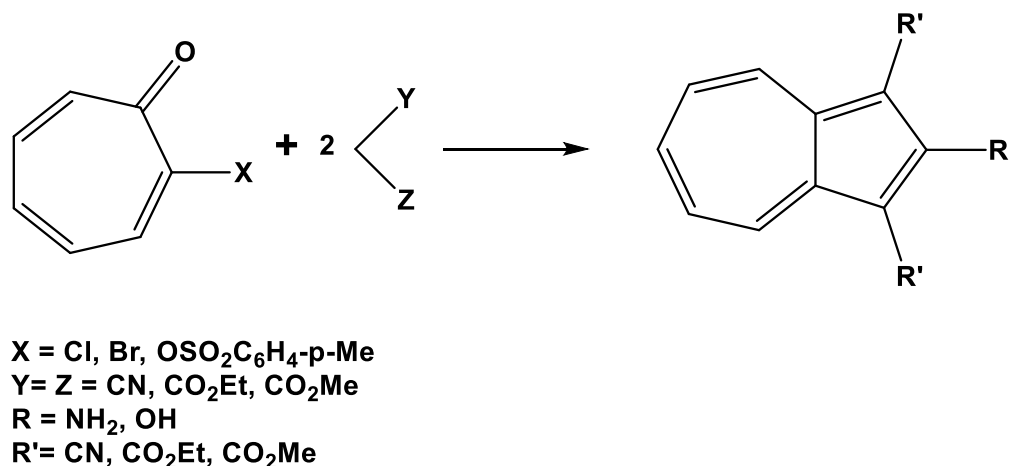


**Figure II.9** Selected mono- and di-functionalized azulene derivatives that have been prepared through EAS reactions (Ref 33).

Even with the presence of a strong deactivating group like a nitro at the 1- position, bromination of the five membered ring at the 3-position still occurs under mild conditions. Both 1,3-diiodoazulene<sup>34</sup> and 1,3-dinitroazulene<sup>35</sup> have also been prepared. The 1- and 3- positions of azulene can also undergo electrochemical polymerization.<sup>36</sup> Direct functionalization of the 6- position can occur through vicarious nucleophilic substitution or EAS for some azulenics derivatives. 6-Aminoazulene can be obtained from treatment of azulene with 4-amino-1,2,4-triazole in the presence of a base.<sup>37</sup> Nitration of azulene at the 6- position has occurred only when the 1- and 3- positions of azulene were blocked and at the 2- position was functionalized with a hydroxyl group.<sup>38</sup> Bromination of the 6- position will occur on either 2-amino<sup>39</sup> or 2-

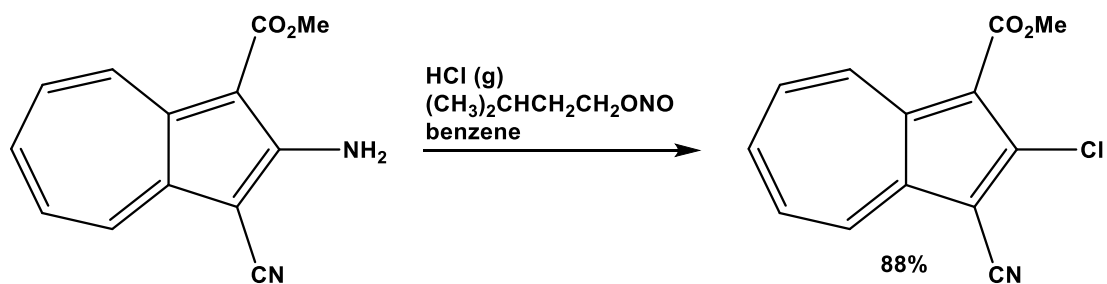
hydroxy-substituted<sup>85</sup> azulenes when ester substituents are present at both the 1- and 3- positions. Direct functionalization the 2-position is much less common. Formation of 2-(4,4,5,5-tetramethyl-1,3,2-dioxaborayl)azulene was observed through reaction with bis(pinacolato)diboron and azulene in the presence of an iridium catalyst.<sup>40</sup> Lithiation was also reported at the 2-position of azulene, although a sulfonyl directing group was required at the 1- position of azulene and the lithiated azulenes were not stable enough to be isolated.<sup>41</sup> 4-aminoazulene can be formed by treatment of azulene with potassium amide.<sup>42</sup>

The work of Nozoe is responsible for many of the 2-functionalized azulenic derivatives as he found that treatment of tropolones with active methylene compounds would yield either 2-hydroxy<sup>43</sup> or 2-aminoazulenes<sup>44</sup> (Scheme II.1).<sup>45</sup>



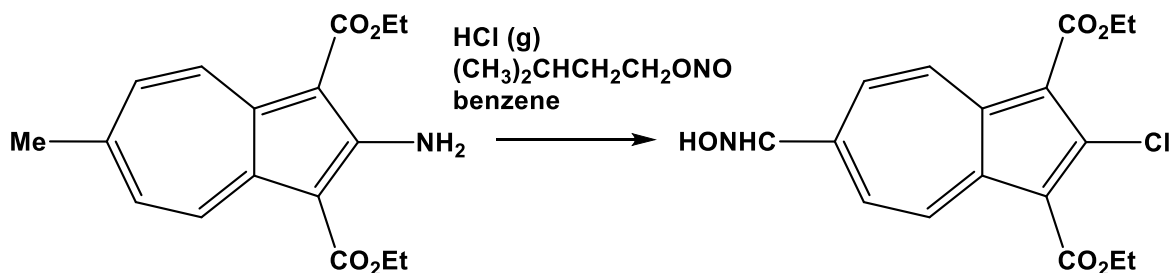
**Scheme II.1** Nozoe's synthesis of substituted azulenes from tropolone (Ref 45).

Diazotization of 2-aminoazulenes with isoamyl nitrite and subsequent replacement of the amine with a halogen typically works well, as long as there are no substituents at the 6- position (Scheme II.2).<sup>46</sup>



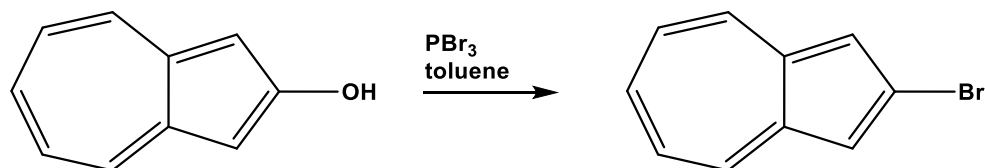
**Scheme II.2** Diazotization of 2-amino-1-cyano-3-methylcarboxylateazulene (Ref 46).

The strong coupling between the 2- and 6-termini of the azulenic scaffold will often lead to additional transformations of functional groups occupying the 6- position following the formation of a diazonium salt at the 2- position (Scheme II.3).<sup>47</sup>



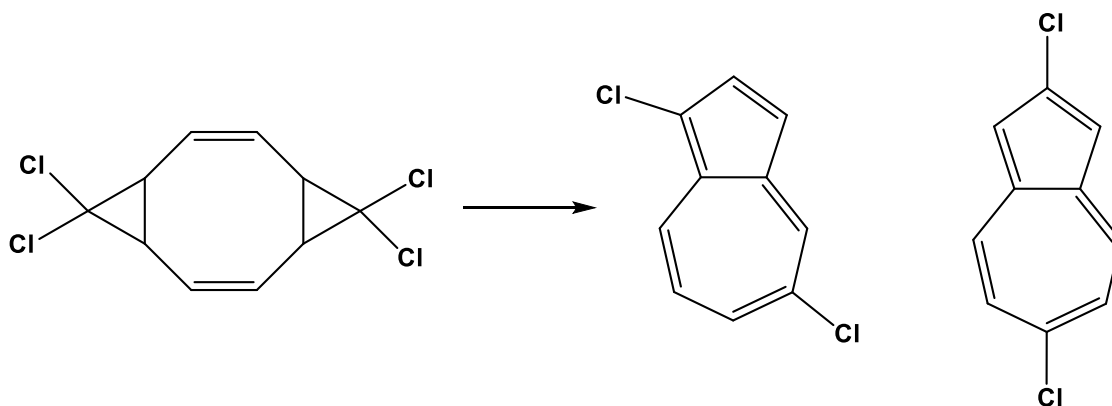
**Scheme II.3** Oxidation of 6-methyl during diazotization of 2-amino (Ref 47).

Replacement of the hydroxyl group of 2-hydroxyazulene with a bromide occurs by treatment with  $\text{PBr}_3$  (Scheme II.4).<sup>48</sup>



**Scheme II.4** Synthesis of 2-bromoazulene (Ref 48)

Dichloroazulenes have been formed by flash pyrolysis of tetrahalotricyclo[7.1.0.0<sup>4,6</sup>] deca-dienes (Scheme II.5)<sup>49</sup>



**Scheme II.5** Synthesis of dichloroazulenes (Ref 49)

Both 2- and 6-halogenated azulenes are known to undergo a variety of different coupling reactions including Ullmann,<sup>50</sup> Stille,<sup>51</sup> Suzuki,<sup>52</sup> and Songashira.<sup>53</sup> In general, Hafner observed that nucleophilic substitution in azulenic halides occurs much more readily for the halogen atoms attached to the seven membered ring rather than the five membered ring.<sup>49</sup>

## II.2. Work Described in Chapter II

This chapter describes the synthesis of 2-mercapto-6-cyanoazulene and work towards the preparation of its isomer 2-cyano-6-mercaptoazulene.

## II.3 Experimental Section

### II.3.1 General Procedure and Starting Materials

Unless specified otherwise, all manipulations were done under an atmosphere of 99.5% argon further purified by passage through columns of activated BASF catalyst and molecular sieves. All connections involving the gas purification systems were made of glass, metal, or other materials impermeable to air. Solutions were transferred via stainless steel cannulas whenever possible. Standard Schlenk techniques were employed with a double manifold vacuum line.  $\text{CH}_2\text{Cl}_2$  and pentane were distilled over calcium hydride. Benzene was dried over molecular sieves and then distilled over freshly cut potassium. THF was doubly distilled over sodium/benzophenone. N,N-dimethylformamide was dried over  $\text{CaCl}_2$  and distilled under an atmosphere of argon. Following purification, all solvents were stored in gas tight containers under an atmosphere of argon. Solid state infrared spectra were recorded on a PerkinElmer Spectrum 100 FTIR spectrometer with samples embedded in KBr pellets. NMR samples were analyzed using Bruker DRX-400 and Bruker Avance 500 spectrometers.  $^1\text{H}$  and  $^{13}\text{C}$  chemical shifts are given with reference to residual  $^1\text{H}$  and  $^{13}\text{C}$  solvent resonances relative to  $\text{Me}_4\text{Si}$ . 2-Hydroxy-6-bromo-1,3-diethoxycarbonylazulene,<sup>54</sup> 2-chloro-1,3-diethoxycarbonylazulene, 2-cyanoazulene, 2-chloroazulene, and 2-idoazulene<sup>38</sup> were prepared as previously reported in the literature. 2,6-Dichloro-1,3-diethoxycarbonylazulene was prepared as described in Chapter 1 of this thesis.

### II.3.2 Synthesis of 6-bromo-2-hydroxyazulene (II.1)

Method A. KOH (0.392 g, 5.984 mmol) and 2-hydroxy-6-bromo-1,3-diethoxycarbonylazulene (0.100 g, 0.272 mmol) was added to 5 mL of 70% aqueous ethanol. The resulting suspension was heated to reflux with stirring for a period of 1 hour. After cooling of the reaction mixture to room temperature, the contents of the flask were poured into 100 mL of distilled H<sub>2</sub>O and acidified dropwise with 10% HCl until a precipitate formed. The precipitate was isolated by vacuum filtration and then dried under vacuum for 4 hours. This solid was dissolved in 2 mL of pyridine and the resulting solution was refluxed for 2 hours. After cooling to room temperature, the solution was poured into 25 mL of 3M H<sub>2</sub>SO<sub>4</sub> and the mixture was extracted with 3 × 15 mL of CH<sub>2</sub>Cl<sub>2</sub>. The organic fractions were combined, washed with 1 × 15 mL of 3M H<sub>2</sub>SO<sub>4</sub>, 2 × 15 mL of H<sub>2</sub>O, dried over anhydrous Na<sub>2</sub>SO<sub>4</sub>, and filtered. The filtrate was concentrated under vacuum and then subjected to column chromatography on silica with a mixture of ethylacetate and CH<sub>2</sub>Cl<sub>2</sub> used as the eluent with the concentration of ethylacetate gradually increasing from 2% to 5%. The dark brownish fraction was collected, concentrated, and dried under vacuum to give 6-bromo-2-hydroxyazulene (0.033 g, 0.149 mmol) in a 55% yield.

Method B. A solution of 6-bromo-2-hydroxy-1,3-diethoxycarbonylazulene (0.3064 g, 0.8344 mmol) in 2 mL of 85% H<sub>3</sub>PO<sub>4</sub> was heated to 130 °C for 25 minutes. After cooling to room temperature, the mixture was poured onto ice and then extracted with 3 × 15 mL of CH<sub>2</sub>Cl<sub>2</sub>. The organic fractions were combined, washed with 3 × 15 mL of distilled H<sub>2</sub>O, dried over anhydrous Na<sub>2</sub>SO<sub>4</sub>, and filtered. Following filtration the solvent was removed from the filtrate under vacuum and 6-bromo-2-hydroxyazulene (0.079 g, 0.354 mmol) was isolated in a

42% yield.  $^1\text{H}$  NMR (400 MHz,  $\text{CDCl}_3$ , 25 °C):  $\delta$  7.81 (s, 2H,  $H^{1,3}$ ), 8.40 (d,  $^3J_{\text{HH}} = 11$  Hz, 2H,  $H^{5,7}$ ), 9.56 (d,  $^3J_{\text{HH}} = 11$  Hz, 2H,  $H^{4,8}$ ) ppm.

### II.3.3 Synthesis of 6-cyano-2-hydroxyazulene (II.2)

A solution/slurry of 6-bromo-2-hydroxyazulene (0.386 g, 1.73 mmol) and CuCN (0.222 g, 2.60 mmol) in 15 mL of DMF was heated to reflux for 8 hours. After cooling to room temperature, the contents of the flask were poured into 75 mL of aqueous ammonium hydroxide and the resulting emulsion was stirred for 12 hours at room temperature and then extracted with  $3 \times 25$  mL of  $\text{CH}_2\text{Cl}_2$ . The organic layers were combined and washed with  $3 \times 10$  mL of  $\text{H}_2\text{O}$ , dried over anhydrous  $\text{Na}_2\text{SO}_4$ , and concentrated under vacuum to a dark residue. The residue was dissolved in a minimum amount of  $\text{CH}_2\text{Cl}_2$  and subjected to column chromatography on silica gel using 5% ether in  $\text{CH}_2\text{Cl}_2$  as the eluent. A dark purple band was collected, concentrated and dried under vacuum to give (0.164 g, 0.969 mmol) of 6-cyano-2-hydroxyazulene as a purple powder in a 56% yield. IR (KBr):  $\nu_{\text{OH}}$  3230,  $\nu_{\text{CN}}$  2215  $\text{cm}^{-1}$ .  $^1\text{H}$  NMR (400 MHz,  $\text{CD}_3\text{CN}$ , 25 °C):  $\delta$  6.96 (s, 2H,  $H^{1,3}$ ), 7.46 (d,  $^3J_{\text{HH}} = 11$  Hz, 2H,  $H^{5,7}$ ), 8.08 (d,  $^3J_{\text{HH}} = 11$  Hz, 2H,  $H^{4,8}$ ) ppm.

### II.3.4 Synthesis of 6-cyano-2-(trifluoromethylsulfonyl)oxyazulene (II.3)

Triethylamine (0.1095 g, 1.08 mmol) was added to a solution of 6-cyano-2-hydroxyazulene (0.185 g, 1.09 mmol) in 10 mL of  $\text{CH}_2\text{Cl}_2$  at room temperature with stirring. Twenty minutes after the addition of triethylamine, trifluoromethanesulfonic anhydride ( $\text{Tf}_2\text{O}$ ) (0.612 g, 2.17 mmol) dissolved in 3 mL of  $\text{CH}_2\text{Cl}_2$  was added dropwise to this solution over a period of 15 minutes. Once the addition of  $\text{Tf}_2\text{O}$  was complete, the resulting solution was left



stirring at room temperature for 1 hour. The contents of the reaction flask were poured into 50 mL of distilled H<sub>2</sub>O and the organic layer was separated. The aqueous layer was extracted once with 10 mL of CH<sub>2</sub>Cl<sub>2</sub> and the organic fractions were combined. The organics were washed with 2 × 25 mL of distilled H<sub>2</sub>O and dried over anhydrous Na<sub>2</sub>SO<sub>4</sub>. Following filtration, the solvent was removed from the filtrate under vacuum and the resulting residue was recrystallized by layering its solution in a minimum amount of CH<sub>2</sub>Cl<sub>2</sub> with pentane. After the solvent diffusion was complete, dark turquoise microcrystals formed. These were isolated by vacuum filtration and dried under vacuum for 3 hours giving 6-cyano-2-(trifluoromethylsulfonyl)oxyazulene (0.2013 g, 0.668 mmol) in a 61% yield. HRMS (*m/z*, ES<sup>+</sup>): found for [M+H]<sup>+</sup> 301.0770; calcd for C<sub>12</sub>H<sub>6</sub>F<sub>3</sub>NO<sub>3</sub>S<sup>+</sup> 301.0020. IR (KBr):  $\nu_{\text{CN}}$  2222 cm<sup>-1</sup>. <sup>1</sup>H NMR (400 MHz, CDCl<sub>3</sub>, 25 °C):  $\delta$  7.37 (s, 2H, *H*<sup>1,3</sup>), 7.60 (d, <sup>3</sup>J<sub>HH</sub> = 10 Hz, 2H, *H*<sup>5,7</sup>), 8.40 (d, <sup>3</sup>J<sub>HH</sub> = 11 Hz, 2H, *H*<sup>4,8</sup>) ppm.

### II.3.5 Synthesis of 6-cyano-2-mercaptoazulene (II.4)

To a solution of 68% aqueous sodium hydrosulfide (1.035 g, 4.310 mmol) in 15 mL of 70% aqueous ethanol was added 6-cyano-2-(trifluoromethylsulfonyl)oxyazulene (0.101 g, 0.336 mmol). The resulting suspension was heated to reflux with stirring for a period of 2 hours. After two hours, the reaction mixture was cooled to room temperature and the contents of the flask were poured into 50 mL of distilled H<sub>2</sub>O. The resulting solution was slowly acidified with 3M H<sub>2</sub>SO<sub>4</sub> until a dark precipitate formed. The precipitate was isolated by vacuum filtration, washed extensively with distilled H<sub>2</sub>O, and dried under vacuum. The precipitate was then dissolved in a minimum amount of CH<sub>2</sub>Cl<sub>2</sub> and subjected to column chromatography on silica gel using neat CH<sub>2</sub>Cl<sub>2</sub> as the eluent. The second band was collected and stripped of solvent on a rotary evaporator. The resulting residue was dissolved in a minimum of CH<sub>2</sub>Cl<sub>2</sub> and this solution was

layered with pentane. After solvent diffusion, dark microcrystals were isolated by filtration and dried under vacuum to give 6-cyano-2-mercaptoazulene (0.0319 g, 0.172 mmol) in a 51% yield. HRMS ( $m/z$ , ES<sup>-</sup>): found for  $[M-H]^-$  184.0032; calcd for  $C_{11}H_6NS^-$  184.0226. IR (KBr):  $\nu_{SH}$  2541,  $\nu_{CN}$  2210  $cm^{-1}$ .  $^1H$  NMR (500 MHz,  $CDCl_3$ , 25 °C):  $\delta$  4.13 (s, 1H,  $SH$ ), 7.27 (s, 2H,  $H^{1,3}$ ), 7.41 (d,  $^3J_{HH} = 10$  Hz, 2H,  $H^{5,7}$ ), 8.03 (d,  $^3J_{HH} = 10$  Hz, 2H,  $H^{4,8}$ ) ppm.  $^{13}C$  NMR (100.6 MHz,  $CDCl_3$ , 25 °C):  $\delta$  116.86, 118.81, 121.37, 126.91, 130.69, 141.57 (azulenic C), 147.86 (CN) ppm.

### II.3.6 Synthesis of 6-cyano-2-N,N-dimethylamino-1,3-diethoxycarbonylazulene (II.5)

A solution/slurry of 2,6-dichloro-1,3-diethoxycarbonylazulene (0.231 g, 0.599 mmol) and CuCN (0.077 g, 0.899 mmol) in 20 mL of DMF was refluxed for 6 hours. During the reflux, the solution color changed from red to a dark yellowish brown. Then the contents of the reaction flask were cooled to room temperature and poured into 200 mL of aqueous ammonium hydroxide solution. The resulting emulsion was left stirring at room temperature for 24 hours to form a deep blue solution. This solution was poured into 500 mL of deionized  $H_2O$  and extracted with  $6 \times 50$  mL of  $CH_2Cl_2$ . All of the organic fractions were combined, washed once with  $\times 100$  mL of deionized  $H_2O$ , and dried over anhydrous  $Na_2SO_4$ . Following filtration, the filtrate was concentrated on a rotary evaporator and then subjected to column chromatography on silica gel using neat  $CHCl_3$  as eluent. A yellow fraction was collected and concentrated to dryness to give 6-cyano-2-N,N-dimethylamino-1,3-diethoxycarbonylazulene (0.067g, 0.197 mmol) in a 29% yield.  $^1H$  NMR (500 MHz,  $CDCl_3$ , 25 °C):  $\delta$  1.49 (t,  $^3J_{HH} = 7$  Hz, 3H,  $CH_3$ ), 3.36 (s, 6H,  $N(CH_3)_2$ ), 4.44 (q,  $^3J_{HH} = 7$  Hz, 4H,  $CH_2$ ), 6.69 (d,  $^3J_{HH} = 12$  Hz, 2H,  $H^{5,7}$ ), 9.00 (d,  $^3J_{HH} = 12$  Hz, 2H,  $H^{4,8}$ ) ppm.  $^{13}C$  NMR (100.6 MHz,  $CDCl_3$ , 25 °C):  $\delta$  14.26 ( $CH_3$ ), 42.52

(N(CH<sub>3</sub>)<sub>2</sub>), 60.44 (CH<sub>2</sub>), 109.68, 114.91, 117.09, 118.82, 133.17, 139.44 (azulenic C), 161.38 (CN), 164.06 (CO<sub>2</sub>Et) ppm.

### II.3.7 Synthesis of 2-amino-6-cyano-1,3-diethoxycarbonylazulene (II.6)

A solution/slurry of 6-bromo-2-formido-1,3-diethoxycarbonylazulene (0.423 g, 1.073 mmol) and CuCN (0.184 g, 2.146 mmol) in 25 mL of DMF was refluxed with stirring for 3.5 hours. The contents of the reaction flask were then cooled to room temperature and poured into aqueous ammonium hydroxide solution. This mixture was stirred at room temperature for 2 hours to form a precipitate, which was isolated by vacuum filtration and redissolved in CH<sub>2</sub>Cl<sub>2</sub>. The filtrate was also extracted with 3 × 20 mL of CH<sub>2</sub>Cl<sub>2</sub> and all organic solutions were combined, washed with 1 × 30 mL H<sub>2</sub>O, dried over anhydrous Na<sub>2</sub>SO<sub>4</sub>, and concentrated under vacuum to a volume of *ca.* 3 mL. This concentrated solution was subjected to column chromatography on silica gel using neat CH<sub>2</sub>Cl<sub>2</sub> as eluent. An orange band was collected and concentrated to dryness under vacuum to give 6-cyano-2-amino-1,3-diethoxycarbonylazulene (0.230 g, 0.736 mmol) as a bright orange powder. <sup>1</sup>H NMR (400 MHz, CDCl<sub>3</sub>, 25 °C): δ 1.50 (t, <sup>3</sup>J<sub>HH</sub> = 7 Hz, 3H, CH<sub>3</sub>), 4.50 (q, <sup>3</sup>J<sub>HH</sub> = 7 Hz, 4H, CH<sub>2</sub>), 7.69 (d, <sup>3</sup>J<sub>HH</sub> = 13 Hz, 2H, H<sup>5,7</sup>), 8.16 (s, 2H, NH<sub>2</sub>), 9.02 (d, <sup>3</sup>J<sub>HH</sub> = 11 Hz, 2H, H<sup>4,8</sup>) ppm.

### II. 3.8 Synthesis of 6-amino-2-cyanoazulene (II.7)

2-cyanoazulene (0.101 g, 0.659 mmol) and 4-amino-1,2,4-triazole (0.168 g, 1.998 mmol) were dissolved in 5 mL of dry DMSO. In a separate flask was placed KO<sup>t</sup>Bu (0.481 g, 4.286 mmol) and 20 mL of dry DMSO was added to form a slurry. Then the solution of 2-cyanoazulene and 4-amino-1,2,4-triazole was slowly transferred into the flask containing the

KO<sup>t</sup>Bu. Once the transfer was completed, the mixture was heated to 70 °C for a period of 18 hrs. The mixture was then cooled to room temperature, poured into 100 mL of deionized H<sub>2</sub>O, and extracted with 3 × 20 mL of CH<sub>2</sub>Cl<sub>2</sub>. The organic fractions were combined, washed with 3 × 15 mL of H<sub>2</sub>O, dried over anhydrous Na<sub>2</sub>SO<sub>4</sub>, and filtered. All solvent was removed from the filtrate under vacuum to give 6-amino-2-cyanoazulene (0.085 g, 0.505 mmol) in a 76% yield. <sup>1</sup>H NMR (400 MHz, CDCl<sub>3</sub>, 25 °C): δ 5.07 (s, 1H, NH<sub>2</sub>), 6.46 (d, <sup>3</sup>J<sub>HH</sub> = 11 Hz, 2H, H<sup>5,7</sup>), 7.31 (s, 2H, H<sup>1,3</sup>), 8.01 (d, <sup>3</sup>J<sub>HH</sub> = 11 Hz, 2H, H<sup>4,8</sup>) ppm.

### II. 3.9 Synthesis of 2-cyano-1,3-diethoxycarbonylazulene (II.8)

A solution/slurry of 2-chloro-1,3-diethoxycarbonylazulene (0.401 g, 1.31 mmol) and CuCN (0.235 g, 2.62 mmol) in 15 mL of DMF was heated to reflux with stirring for 8 hours. After this time, the reaction mixture was cooled to room temperature and the contents of the reaction flask were poured into 150 mL of ammonium hydroxide solution and left stirring for 12 hours. The mixture was extracted with 3 × 25 mL of CH<sub>2</sub>Cl<sub>2</sub>. The organic fractions were combined, washed with 3 × 10 mL of H<sub>2</sub>O, dried over anhydrous Na<sub>2</sub>SO<sub>4</sub>, and filtered. The filtrate was concentrated to dryness under vacuum to give a dark residue which was recrystallized by layering its solution in a minimum amount of CH<sub>2</sub>Cl<sub>2</sub> with pentane and allowing solvent diffusion to occur. Following filtration, 2-cyano-1,3-diethoxycarbonylazulene was isolated as dark microcrystals (0.176 g, 0.592 mmol) in a 45% yield. <sup>1</sup>H NMR (500 MHz, CDCl<sub>3</sub>, 25 °C): δ 1.53 (t, <sup>3</sup>J<sub>HH</sub> = 7 Hz, 3H, CH<sub>3</sub>), 4.54 (q, <sup>3</sup>J<sub>HH</sub> = 7 Hz, 4H, CH<sub>2</sub>), 7.88 (t, <sup>3</sup>J<sub>HH</sub> = 10 Hz, 2H, H<sup>5,7</sup>), 8.15 (t, <sup>3</sup>J<sub>HH</sub> = 10 Hz, 1H, H<sup>6</sup>), 9.94 (d, <sup>3</sup>J<sub>HH</sub> = 10 Hz, 2H, H<sup>4,8</sup>) ppm.

### II. 3.10 Synthesis of 2-chloro-6-hydroxy-1,3-diethoxycarbonylazulene (II.9)

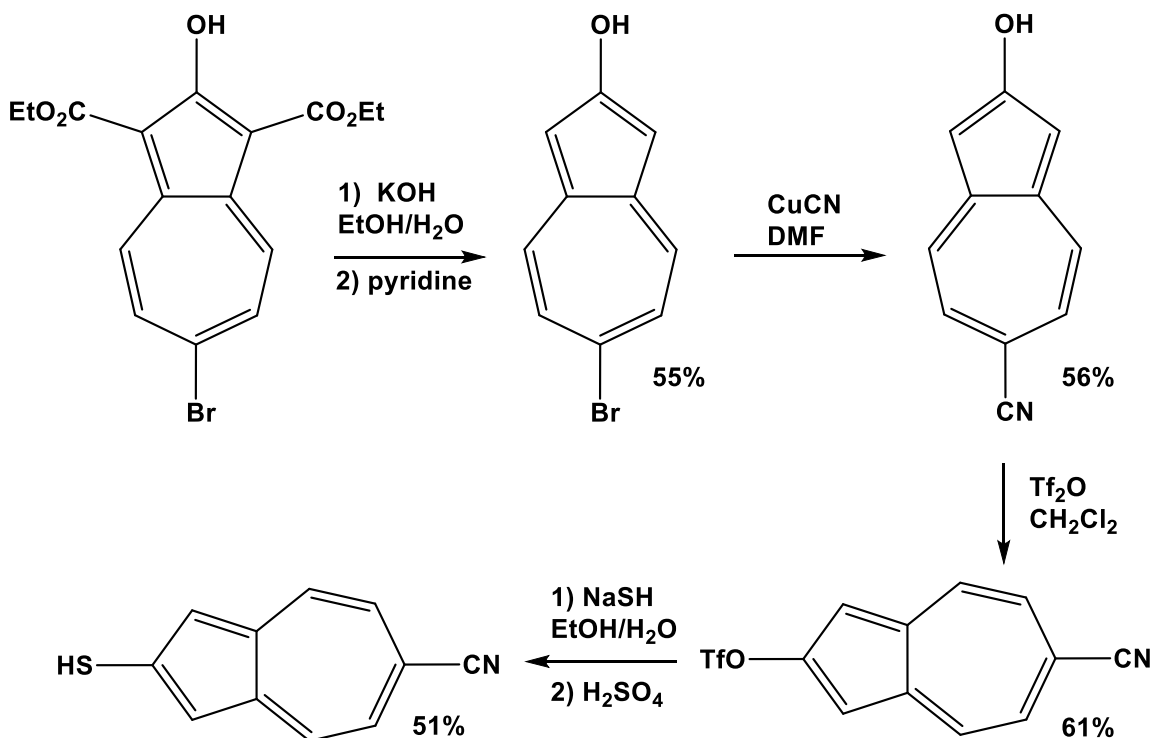
A solution of 2,6-dichloro-1,3-diethoxycarbonylazulene (0.234 g, 0.686 mmol) and NaOH (0.626 g, 15.65 mmol) in 30 mL of 70% aqueous ethanol was heated to reflux with stirring for 1 hour. The contents of the flask were then cooled to room temperature and poured into 100 mL of H<sub>2</sub>O. The resulting mixture was slowly acidified drop wise with 3M H<sub>2</sub>SO<sub>4</sub> until a precipitate formed. The precipitate was isolated by vacuum filtration and then dried under vacuum to give 2-chloro-6-hydroxy-1,3-diethoxycarbonylazulene (0.266 g, 0.824 mmol) in a 79% yield. <sup>1</sup>H NMR (400 MHz, CDCl<sub>3</sub>, 25 °C): δ 1.46 (t, <sup>3</sup>J<sub>HH</sub> = 7 Hz, 3H, CH<sub>3</sub>), 4.46 (q, <sup>3</sup>J<sub>HH</sub> = 7 Hz, 4H, CH<sub>2</sub>), 7.37 (d, <sup>3</sup>J<sub>HH</sub> = 11 Hz, 2H, H<sup>5,7</sup>), 9.28 (d, <sup>3</sup>J<sub>HH</sub> = 11 Hz, 2H, H<sup>4,8</sup>) ppm.

### II. 3.11 Synthesis of 2-chloro-6-hydroxyazulene (II.10)

2-Chloro-6-1,3-diethoxycarbonylazulene (0.110 g, 0.341 mmol) was added to 7 mL of 85% H<sub>3</sub>PO<sub>4</sub> and the mixture was heated at 120 °C for 40 minutes. The dark solution was cooled to room temperature, poured onto ice and then extracted with 3 × 20 mL of CH<sub>2</sub>Cl<sub>2</sub>. The organic fractions were combined, washed with 2 × 15 mL H<sub>2</sub>O, and dried over anhydrous Na<sub>2</sub>SO<sub>4</sub>. Following filtration, the filtrate was concentrated under vacuum and then subjected to column chromatography on silica gel using neat CH<sub>2</sub>Cl<sub>2</sub> as the eluent. A red band was collected. The solvent was removed under vacuum giving 2-chloro-6-hydroxyazulene (0.041 g, 0.230 mmol) as an orange-red powder in a 67% yield. <sup>1</sup>H NMR (400 MHz, CDCl<sub>3</sub>, 25 °C): δ 5.87 (s, 1H, OH), 6.81 (d, <sup>3</sup>J<sub>HH</sub> = 11 Hz, 2H, H<sup>5,7</sup>), 7.14 (s, 2H, H<sup>1,3</sup>), 8.05 (d, <sup>3</sup>J<sub>HH</sub> = 11 Hz, 2H, H<sup>4,8</sup>) ppm.

## II.4 Results and Discussion

Synthesis of 6-cyano-2-mercaptoazulene was accomplished in 4 steps from 6-bromo-2-hydroxy-1,3-diethoxycarbonylazulene (Scheme II.6).



**Scheme II.6** Synthesis of 6-cyano-2-mercaptoazulene

Removal of the ester groups from 6-bromo-2-hydroxy-1,3-diethoxycarbonylazulene can be achieved under either basic or acidic conditions. The harsh nature of both methods can cause product decomposition resulting in mediocre yields if sufficient care is not taken during these reactions. In the case of the acid-catalyzed hydrolysis of the ester groups, prolonged heating in 85% H<sub>3</sub>PO<sub>4</sub> will result in product decomposition. Heating at lower temperatures or insufficient reaction time only removes one of the ester groups. Removal of the ester groups under basic

conditions requires two steps: first the generation of 1,3-dicarboxylic acid through treatment of the starting compound with NaOH in 70% aqueous ethanol followed by an acidic work up and then a reflux in pyridine. A slight decrease in yield from the acid method for the removal of the ester groups is offset by an easier workup and the avoidance of a chromatographic separation required by the basic method for the isolation of the pure product.

The cyano substituent was introduced by treatment of the 6-bromo-2-hydroxyazulene with a slight excess of CuCN in DMF at high temperature. Following the workup with aqueous ammonium hydroxide and a chromatographic separation, 6-cyano-2-hydroxyazulene was isolated in ~50% yield. The solid state IR spectrum of the product confirmed the presence of both the hydroxyl and cyano groups (Figure II.10).

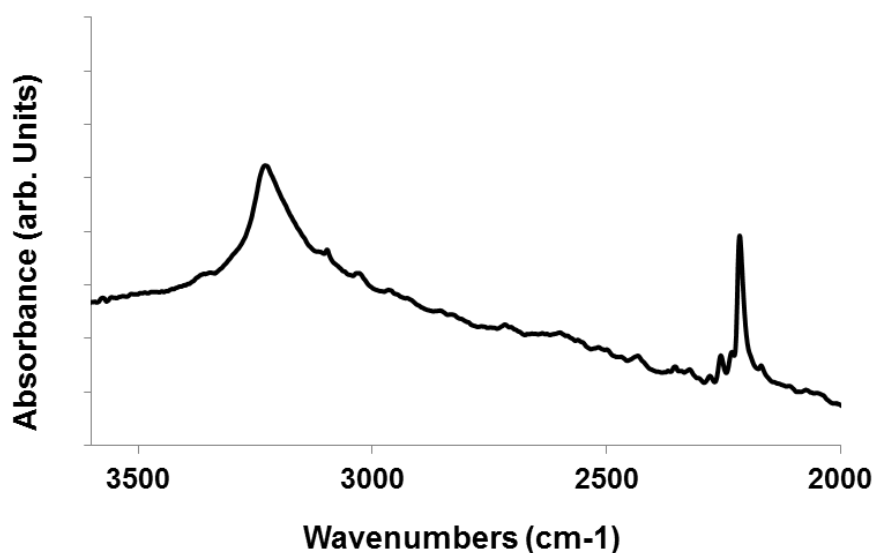
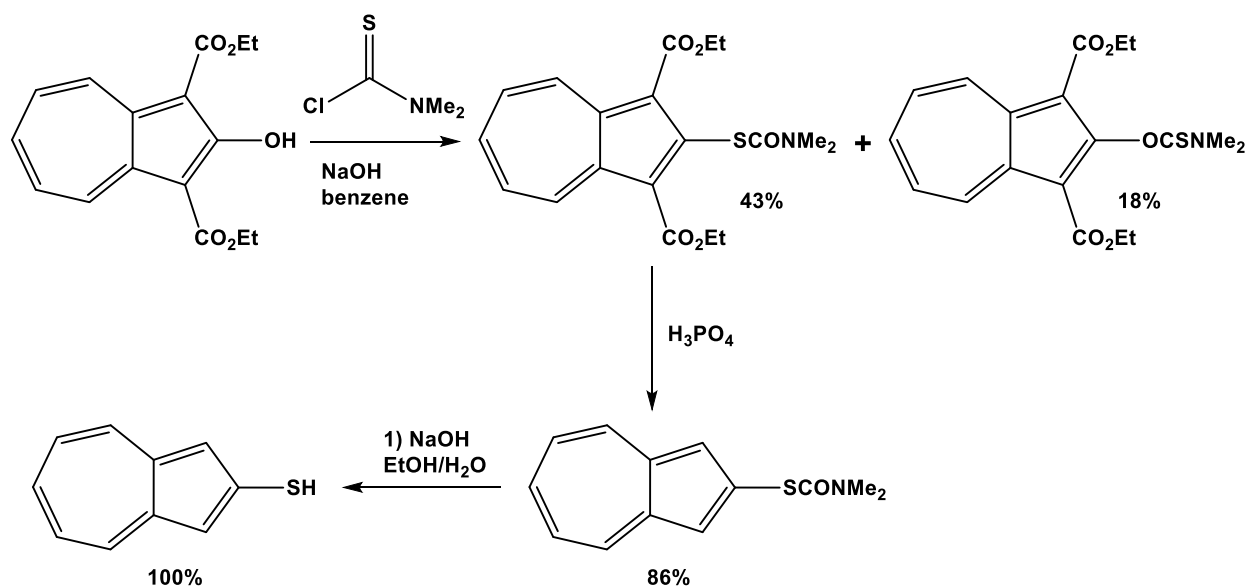


**Figure II.10** FTIR spectrum of 6-cyano-2-hydroxyazulene in a KBr pellet.

Previous studies have shown that 2-hydroxyazulenes have a solvent dependent tautomerism between 2-(1*H*)-azulenone and 2-azulenol,<sup>55</sup> so it is not surprising that no resonance for the hydroxyl proton was observed in the <sup>1</sup>H NMR spectrum 6-cyano-2-hydroxyazulene.

Although formation of 2-mercaptoazulene has been reported from 2-hydroxy-1,3-diethoxycarbonylazulene the low yield of the intermediate and formation of a side product made this route unattractive (Scheme II.7).<sup>30a</sup>



**Scheme II.7** Synthesis of 2-mercaptoazulene (Ref 30a).

Additionally, subsequent treatments with NaOH and H<sub>3</sub>PO<sub>4</sub> caused concern about potential loss of the nitrile substituent. While formation of aryl halides from aryl alcohols is well known to proceed with the reagents thionyl chloride and PBr<sub>3</sub>, attempts at such reactions with 6-cyano-2-hydroxyazulene were not successful. Alternatively, it was found that a triflate could be easily installed in a high yield by treatment of 6-cyano-2-hydroxyazulene with triflic anhydride. <sup>19</sup>F NMR and high resolution mass spectrometry were used confirm the successful formation of the



aryl triflate, while the IR spectrum of the product showed the presence of the nitrile group (Figure II.11).

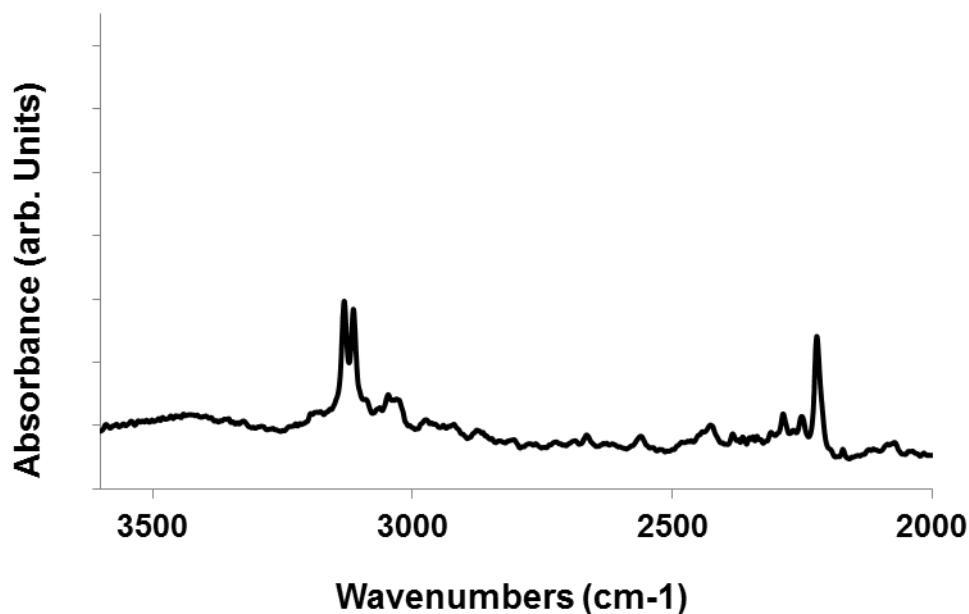


**Figure II.11** Solid state FTIR spectrum of 6-cyano-2-(trifluoromethylsulfonyl)oxyazulene in KBr

The displacement of the aryl triflate with NaSH was done under mild conditions in 70% aqueous ethanol and formation of the thiol was completed after acidification with dilute mineral acid. The 6-cyano-2-mercaptoazulene is thermally robust and does not appear to be air- or moisture sensitive under ambient conditions. After column chromatography and recrystallization, its small dark crystals were isolated in a 51% yield. The solid state IR spectrum of 6-cyano-2-mercaptoazulene shows sharp bands for both the thiol at  $\nu_{\text{SH}} = 2541 \text{ cm}^{-1}$  and the nitrile at  $\nu_{\text{CN}} = 2210 \text{ cm}^{-1}$  (Figure II.12).

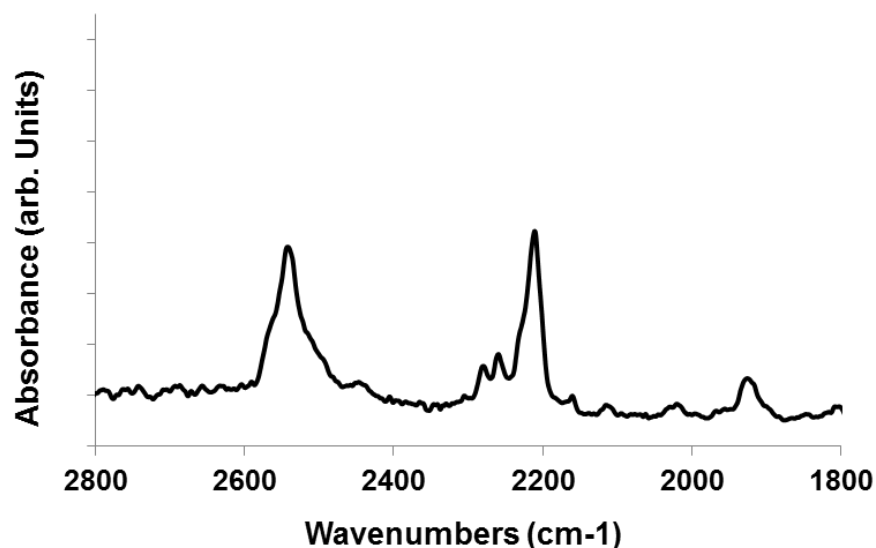
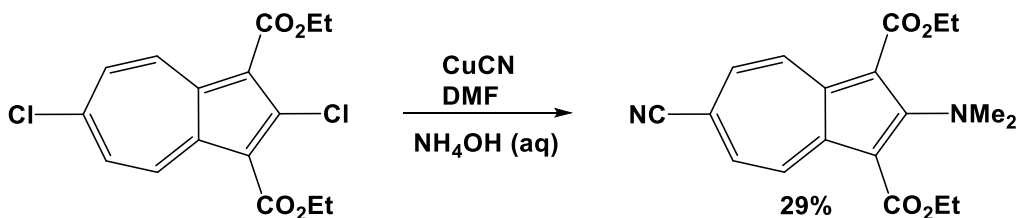


**Figure II.12** FTIR spectrum of 6-cyano-2-mercaptoazulene in KBr

The  $^1\text{H}$  NMR spectrum of this compound features a characteristic *SH* resonance at 4.13 ppm, which is similar to other azulenic thiols.<sup>25,30</sup> Prior to the successful synthesis of 6-cyano-2-mercaptoazulene, two other routes to this novel species were attempted. In the first, 6-bromo-2-formido-1,3-diethoxycarbonylazulene was reacted with an excess of CuCN in DMF at elevated temperatures. After a basic work up, 2-amino-6-cyano-1,3-diethoxycarbonylazulene was obtained in a reasonable yield as a bright orange powder. Notably, attempts to generate the same product from 2-amino-6-bromo-1,3-diethoxycarbonylazulene were unsuccessful resulting only in the recovery of a small fraction of the starting material. Given this outcome, it is likely that the amine was generated during the basic work up with ammonium hydroxide. Attempts to access the corresponding azulenyl halide from this amine through the generation and subsequent decomposition of a diazonium salt were not successful as there was no evidence of any reaction occurring. Formylation of the amine with acetic-formic anhydride was not successful either,

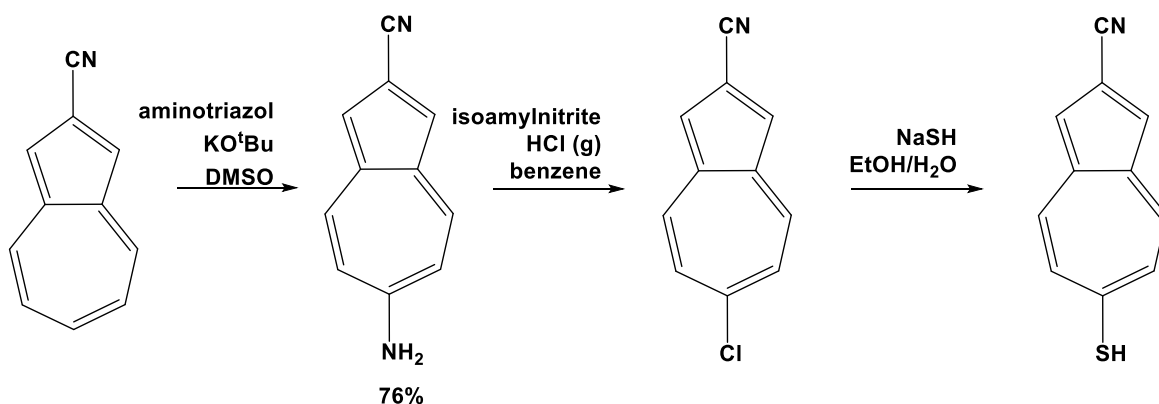
even at elevated temperatures. Thus, the presence of three electron withdrawing groups around azulenic core appears to substantially deactivate the amine functionality toward substitution.

In a similar fashion, 2,6-dichloro-1,3-diethoxycarbonylazulene was reacted with a stoichiometric amount of CuCN in DMF at elevated temperatures. It was hoped that the sterically crowded environment around the 2-chloro substituent would render it less reactive, thereby leading to the regioselective cyanation at only the 6-position. Initial results of this reaction appeared promising as the isolated yellow powder featured a strong CN stretching band at  $2220\text{ cm}^{-1}$  in its IR spectrum. However, its  $^1\text{H}$ -NMR spectrum revealed that during the course of the reaction and/or workup the 2-chloro substituent had been replaced with an N,N-dimethylamino functionality (Scheme II.8).



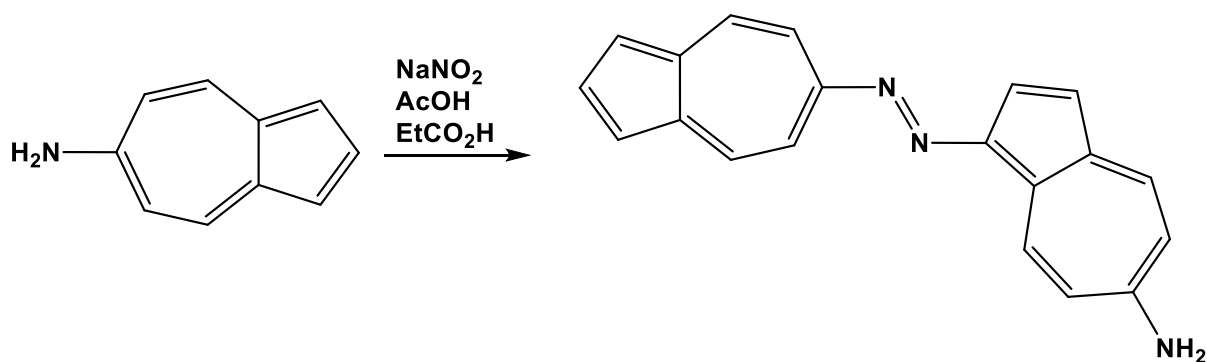
**Scheme II.8** Synthesis of 6-cyano-2-N,N-dimethylamino-1,3-diethoxycarbonylazulene

The first synthetic route to 2-cyano-6-mercaptoazulene that was attempted is shown in scheme II.9.



**Scheme II.9** Proposed synthesis of 2-cyano-6-mercaptoazulene

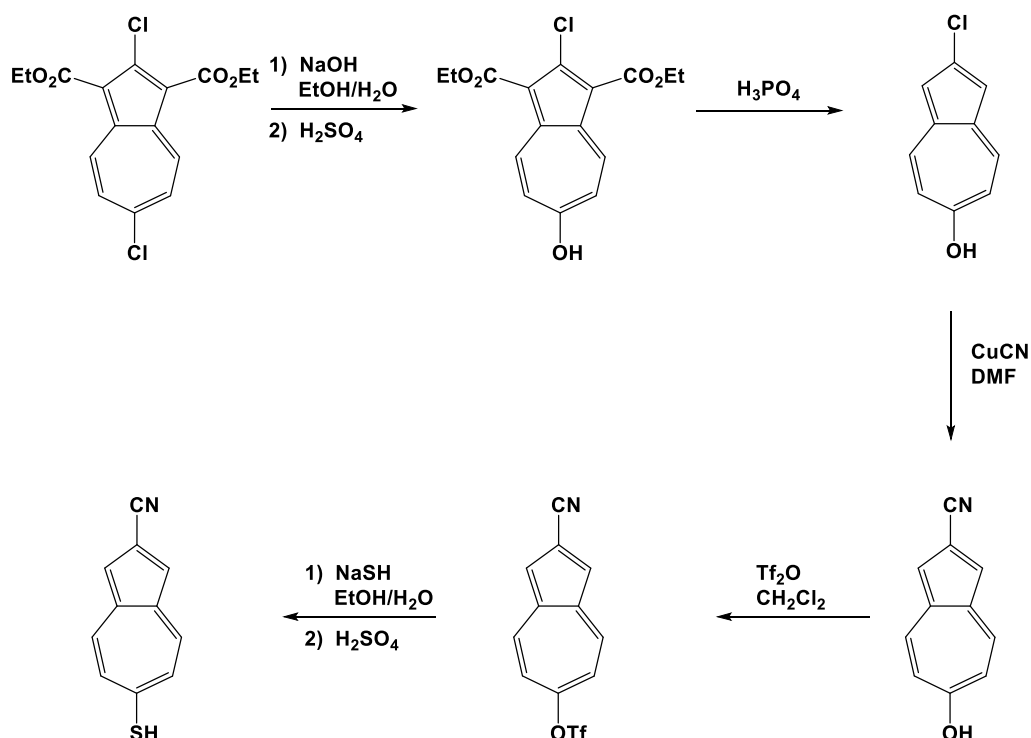
Treatment of 2-cyanoazulene with 4-amino-1,2,4-triazole in dry DMSO at 40 °C provided 6-amino-2-cyanoazulene in a good yield. However, the diazotation of the 6-amino-2-cyanoazulene with isoamyl nitrite did not result in the formation of the corresponding aryl halide but instead gave a dark brown powder that was surprisingly insoluble in organic solvents and had extremely limited solubility in H<sub>2</sub>O. Solubility limitations prevented analysis of the product by <sup>1</sup>H NMR. Separation and characterization of azulenic product(s) was not possible even after chromatography and multiple attempts at recrystallization. The preparation of diazonium salts from 6- amino azulenes is extremely difficult as they are highly unstable and are known to convert to diazo compounds (Scheme II.10).<sup>37</sup>



**Scheme II.10** Synthesis of 1-(azulen-6-ylazo)-azulen-6-yl-amine (Ref 37)

Formation of oligomers of various lengths with a diazo-linkage between the 1- and 6-positions of the azulenic scaffold could account for the nearly insoluble nature of the brown precipitate. Since the diazotization of 6-amino-2-cyanoazulene did not proceed as anticipated a new approach was necessary. A sample of 2-cyano-1,3-diethoxycarbonyl azulene was prepared from 2-chloro-1,3-diethoxycarbonylazulene in hope that the ethyl ester substituents would block the potential diazocoupling from occurring. However, the amination of the **II.8** failed with both 4-amino-1,2,4-triazole and methoxyaminehydrochloride. It has not been determined if the presence of electron withdrawing groups at the 1- and 3-positions would prevent diazo coupling and lead to the formation of the corresponding azulenyl halide at the 6- position.

Another route to currently unknown 2-cyano-6-mercaptoazulene was envisioned with 2,6-dichloro-1,3-diethoxycarbonylazulene as a potential precursor (Scheme II.11).

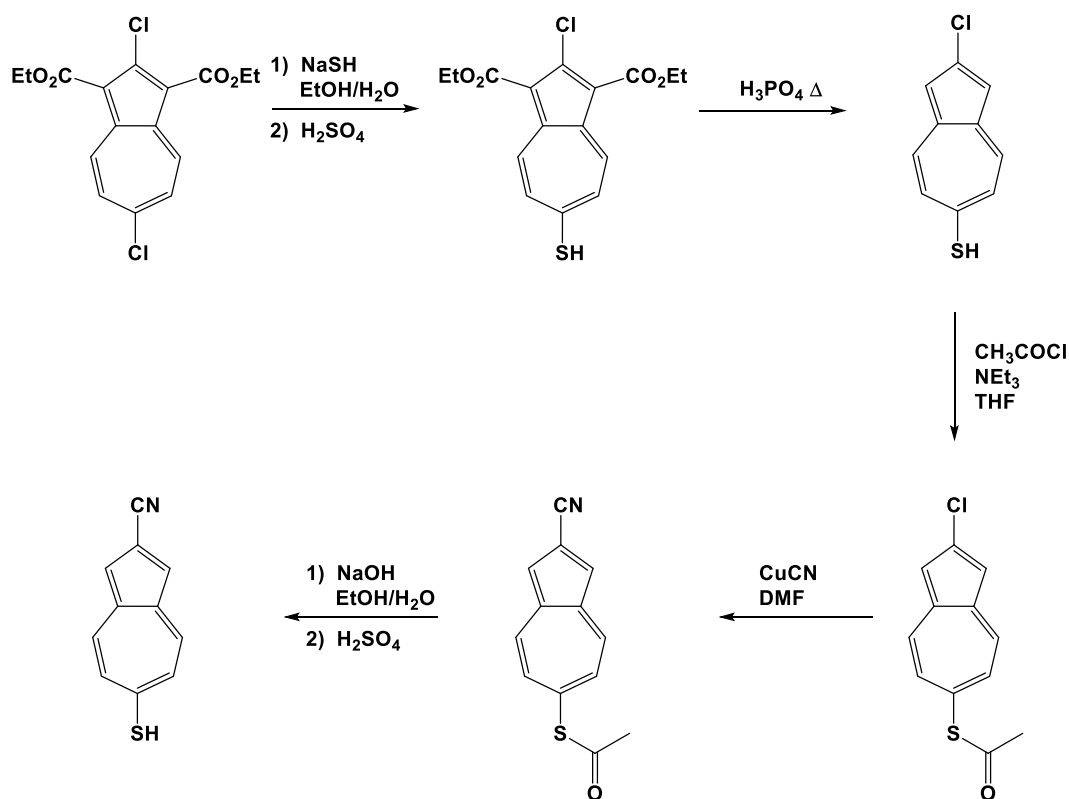


**Scheme II.11** Proposed synthesis of 2-cyano-6-mercaptoazulene

2-Chloro-6-hydroxy-1,3-diethoxycarbonylazulene was synthesized from 2,6-dichloro-1,3-diethoxycarbonylazulene in good yield by treatment of the latter with an excess of KOH in 70% aqueous ethanol, followed by an acidic workup. Decarboxylation of 2-chloro-6-hydroxy-1,3-diethoxycarbonylazulene was accomplished by heating it in a solution of 85%  $\text{H}_3\text{PO}_4$  at 120 °C for thirty minutes. The resulting 2-chloro-6-hydroxyazulene was treated with CuCN in DMF at elevated temperatures but the reaction did not produce 2-cyano-6-hydroxyazulene and only a small amount of the starting material was recovered. Attempts to form 6-hydroxy-2-iodoazulene from 2-chloro-6-hydroxyazulene using a slightly modified method of Nozoe's preparation of 2-iodoazulene<sup>38</sup> was not successful either.

## II.5 Conclusions and Outlook

While the synthesis of 6-cyano-2-mercaptoazulene was accomplished in four steps from 2-hydroxy-1,3-diethoxycarbonylazulene, its isomer 2-cyano-6-mercaptoazulene still remains elusive. Installation of a halide at the 6- position of azulenic scaffold through the diazotization of 6-amino-2-cyanoazulene proved to be futile. Attempts to access 2-cyano-6-hydroxyazulene by treating 2-chloro-6-hydroxyazulene with CuCN were also unsuccessful. A potential route that has not yet been attempted would involve the decarboxylation of 2-chloro-6-mercapto-1,3-diethoxycarbonylazulene to access 2-chloro-6-mercaptoazulene. Following protection of the mercaptan functionality with an acetyl group, it may be possible to install the cyano group at the 2- position by treatment of the protected mercaptoazulene with CuCN. Deprotection of the acetylated mercaptan should be possible under mildly basic conditions to generate the 2-cyano-6-mercaptoazulene (Scheme II.12).



**Scheme II.12** Proposed synthesis of 2-cyano-6-mercaptoazulene

The successful synthesis of 2-cyano-6-mercaptoazulene will afford an opportunity to probe the charge transport dynamics within the azulenic motif along its molecular axis. These new additions to the expanding family of 2,6- functionalized azulene derivatives may also be useful in further studies of azulenic thin film assemblies.



---

## II.6 References

- (1) Dewar, M. J. S. *The Molecular Orbital Theory of Organic Chemistry*, McGraw-Hill: New York, 1969.
- (2) Anderson, A. G., Jr.; Steckler, B. M. *Journal of the American Chemical Society*, **1959**, *81*, 4941-4946.
- (3) (a) Liu, R. S. H.; Asato, A. E. *Journal of Photochemistry and Photobiology C-Photochemistry*, **2003**, *4*, 179-194. (b) Lacroix, P. G.; Malfant, I.; Iftime, G.; Razus, A. C.; Nakatani, K.; Delaire, J. A. *Chemistry-a European Journal*, **2000**, *6*, 2599-2608. (c) Herrmann, R.; Pedersen, B.; Wagner, G.; Youn, J. H. *Journal of Organometallic Chemistry*, **1998**, *571*, 261-266.
- (4) (a) Estdale, S. E.; Brettler, R.; Dunmur, D. A.; Marson, C. M. *Journal of Materials Chemistry*, **1997**, *7*, 391-401. (b) Ito, S.; Inabe, H.; Morita, N.; Ohta, K.; Kitamura, T.; Imafuku, K. *Journal of the American Chemical Society*, **2003**, *125*, 1669-1680.
- (5) Barman, S.; Furukawa H.; Blacque, O.; Venkatesan, K.; Yaghi, O. M.; Berke, H. *Chemical Communications*, **2010**, *46*, 7981-7983.
- (6) (a) Amir, E.; Amir, R. J.; Campos, L. M.; Hawker, C. J. *Journal of the American Chemical Society*, **2011**, *133*, 10046-10049. (b) Feringa, B. L.; van Delden, R. A.; Koumura, N.; Geertsema, E. M. *Chemical Reviews*, **2000**, *100*, 1789-1816.
- (7) (a) Wang, F. K.; Lai, Y. H.; Han, H. Y. *Macromolecules*, **2004**, *37*, 3222-3230. (b) Redl, F. X.; Kothe, O.; Rockl, K.; Bauer, W.; Daub, J. *Macromolecular Chemistry and Physics*, **2000**, *201*, 2091-2100. (c) Nie, G. Cai, T.; Zhang, S.; Hou, J.; Xu, J.; Han, X. *Materials Letters*, **2007**, *61*, 3079-3082.
- (8) Zhang, X. H.; Li, C.; Wang, W. B.; Cheng, X. X.; Wang, X. S.; Zhang, B. W. *Journal of Materials Chemistry*, **2007**, *17*, 642-649.
- (9) Yamaguchi, Y.; Maruya, Y.; Katagiri, H.; Nakayama, K; Ohba, Y. *Organic Letters*, **2012**, *14*, 2316-2319
- (10) Coropceanu, V.; Cornil, J.; Demtrio, A. Olivier, Y.; Silbey, R.; Bredas, J-L. *Chemical Reviews*, **2007**, *107*, 926-952.
- (11) Aviram, A.; Ratner, M. A. *Chemical Physics Letters*, **1974**, *29*, 277-283.
- (12) Kornilovitch, P.; Bratkovsky, A.; Williams, S. *Annals of the New York Academy of Sciences*, **2006**, *1006*, 198-211.

- 
- (13) Elbing, M.; Ochs, R.; Koentop, M.; Fischer, M.; Hanisch, C. V.; Weigend, F.; Evers, F.; Weber, H. B.; Mayor, M. *Proceedings of the National Academy of Sciences*, **2005**, *102*, 8815-8820.
- (14) Zhou, K.-G.; Zhang, Y.-H.; Wang, L.-J.; Xie, K.-F.; Xiong, Y.-Q.; Zhang, H.-L.; Wang, C.-W.; *Physical Chemistry Chemical Physics*, **2011**, *13*, 15882-15890.
- (15) Treboux, G.; Lapstun, P.; Silverbrook, K. *Journal of Physical Chemistry B*, **1998**, *102*, 8978-8980.
- (16) a) King, R. B.; Ackermann, M. N. *Inorganic Chemistry*, **1973**, *13*, 637. b) Tofke, V. S.; Behrens, U. *Angewandte Chemie*, **1986**, *99*, 134. c) Churchill, M. R. *Progress in Inorganic Chemistry* **1970**, *11*, 53.
- (17) Holovics, T. C.; Robinson, R. E.; Weintrop, E. C.; Toriyama, M.; Lushington, G. H.; Barybin, M. V. *Journal of the American Chemical Society*, **2006**, *128*, 2300-2309.
- (18) Barybin, M. V.; Chisholm, M. H.; Dalal, N. S.; Holovics, T. H.; Patmore, N. J.; Robinson, R. E.; Zipse, D. J. *Journal of the American Chemical Society*, **2005**, *127*, 15182-15190.
- (20) Tsutsui, M.; Taniguchi, M. *Sensors*, **2012**, *12*, 7259-7298.
- (21) Mativetsky, J. M.; Palma, M.; Samori, P. *Topics in Current Chemistry*, **2008**, *285*, 157-202.
- (22) Angelici, R. J.; Lazar, M. *Inorganic Chemistry*, **2008**, *47*, 9155-9165.
- (23) Ullman, A. *Accounts of Chemical Research*, **2001**, *34*, 855-863.
- (24) Dubose, D. L.; Robinson, R. E.; Holovics, T. C.; Moody, D. R.; Weintrob, E. C.; Berrie, C. L.; Barybin, M. V. *Langmuir*, **2006**, *22*, 4599-4606.
- (25) Neal, B.; Vorushilov, A. S.; DeLaRosa, A. M.; Robinson, R. E.; Berrie, C. L.; Barybin, M. V. *Chemical Communications*, **2011**, *47*, 10803-10805.
- (26) Lortscher, E.; Cho, C. J.; Mayor, M.; Tschudy, M.; Rettner, C.; Riel, H. *ChemPhysChem*, **2011**, *12*, 1677-1682.
- (27) Neppl, S.; Bauer, U.; Menzel, D.; Feulner, P.; Shaporenko, A.; Zharnikov, M.; Kao, P.; Allara, D. L. *Chemical Physics Letters*, **2007**, *447*, 227-231.
- (28) Hamoudi, H.; Neppl, S.; Kao, P.; Schupbach, B.; Feulner, P.; Terfort, A.; Allara, D.; Zharnikov, Z. *Physical Review Letters*, **2011**, *107*, 027801-1 – 027801-4.
- (29) Schkolnik, G.; Salewski, J.; Millo, D.; Zebger, I.; Franzen, S.; Hildebrandt, P. *International*

- (30) a) Asao, T. *Pure and Applied Chemistry*, **1990**, *62*, 507-512. b) Fujimori, K.; Kitahashi, H.; Koyama, S.; Yamane, K. *Bulletin of the Chemical Society of Japan*, **1986**, *59*, 3320-3322.
- (31) a) Nozoe, T.; Seto, S.; Matsumura, S. *Bulletin of the Chemical Society of Japan*, **1962**, *35*, 1990-1998 (b) Schmitt, S.; Baumgarten, M.; Simon, J.; Hafner, K. *Angewandte Chemie, International Edition*, **1998**, *37*, 1078-1081.
- (32) Liu, R. S. H. *Journal of Chemical Education*, **2002**, *79*, 183-185
- (33) Anderson Jr., A. G.; Nelson, J. A.; Tazuma, J. J. *Journal of the American Chemical Society*, **1953**, 4980-4989.
- (34) Anderson Jr., G. A.; Gale, D. J.; McDonald, R. N. Anderson, R. G.; Rhodes, R. C. *Journal of Organic Chemistry*, **1964**, *29*, 1373-1377.
- (35) Anderson Jr., G. A.; Scotoni Jr., R.; Cowles, E. J.; Fritz, C. G. *Journal of Organic Chemistry*, **1957**, *22*, 1193-1197.
- (36) Redl, F. X.; Kothe, O.; Rocki, K.; Bauer, W.; Daub, J. *Macromolecular Chemistry and Physics*, **2000**, *201*, 2091-2100.
- (37) Makosza, M.; Osinski, P. W.; Ostrowski, S. *The Polish Journal of Chemistry*, **2001**, *75*, 275-281.
- (38) Nozoe, T.; Asao, T.; Oda, M. *Bulletin of the Chemical Society of Japan*, **1974**, *47*, 681-686.
- (39) Nozoe, T.; Seto, S.; Matsumura, S. *Bulletin of the Chemical Society of Japan*, **1962**, *35*, 1990-1998.
- (40) Fujinaga, M.; Murafuji, T.; Kurotobi, K.; Sugihara, Y. *Polyhedron*, **2009**, *65*, 7115-7121.
- (41) Shibasaki, T.; Ooishi, T.; Yamanouchi, N.; Murafuji, T.; Kurotobi, Kei, and Yoshikaza, S. *Journal of Organic Chemistry*, **2008**, *73*, 7971-7977.
- (42) Anderson Jr., A. G.; Gale, D. J.; McDonald, R. N.; Anderson, R. G.; Rhodes, R. C. *Journal of Organic Chemistry*, **1964**, *29*, 1373.
- (43) Nozoe, T. Takase, K.; Norboru, S. *Bulletin of the Chemical Society of Japan*, **1964**, *37*, 1644-1648.
- (44) Nozoe, T.; Matsumura, S.; Murase, Y.; Seto, S.; *Chemistry & Industry*, **1955**, 1257.

- 
- (45) Machiguchi, T.; Hasegawa, T.; Yamabe, S.; Minato, T.; Yamazaki, S. Nozoe, T. *Journal of Organic Chemistry*, **2012**, 77, 5318-5330.
- (46) Morita, T.; Fujita, T.; Takase, K. *Bulletin of the Chemical Society of Japan*, **1980**, 53, 1647-1651.
- (47) (a) Kato, N.; Fukazawa, Y.; Ito, S. *Tetrahedron Letters*, **1976**, 24, 2045-2048. (b) Nozoe, T.; Asao, T.; Susumago, H.; Ando, M. *Bulletin of the Chemical Society of Japan*, **1974**, 47, 1471-1476
- (48) Yokoyama, R.; Ito, S.; Okujima, T.; Kubo, T.; Yasunami, M.; Tajiri, A.; Morita, N. *Tetrahedron*, **2003**, 59, 8191-8198.
- (49) Hafner, K. *Justus Liebigs Annalen der Chemie*, **1962**, 656, 24-33.
- (50) Morita, T.; Takase, T. *Bulletin of the Chemical Society of Japan*, **1982**, 55, 1144-1152.
- (51) Okujima, T.; Ito, S.; Morita, N. *Tetrahedron*, **2002**, 43, 1261-1264.
- (52) Kurotobi, K.; Tabata, H.; Miyauchi, M.; Murafuji, T.; Sugihara, Y. *Synthesis*, **2002**, 8, 1013-1016.
- (53) Ito, S.; Nomura, A.; Mortia, N.; Kabuto, C.; Kobayashi, H.; Maejima, S.; Fujimori, K.; Yasunami, M. *Journal of Organic Chemistry*, **2002**, 67, 7295-7302.
- (54) Nozoe, T.; Asao, T.; Oda, M. *Bulletin of the Chemical Society of Japan*, **1974**, 47, 681-686.
- (55) Takase, K.; Asao, T.; Takagi, Y.; Nozoe, T.; *Chemical Communications*, **1968**, 368-370.

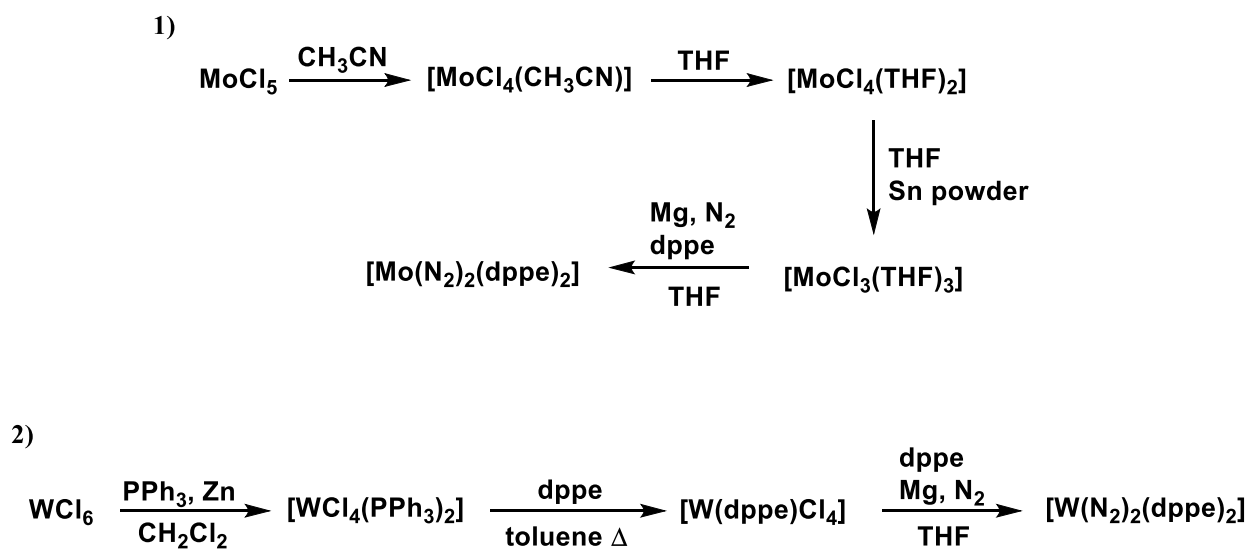
## **Chapter 3**

Coordination Chemistry of Nonbenzenoid Isocyanoarenes with

Low Valent Molybdenum and Tungsten

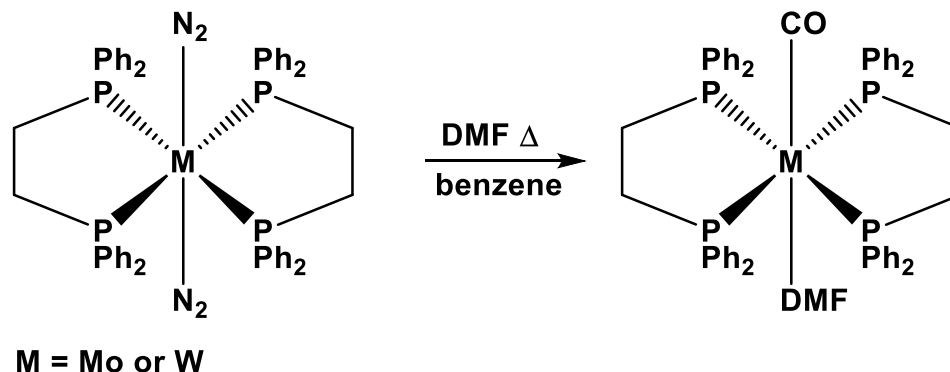
### III.1 Historical Perspective

The fixation of N<sub>2</sub> and its reduction to NH<sub>3</sub> by transition metal complexes has led to the preparation of many coordination complexes featuring N<sub>2</sub> as a ligand.<sup>1</sup> In addition to probing the reactivity of N<sub>2</sub>, some of these complexes provide convenient adducts for the formation of complexes with low valent metal centers.<sup>2</sup> The first example of a complex featuring *trans* configuration of two N<sub>2</sub> ligands was reported in 1969 when Hidai and co-workers isolated *trans*-[Mo(N<sub>2</sub>)<sub>2</sub>(dppe)<sub>2</sub>].<sup>3</sup> A similar complex *trans*-[W(N<sub>2</sub>)<sub>2</sub>(dppe)<sub>2</sub>] has also been prepared.<sup>4</sup> These zero valent metal complexes display a wide range of chemical activity including P-H bond activation,<sup>5</sup> protonation of N<sub>2</sub>,<sup>6</sup> transformations of cyanamides,<sup>7</sup> and the formation of group 6 metal hydrides.<sup>8</sup> Upon treatment of [Mo(N<sub>2</sub>)<sub>2</sub>(dppe)<sub>2</sub>] with HBF<sub>4</sub>, loss of one N<sub>2</sub> ligand and protonation of the other occurs to form the [Mo(N<sub>2</sub>H<sub>2</sub>)F(dppe)<sub>2</sub>]BF<sub>4</sub>•CH<sub>2</sub>Cl<sub>2</sub> complex.<sup>9</sup> Although these complexes are unstable under ambient laboratory conditions, they may be stored for extended periods of time under an inert atmosphere.<sup>4</sup> Preparation of [M(N<sub>2</sub>)<sub>2</sub>(dppe)<sub>2</sub>], where M is either Mo or W, is shown in Scheme III.1.<sup>4</sup>

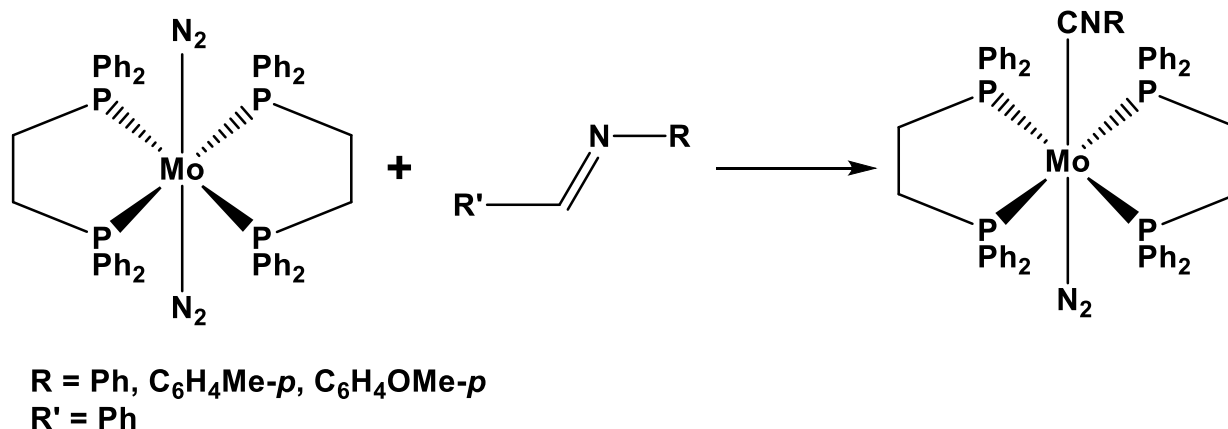


**Scheme III.1** Synthesis of [Mo(N<sub>2</sub>)<sub>2</sub>(dppe)<sub>2</sub>] and [W(N<sub>2</sub>)<sub>2</sub>(dppe)<sub>2</sub>] (Ref 4)

Both the W and Mo  $[M(N_2)_2(dppe)_2]$  complexes react with DMF to form  $[M(CO)(DMF)(dppe)_2]$  (Scheme III.2).<sup>10,11</sup> The DMF ligand was readily displaced by CO to form the W and Mo  $[M(CO)_2(dppe)_2]$  complexes.<sup>10,11</sup> Treatment of  $[Mo(N_2)_2(dppe)_2]$  with various benzyldeneanilines resulted in the formation of isocyano-dinitrogen complexes *trans*- $[Mo(CNR)(N_2)(dppe)_2]$  (Scheme III.3).<sup>12, 13</sup> The dinitrogen ligand in the  $[Mo(CNR)(N_2)(dppe)_2]$  complex could be displaced with either CO or an isocyanide.



**Scheme III.2** Synthesis of W and Mo  $[M(CO)(DMF)(dppe)_2]$ <sup>10,11</sup>



**Scheme III.3** Synthesis of  $[Mo(CNR)(N_2)(dppe)_2]$ <sup>13</sup>

Isocyanides have been shown to be excellent ligands in the stabilization of low valent transition metal complexes.<sup>14</sup> Being isoelectronic with CO, isocyanides function as both  $\sigma$ -donors and  $\pi$ -acceptor ligands (Figure III.1). The relatively strong  $\pi$  accepting ability of isocyanide ligands allows stabilization of a variety of low valent transition metal atoms and ions.<sup>14</sup> In the case of isocyanoarenes, introduction of electron donating/withdrawing substituents at the aromatic ring allows, to some extent, tuning the isocyanide ligand's  $\sigma$ -donor and/or  $\pi$ -acceptor characteristics.<sup>14</sup>

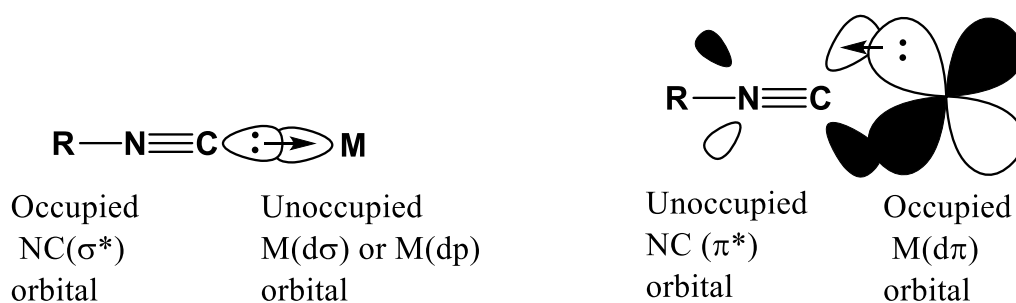
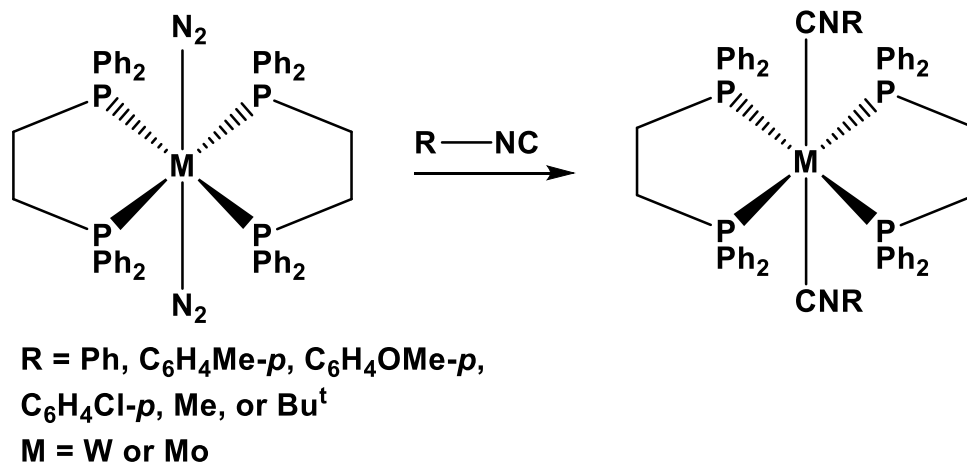


**Figure III.1** Isocyanides as  $\sigma$ -donors and  $\pi$ -acceptors.

Chatt *et. al.* described the displacement of both dinitrogen ligands from the  $[\text{M}(\text{N}_2)_2(\text{dppe})_2]$  complexes where  $\text{M} = \text{W}$  or  $\text{Mo}$  with aryl and alkyl isocyanides (Scheme III.4).<sup>2,15</sup> They found the resulting  $[\text{M}(\text{CNR})_2(\text{dppe})_2]$  complexes ( $\text{M} = \text{Mo}$  or  $\text{W}$ ) to be air stable in the solid state, but noted that they decomposed in halogenated solvents.<sup>4</sup>





**Scheme III.4** Synthesis of *trans*-[M(CNR)<sub>2</sub>(dppe)<sub>2</sub>]<sup>15</sup>

In 2000, Bennet *et. al.* described electronic and steric factors that dictate *cis* and *trans* complexation of several different benzenoid isocyanides in octahedral zero-valent group 6 transition metal complexes.<sup>16</sup> The authors found that isocyanobenzenes substituted at the *para*-position with electron-withdrawing group formed *cis* complexes while those featuring an electron-donating *para*-substitution formed *trans* complexes.<sup>16</sup> They argued that the electron-withdrawing groups increased the electronic stabilization enough to overcome the steric interactions for the *cis* complexes.<sup>16</sup> Table III.1 summarizes the different isocyanobenzenes considered in that study and the characteristic  $\nu_{\text{CN}}$  stretching bands of the bound isocyanide ligands in the various *cis* or *trans* complexes they formed with the W(dppe)<sub>2</sub> motif.<sup>16</sup>

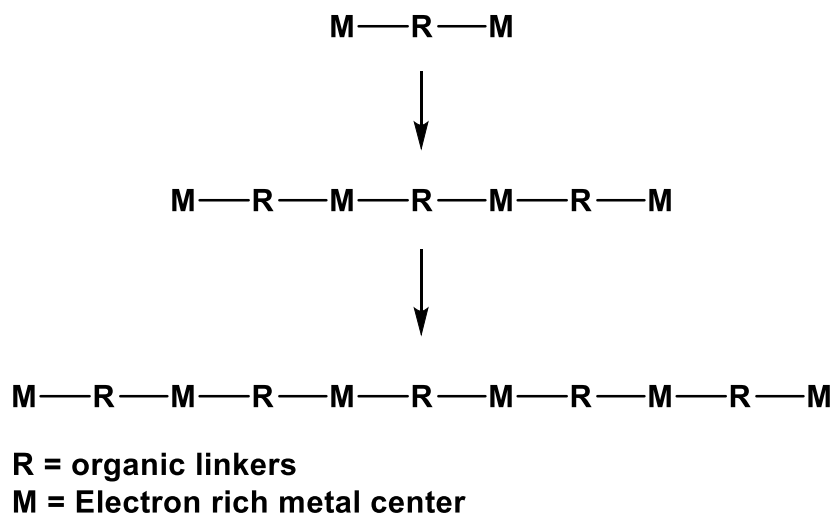
**Table III.1** Stereochemistry of the  $(p\text{-R-C}_6\text{H}_4\text{-NC})_2\text{W(dppe)}_2$  complexes and the corresponding  $\nu_{\text{CN}}$  data adapted from reference 16.

Isocyanide ligand	complex	$\nu_{\text{CN}}, \text{cm}^{-1}$
$p\text{-O}_2\text{N-C}_6\text{H}_4\text{-NC:}$	cis	1743, 1662
$p\text{-CN-C}_6\text{H}_4\text{-CN:}$	cis	1772, 1669
$p\text{-CN-C}_6\text{H}_2(\text{CH}_3)_2\text{-NC:}$	cis	1761, 1662
$p\text{-CF}_3\text{-C}_6\text{H}_4\text{-NC:}$	cis	1834, 1693
$p\text{-CN-C}_6(\text{CH}_3)_4\text{-NC:}$	trans	1819
$p\text{-F-C}_6\text{H}_4\text{-NC:}$	trans	1865
$p\text{-CH}_3\text{-C}_6\text{H}_4\text{-NC:}$	trans	1873
$p\text{-H}_3\text{CO-C}_6\text{H}_4\text{-NC:}$	trans	1822

### III.2 Introduction

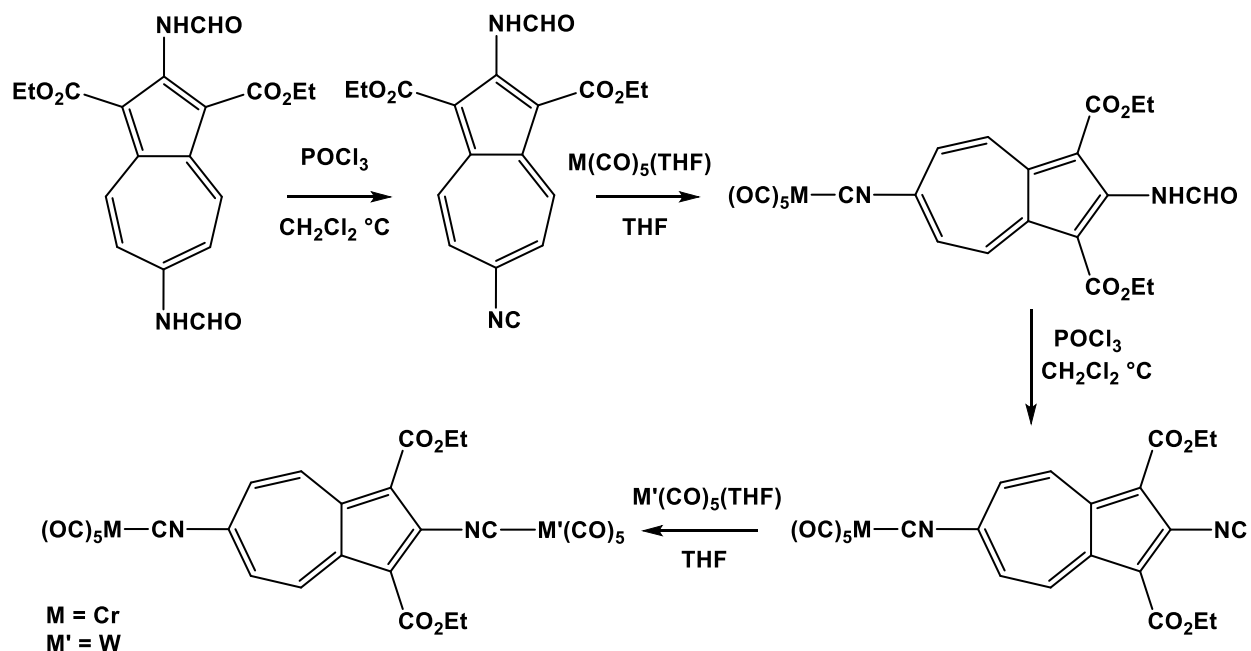
The growing field of molecular electronics dictates a need for the controlled construction of 1-D materials for charge transport, i.e., molecular wires. Electron transfer across organic bridges in dinuclear complexes is of great importance for future construction of organometallic molecular wires.<sup>17</sup> On a molecular level, electron rich metal centers may function as electron reservoirs connected via an organic bridge. Organic bridges constructed of arenes offer the ability to fine tune the extended  $\pi$ - system of the bridge. To ensure controlled coordination of the arene bridging motif, isocyano or thiolate junction groups are often employed. As the thiolate junction has been discussed in detail in Chapters 1 and 2 of this Thesis, the following discussion will address the function of the isocyanide junction group. Linear disocyanoarenes have been suggested to function as mediators for charge delocalization between transition metal

centers.<sup>14</sup> Of particular recent interest is the development of strategies for assembling one-dimensional metal-diisocynoarene “wires” possessing well-defined chain lengths. An approach for the formation of such wires by the systematic addition one metal center to each terminus of the unit in a stepwise fashion is shown in Scheme 5.



**Scheme III.5** Proposed approach for the formation of uniform 1-D organometallic materials by the systematic addition of metal centers.

Previously, the Barybin group has published synthetic routes to a number of new non-benzenoid aromatic isocyanides and began exploration of their coordination chemistry.<sup>18</sup> Later in 2006 the Barybin group published the synthesis of 2,6-diisocyano-1,3-diethoxycarbonylazulene and demonstrated that it could be implemented as an organic linker between either metal centers.<sup>19</sup> They discovered that dehydration of the 2,6-diformamido-1,3-diethoxycarbonylazulene at low temperature was regioselective and generated 2-formamido-6-isocyano-1,3-diethoxycarbonylazulene.<sup>19</sup> This discovery led to the development of a method for a controlled stepwise complexation of metal centers to their 2,6-diisocyano-1,3-diethoxycarbonylazulene (Scheme III.6).<sup>19</sup>



**Scheme III.6** Controlled Mono- and Heterobimetallic Complexation of 2,6-diisocyano-1,3-diethoxycarbonylazulene (Ref 19)

### III.3 Work Described in Chapter III

This chapter describes a systematic investigation of the interactions of non-benzenoid aromatic isocyanides with  $[\text{W}(\text{N}_2)_2(\text{dppe})_2]$  and  $[\text{Mo}(\text{N}_2)(\text{CO})(\text{dppe})_2]$ .

## III.4 Experimental

### III.4.1 General Procedures

Unless otherwise specified, 99.5% argon and nitrogen were further purified by passage through columns of activated BASF catalyst and molecular sieves. All connections involving the gas purification systems were made of glass, metal, or other materials impermeable to air. Solutions were transferred via stainless steel cannulas whenever possible. Standard Schlenk techniques were employed with a double manifold vacuum line. Pentane was distilled over calcium hydride. Benzene was dried over molecular sieves and then distilled over freshly cut potassium. THF was distilled over sodium/benzophenone. N,N-dimethylformamide was dried over  $\text{CaCl}_2$  and distilled under argon. Following purification, all solvents were stored under argon. Solution infrared spectra were recorded on a PerkinElmer Spectrum 100 FTIR spectrometer with samples sealed in 0.1mm gas tight NaCl cells. Solid state infrared spectra were recorded with samples embedded in KBr pellets. All glassware was thoroughly dried in an oven at 90 °C for at least 12 hours prior to use. 2-Isocyano-1,3-diethoxycarbonylazulene ( $\text{CN}^2\text{CO}_2\text{Et}^{1,3}\text{Az}$ ),<sup>13</sup> 1-isocyanoazulene ( $\text{CN}^1\text{Az}$ ),<sup>14</sup> isocyanoferrocene ( $\text{CNFc}$ ),<sup>15</sup> 2,6-diisocyano-1,3-diethoxycarbonylazulene ( $\text{CN}^2\text{AzNC}^6$ ),<sup>11b</sup>  $[\text{W}(\text{N}_2)_2(\text{dppe})_2]$ ,<sup>4</sup>  $[\text{Mo}(\text{N}_2)_2(\text{dppe})_2]$ ,<sup>4</sup> and  $[\text{Mo}(\text{CO})(\text{N}_2)(\text{dppe})_2]$ ,<sup>8</sup> were prepared according to literature procedures.

### III.4.2 Synthesis of *trans*- $[\text{W}(\text{dppe})_2(\text{CN}^2\text{CO}_2\text{Et}^{1,3}\text{Az})_2]$ (III.1)

A 250 mL single armed round bottom flask (SARB) was charged with  $[\text{W}(\text{dppe})_2(\text{N}_2)_2]$  (0.220 g, 0.212 mmol) and 2-isocyano-1,3-diethoxycarbonylazulene (0.132 g, 0.444 mmol). This mixture was dissolved in 25 mL of THF and then heated to reflux with stirring for 18 hours. When the contents of the reaction flask had cooled to room temperature, the resulting dark solution was

carefully layered with 100 mL of pentane. Upon solvent diffusion, dark green microcrystals formed. These microcrystals were isolated from the mother liquor by filtration and dried under vacuum ( $10^{-2}$  torr) for 12 hours to afford **III.1** (0.2095 g, 0.134 mmol) in a 63% yield. IR (THF):  $\nu_{\text{CN}}$  1803  $\text{cm}^{-1}$ .

#### **III.4.3 Synthesis of *trans*-[W(dppe)<sub>2</sub>(CN<sup>1</sup>Az)<sub>2</sub>] (III.2)**

A solution of 1-isocyanoazulene (0.052 g, 0.339 mmol) in 25 mL of THF was carefully transferred to a 100 mL SARB charged with [W(dppe)<sub>2</sub>(N<sub>2</sub>)<sub>2</sub>] (0.150 g, 0.145 mmol). After the transfer was complete, the resulting mixture was heated to reflux with stirring for 18 hours. When the contents of the flask had cooled to room temperature, 50 mL of pentane was transferred into the reaction flask to form a dark purple precipitate. This solid was filtered off and dried under vacuum at  $10^{-2}$  torr for 12 hours to afford **III.2** (0.1489 g, 0.116 mmol) in an 80% yield. IR (THF)  $\nu_{\text{CN}}$  1861  $\text{cm}^{-1}$ .

#### **III.4.4 Synthesis of [W(dppe)<sub>2</sub>(CNFc)<sub>2</sub>] (III.3)**

A solution of [W(dppe)<sub>2</sub>(N<sub>2</sub>)<sub>2</sub>] (0.0943 g, 0.091 mmol) in 25 mL of THF was transferred to a 100 mL SARB charged with isocyanoferrrocene (0.040 g, 0.190 mmol). After the transfer was complete, the solution was heated to reflux for 18 hours. The reaction mixture was then cooled to room temperature, concentrated to a volume of approximately 10 mL, and carefully layered with 50 mL of pentane. Following solvent diffusion, red brick-like crystals formed. These crystals were filtered off and then dried under vacuum at  $10^{-2}$  torr to afford **III.3** (0.0664 g, 0.047 mmol) in a 52% yield. IR (THF):  $\nu_{\text{CN}}$  1884  $\text{cm}^{-1}$ .

#### III.4.5 Synthesis of $[\text{Mo}(\text{CO})(\text{dppe})_2(\text{CN}^2\text{CO}_2\text{Et}^{1,3}\text{Az})]$ (III.4)

A solution prepared by dissolving  $[\text{Mo}(\text{CO})(\text{DMF})(\text{dppe})_2]$  (0.400 g, 0.422 mmol) and 2-isocyano-1,3-diethoxycarbonylazulene (0.1256 g, 0.422 mmol) in 50 mL of THF was refluxed for 6 hours. After being cooled to room temperature, the mixture was concentrated under vacuum to a volume of approximately 10 mL. Then 50 mL of pentane was transferred to the reaction flask to form a precipitate. This solid was filtered off and dried under vacuum at  $10^{-2}$  torr to afford III.4 (0.155 g, 0.126 mmol) in a 30% yield. IR (THF):  $\nu_{\text{CN}}$  1949,  $\nu_{\text{CO}}$  1832  $\text{cm}^{-1}$ .

#### III.4.6 Synthesis of $[\text{Mo}(\text{CO})(\text{dppe})_2(\text{CN}^2\text{AzNC}^6)\text{Mo}(\text{CO})(\text{dppe})_2]$ (III.5)

A solution prepared by dissolving  $[\text{Mo}(\text{CO})(\text{N}_2)(\text{dppe})_2]$  (0.300 g, 0.333 mmol) and 2,6-diisocyano-1,3-diethoxycarbonylazulene (0.0536 g, 0.166 mmol) in 30 mL of THF was refluxed for 4 hours. After being cooled to room temperature, the mixture was concentrated under vacuum to a volume of approximately 10 mL. Addition of 50 mL of pentane afforded a precipitate, which was filtered off, washed with a small amount of benzene, and dried under vacuum at  $10^{-2}$  torr to give III.5 (0.288 g, 0.139 mmol) in an 83% yield. IR (THF):  $\nu_{\text{CN}}$  1971, 1954,  $\nu_{\text{CO}}$  1825, 1802  $\text{cm}^{-1}$ .

### III.5 Results and Discussion

The goal of this investigation was to determine if *trans*-[M(CNR)<sub>2</sub>(dppe)<sub>2</sub>] complexes would form upon the displacement of dinitrogen by non-benzenoid aromatic isocyanides. This determination would indicate whether such nonbenzenoid isocyanides could be utilized as organic linkers in the construction of 1-D materials featuring either the W or Mo M(dppe)<sub>2</sub> motifs. In general, the complexes described in this chapter were found to be extremely air and moisture sensitive. Upon exposure to air, solutions containing these complexes quickly darkened and eventually turned black. After their isolation, these complexes were virtually insoluble in any non-halogenated solvents. Even though they initially dissolved in halogenated solvents, such as CD<sub>2</sub>Cl<sub>2</sub> and CDCl<sub>3</sub>, rapid decomposition and precipitation prevented acquisition of useful NMR data. The complexes that were synthesized in this investigation are shown in Figure III.2.



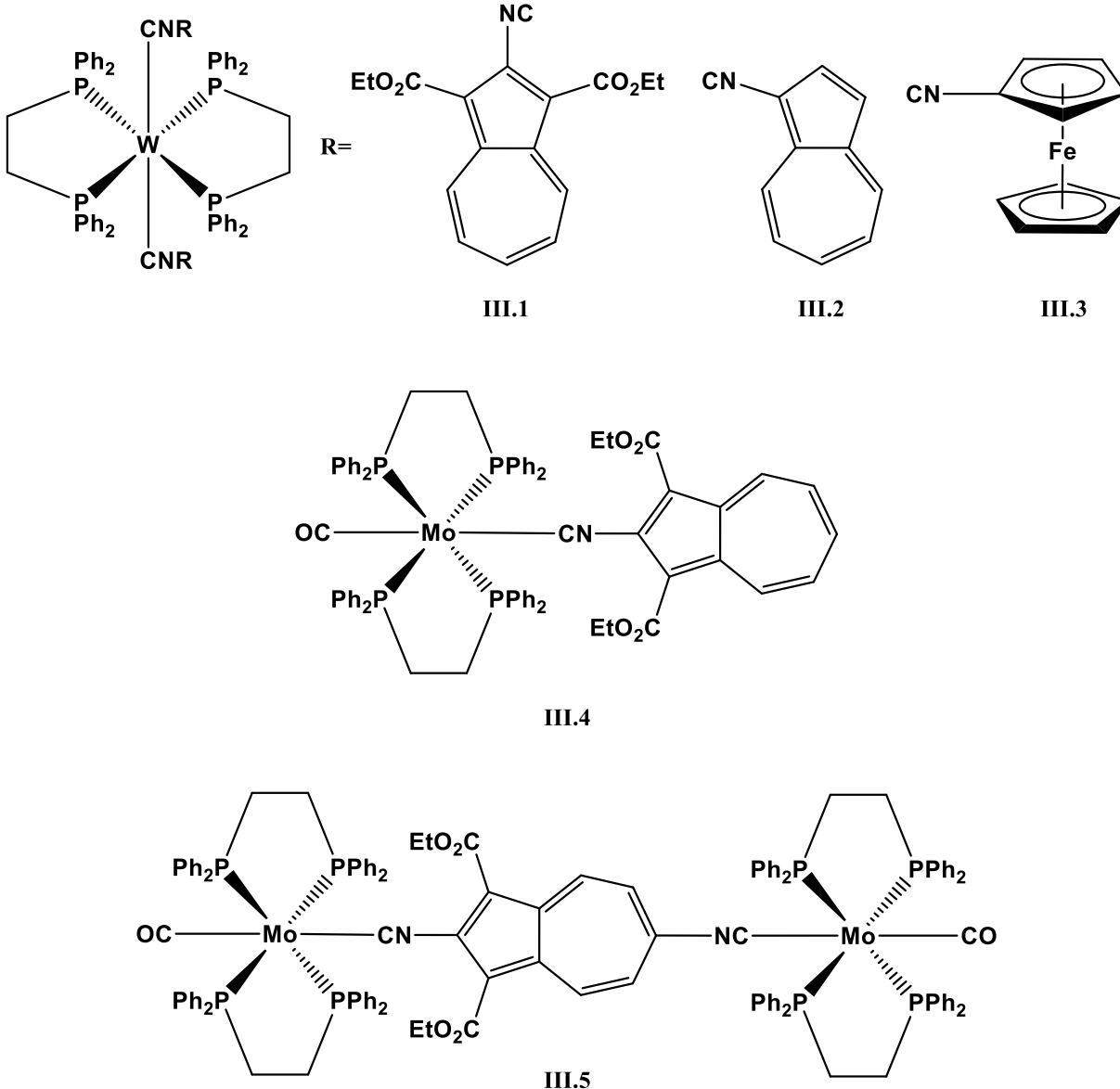


**Figure III.2** Structures of the complexes that were prepared in this investigation.

According to the arguments of Bennett *et al.* there is a fine balance between electronic stabilization and steric repulsion that dictates whether these complexes will form in a cis or trans configuration.<sup>16</sup> Since the isocyano ligands in complexes **III.1**, **III.2**, and **III.3** are relatively bulky compared to the benzenoid isocyanides used by Bennett, the additional steric repulsion should impede the formation of complexes in a cis configuration. The formation of the

complexes described in the experimental section could be conveniently monitored by FTIR as there was a significant shift in the  $\nu_{\text{CN}}$  stretching bands between the free and coordinated isocyanides.

The two possible configurations of these complexes have an idealized local symmetry of  $D_{4h}$  or  $C_{2v}$  (Figure III.3)<sup>16</sup> Octahedral complexes  $\text{ML}_4(\text{CNR})_2$  in the trans configuration should only exhibit one  $\nu_{\text{CN}}$  band since only the asymmetric  $A_{2u}$  stretching mode is IR active, while those in the cis configuration would be expected to have two bands since both the symmetric  $A_1$  and asymmetric  $B_1$  stretching modes are IR active.

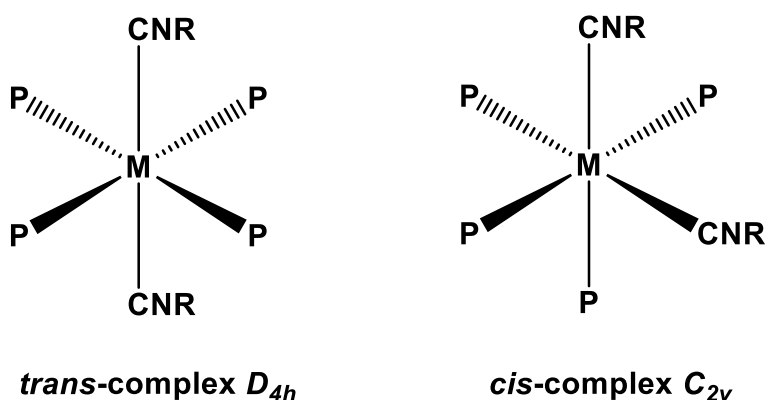


**Figure III.3** Local symmetry around the metal center in bis-isocyano octahedral coordination complexes.

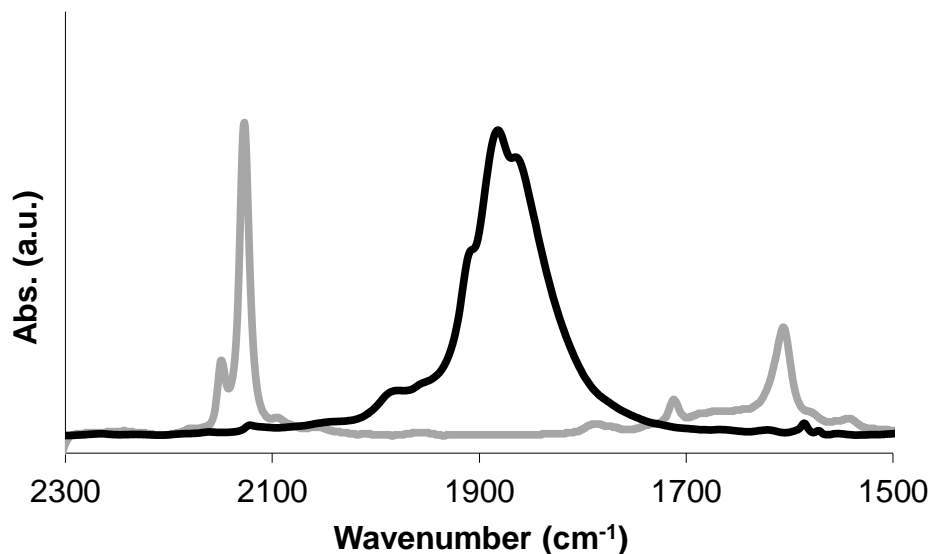
Analysis of the FTIR spectra of complexes **III.1**, **III.2**, and **III.3** was indicative that they had adopted a trans configuration. For complexes **III.1** and **III.2** this determination was unambiguous as only a  $\nu_{\text{CN}}$  band was observed. Table III.2 compares the  $\nu_{\text{CN}}$  stretches of the free and bound isocyanides. The substantial shift to lower energy in the  $\nu_{\text{CN}}$  bands of the bound isocyanides in these complexes suggest substantial back bonding is occurring.

**Table III.2** FTIR  $\nu_{\text{CN}}$  stretches of free and bound isocyanides

Complex	$\nu_{\text{CN}}$ $\text{cm}^{-1}$ of free ligand	$\nu_{\text{CN}}$ $\text{cm}^{-1}$ of bound ligand
<b>III.1</b>	2130	1803
<b>III.2</b>	2118	1861
<b>III.3</b>	2127	1884

FTIR solution (THF)

Of the three complexes the configuration of **III.3** is the most difficult to definitively determine by only an FTIR analysis. The intense  $\nu_{\text{CN}}$  stretch at  $1884\text{ cm}^{-1}$  is accompanied by two shoulders at  $1913$  and  $1874\text{ cm}^{-1}$  (Figure III.4). The presence of these shoulders may be due to deviations from the idealized  $D_{4h}$  symmetry of the complex caused by steric bulk of the isocyanoferrrocene ligands. Additionally, all of the aryl isocyanides that formed *cis*- $[\text{W}(\text{CNR})_2(\text{dppe})_2]$  complexes displayed two distinct  $\nu_{\text{CN}}$  bands at a much lower energy which were separated by a minimum of  $80\text{ cm}^{-1}$  (Table III.1).<sup>16</sup>

**Figure III.4** FTIR spectra of **III.3** (black) and free ligand (grey) in THF.

After establishing that complexes **III.1**, **III.2**, and **III.3** did form in a *trans* configuration, the focus of the study was shifted to controlling the complexation so only one isocyanide would bind to each metal center. Several attempts to form these  $[\text{W}(\text{CNR})(\text{N}_2)(\text{dppe})_2]$  complexes by the combination of  $[\text{W}(\text{N}_2)_2(\text{dppe})_2]$  and the isocyano ligand in a 1 to 1 molar ratio were unsuccessful. When analyzing the FTIR spectrum it appeared that these reactions were producing a mixture of the starting metal complex and  $[\text{W}(\text{CNR})_2(\text{dppe})_2]$ .

Since the preparation of  $[\text{Mo}(\text{CO})(\text{N}_2)(\text{dppe})_2]$  was previously described by Hidai *et al.*<sup>11</sup> this complex was chosen as a starting point for the controlled complexation of one isocyano ligand. Treatment of  $[\text{Mo}(\text{CO})(\text{N}_2)(\text{dppe})_2]$  with one molar equiv. of 2-isocyano-1,3-diethoxycarbonylazulene generated complex **III.4**. Treatment of  $[\text{Mo}(\text{CO})(\text{N}_2)(\text{dppe})_2]$  with 0.5 molar equiv. of 2,6-diisocyano-1,3-diethoxycarbonylazulene resulted in the formation of **III.5**. The configuration of these complexes cannot be unambiguously determined by the analysis of their IR spectra. The  $\nu_{\text{CN}}$  and  $\nu_{\text{CO}}$  stretches of these complexes are listed in Table III.3. While the  $^{31}\text{P}$  NMR analysis would have allowed the determination of the configuration of these complexes, their poor solubility prevented acquisition of such data. It should be noted that other similar complexes featuring aryl and alkyl isocyanide ligands do have a *trans* configuration, at least in the solid state.<sup>13</sup>

**Table III.3** FTIR  $\nu_{\text{CN}}$  and  $\nu_{\text{CO}}$  stretches of complexes **III.4** and **III.5**

Complex	$\nu_{\text{CN}} \text{ cm}^{-1}$	$\nu_{\text{CO}} \text{ cm}^{-1}$
<b>III.4</b>	1949	1832
<b>III.5</b>	1971, 1954	1825, 1802
Solution FTIR (THF)		

### III.6 Conclusions and Outlook

The formation of complexes III.1, III.2, and III.3 was accomplished. Their adoption of a trans configuration in the  $[\text{W}(\text{CNR})_2(\text{dpppe})_2]$  complexes demonstrates that related non-benzenoid aromatic isocyanides shown in Figure III.5 might be suitable for the construction of 1-D organometallic materials featuring either an electron rich W or Mo  $\text{M}(\text{dppe})_2$  motif.

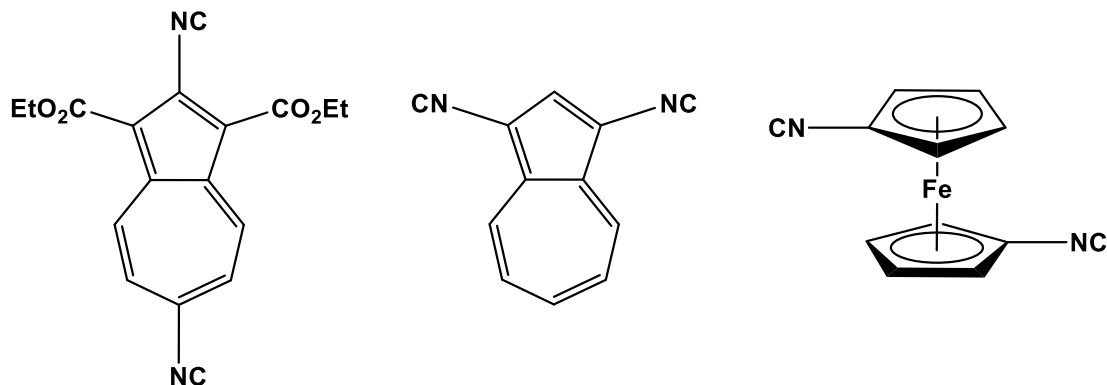


**Figure III.5** Diisocyanoarenes that may be suitable for the construction of 1-D organometallic materials

The formation of complexes III.4 and III.5 demonstrated that a single isocyanide ligand could be selectively installed. These complexes might serve as starting materials for the construction of 1-D materials if a suitable method is found for the displacement of the CO ligand. Since the formation of  $[\text{Mo}(\text{CNR})(\text{N}_2)(\text{dppe})_2]$  occurs from reaction of immines with  $[\text{Mo}(\text{N}_2)_2(\text{dppe})_2]$  (Scheme III.3) and the remaining dinitrogen ligand is readily displaced these complexes are also appealing for the controlled construction of 1-D materials.<sup>12,13</sup>

### III.7 References

---

- (1) Hidai, M.; Mizobe, Y. *Chemical Reviews*, **1995**, 95, 1115-1133.
- (2) Chatt, J.; Pombeiro, A. J. L.; Richards, R. L.; Royston, G. H. D. *Journal of the Chemical Society-Chemical Communications*, **1975**, 17, 708-709.
- (3) Hidai, M.; Tominari, K.; Uchida, Y.; Misono, A. *Journal of the Chemical Society D-Chemical Communications*, **1969**, 1392.
- (4) Dilworth, J. R.; Richards, R. L. *Inorganic Synthesis*, **1980**, 119.
- (5) Field, L. D.; Jones, N. G. Turner, P. *Journal of Organometallic Chemistry*, **1998**, 571, 195-199.
- (6) Nishibayashi, Y.; Wakiji, I.; Hirata, K.; Dubois, M. R.; Hidai, M. *Inorganic Chemistry*, **2001**, 40, 578-580
- (7) Cunha, S.; Guedes da Silva, M.; Pobeiro, A. J. L. *Inorganic Chemistry*, **2003**, 42, 2157-2164.
- (8) Eguillor, B.; Caldwell, P. J.; Cockett, M. C. R.; Duckett, S. B. John, R. O. Lynam, J. M.; Sleigh, C. J.; Wilson, I. *Journal of the American Chemical Society*, **2012**, 134, 18257-18265.
- (9) Hidai, M.; Kodama, T.; Sato, M.; Harakawa, M.; Uchida, Y. *Inorganic Chemistry*, **1976**, 15, 2694-2697
- (10) Ishida, T.; Mizobe, Y.; Tanase, T.; Hidai, M. *Chemistry Letters*, **1988**, 441-444.
- (11) Sato, M.; Tatsumi, T. Kodama, T.; Hidai, M.; Uchida, T.; Uchida Y. *Journal of the American Chemical Society*, **1978**, 100, 4447-4452.
- (12) Nakamura, G.; Harada, Y.; Arita, C.; Seino, H.; Mizobe, Y.; Hidai, M. *Organometallics*, **1998**, 17, 1010-1012.
- (13) Seino, H.; Arita, C.; Nonokawa, D.; Nakaumura, G.; Harada, Y.; Mizobe, Y.; Hidai M. *Organometallics*, **1999**, 18, 4165-4173
- (14) Barybin, M. V.; Meyers, J. J., Jr.; Neal, B. M. Renaissance of Isocyanoarenes as Ligands in Low-Valent Organometallic Chemistry. In *Isocyanide Chemistry: Applications in Synthesis and Material Science*. Nenajdenko, V., Ed. Wiley-VCH: Weinheim, **2012**, pp 493-529.
- (15) Chatt, J.; Elson C. M.; Pombeiro, A. L. J.; Richards, R. L.; Royston, G. H. D. *Journal of*

---

*the Chemical Society-Dalton Transactions*, **1978**, 2, 165-169.

- (16) Wagner, N. L.; Laib, F. E.; Bennett, D. W. *Journal of the American Chemistry Society*, **2000**, 122, 10856-10867.
- (17) Launy, J-P. *Coordination Chemistry Reviews*, **2013**, 257, 1544-1554.
- (18) a) Barybin, M. V.; Holovics, T. C.; Deplazes, S. F.; Lushington, G. H.; Powell, D. R.; Toriyama, M. *Journal of the American Chemical Society*, **2002**, 124, 13668-13669. b) Robinson, R. E.; Holovics, T. C.; Deplazes, S. F.; Powell, D. R.; Lushington, G. H.; Thompson, W. H.; Barybin, M. V. *Organometallics*, **2005**, 24, 2386-2397. c) Dubose, D. L.; Robinson, R. E.; Holovics, T. C.; Moody, D. R.; Weintrob, E. C.; Berrie, C. L.; Barybin, M. V. *Langmuir*, **2006**, 22, 4599-4606. d) Robinson, R. E.; Holovics, T. C.; Deplazes, S. F.; Lushington, G. H.; Powell, D. R.; Barybin, M. V. *Journal of the American Chemical Society*, **2003**, 125, 4432-4433.
- (19) Holovics, T. C.; Robinson, R. E.; Weintrop, E. C.; Toriyama, M.; Lushington, G. H.; Barybin, M. V. *Journal of the American Chemical Society*, **2006**, 128, 2300-2309.

## **Appendix 1**

### **Crystallographic Data for Compound I.1**



**Table 1.** Crystal data and structure refinement for **I.1**.

Empirical formula	$\text{C}_{16}\text{H}_{14}\text{Cl}_2\text{O}_4$	
Formula weight	341.17	
Crystal system	triclinic	
Space group	$P\bar{1}$	
Unit cell dimensions	$a = 3.9099(11) \text{ \AA}$	$\alpha = 82.606(5)^\circ$
	$b = 13.413(4) \text{ \AA}$	$\beta = 86.888(6)^\circ$
	$c = 14.207(4) \text{ \AA}$	$\gamma = 82.453(6)^\circ$
Volume	$731.9(4) \text{ \AA}^3$	
Z, Z'	2, 1	
Density (calculated)	$1.548 \text{ Mg/m}^3$	
Wavelength	$0.71073 \text{ \AA}$	
Temperature	$100(2) \text{ K}$	
$F(000)$	352	
Crystal size	$0.46 \times 0.18 \times 0.07 \text{ mm}^3$	
Absorption coefficient	$0.459 \text{ mm}^{-1}$	
Absorption correction	Semi-empirical	
Max. and min. transmission	0.9686 and 0.8167	
Theta range for data collection	$1.54$ to $25.25^\circ$	
Reflections collected	7409	
Independent reflections	2654 [ $R(\text{int}) = 0.0499$ ]	
Data / restraints / parameters	2654 / 0 / 201	
	101	

$wR(F^2 \text{ all data})$	$wR2 = 0.1876$
$R(F \text{ obsd data})$	$R1 = 0.0700$
Goodness-of-fit on $F^2$	1.017
Observed data [ $I > 2\sigma(I)$ ]	1994
Largest and mean shift / s.u.	0.000 and 0.000
Largest diff. peak and hole	2.253 and -0.309 e/Å <sup>3</sup>

---


$$R_1 = \Sigma ||F_O| - |F_C|| / \Sigma |F_O|$$

$$wR_2 = \{ \Sigma [w(F_O^2 - F_C^2)^2] / \Sigma [w(F_O^2)^2] \}^{1/2}$$

**Table 2.** Atomic coordinates and equivalent isotropic displacement parameters for **I.1**.  
 $U(\text{eq})$  is defined as one third of the trace of the orthogonalized  $U_{ij}$  tensor.

	x	y	z	$U(\text{eq})$
Cl(1)	0.9917(3)	0.15437(7)	0.34224(7)	0.0186(3)
Cl(2)	0.0842(3)	0.77431(8)	0.17220(7)	0.0218(3)
O(1)	0.2612(8)	0.3645(2)	0.5094(2)	0.0276(8)
O(2)	0.5872(7)	0.2155(2)	0.50316(19)	0.0182(7)
O(3)	1.0970(8)	0.3471(2)	0.0581(2)	0.0253(8)
O(4)	1.2189(7)	0.2006(2)	0.15037(19)	0.0177(7)
C(1)	0.5927(11)	0.3373(3)	0.3672(3)	0.0141(9)
C(2)	0.8106(11)	0.2761(3)	0.3073(3)	0.0169(9)
C(3)	0.8582(11)	0.3307(3)	0.2163(3)	0.0159(9)
C(4)	0.6400(10)	0.5042(3)	0.1409(3)	0.0152(9)
C(5)	0.4595(11)	0.6022(3)	0.1353(3)	0.0184(9)
C(6)	0.2636(11)	0.6481(3)	0.2051(3)	0.0176(9)
C(7)	0.1856(11)	0.6100(3)	0.2979(3)	0.0169(9)
C(8)	0.2900(10)	0.5136(3)	0.3455(3)	0.0148(9)
C(9)	0.5005(10)	0.4320(3)	0.3123(3)	0.0135(9)
C(10)	0.6667(10)	0.4280(3)	0.2173(3)	0.0139(9)
C(11)	0.4649(11)	0.3103(3)	0.4641(3)	0.0153(9)
C(12)	0.4416(11)	0.1829(3)	0.5944(3)	0.0163(9)
C(13)	0.5748(11)	0.0729(3)	0.6202(3)	0.0216(10)
C(14)	1.0635(11)	0.2969(3)	0.1342(3)	0.0166(9)

C(15)	1.4241(11)	0.1627(3)	0.0722(3)	0.0165(9)
C(16)	1.5966(11)	0.0584(3)	0.1078(3)	0.0182(9)

---

**Table 3.** Bond lengths [Å] for **I.1**.

---

Cl(1)-C(2)	1.714(4)	C(6)-C(7)	1.385(6)
Cl(2)-C(6)	1.759(4)	C(7)-C(8)	1.401(6)
O(1)-C(11)	1.220(5)	C(7)-H(7)	0.9500
O(2)-C(11)	1.356(5)	C(8)-C(9)	1.397(6)
O(2)-C(12)	1.426(5)	C(8)-H(8)	0.9500
O(3)-C(14)	1.208(5)	C(9)-C(10)	1.470(6)
O(4)-C(14)	1.351(5)	C(12)-C(13)	1.504(5)
O(4)-C(15)	1.441(5)	C(12)-H(12A)	0.9900
C(1)-C(9)	1.417(5)	C(12)-H(12B)	0.9900
C(1)-C(2)	1.429(6)	C(13)-H(13A)	0.9800
C(1)-C(11)	1.457(6)	C(13)-H(13B)	0.9800
C(2)-C(3)	1.417(6)	C(13)-H(13C)	0.9800
C(3)-C(10)	1.419(6)	C(15)-C(16)	1.508(5)
C(3)-C(14)	1.466(6)	C(15)-H(15A)	0.9900
C(4)-C(10)	1.390(5)	C(15)-H(15B)	0.9900
C(4)-C(5)	1.403(6)	C(16)-H(16A)	0.9800
C(4)-H(4)	0.9500	C(16)-H(16B)	0.9800
C(5)-C(6)	1.379(6)	C(16)-H(16C)	0.9800
C(5)-H(5)	0.9500		

---

**Table 4.** Bond angles [°] for **I.1**.

C(11)-O(2)-C(12)	115.9(3)	C(8)-C(7)-H(7)	115.7
C(14)-O(4)-C(15)	116.1(3)	C(9)-C(8)-C(7)	129.2(4)
C(9)-C(1)-C(2)	106.7(4)	C(9)-C(8)-H(8)	115.4
C(9)-C(1)-C(11)	124.4(4)	C(7)-C(8)-H(8)	115.4
C(2)-C(1)-C(11)	128.8(4)	C(8)-C(9)-C(1)	124.5(4)
C(3)-C(2)-C(1)	110.4(4)	C(8)-C(9)-C(10)	127.4(3)
C(3)-C(2)-Cl(1)	125.3(3)	C(1)-C(9)-C(10)	108.0(3)
C(1)-C(2)-Cl(1)	124.3(3)	C(4)-C(10)-C(3)	125.4(4)
C(2)-C(3)-C(10)	107.2(4)	C(4)-C(10)-C(9)	127.0(4)
C(2)-C(3)-C(14)	128.4(4)	C(3)-C(10)-C(9)	107.6(3)
C(10)-C(3)-C(14)	124.4(4)	O(1)-C(11)-O(2)	120.1(4)
C(10)-C(4)-C(5)	129.5(4)	O(1)-C(11)-C(1)	125.5(4)
C(10)-C(4)-H(4)	115.3	O(2)-C(11)-C(1)	114.4(4)
C(5)-C(4)-H(4)	115.3	O(2)-C(12)-C(13)	108.0(3)
C(6)-C(5)-C(4)	128.7(4)	O(2)-C(12)-H(12A)	110.1
C(6)-C(5)-H(5)	115.7	C(13)-C(12)-H(12A)	110.1
C(4)-C(5)-H(5)	115.7	O(2)-C(12)-H(12B)	110.1
C(5)-C(6)-C(7)	129.7(4)	C(13)-C(12)-H(12B)	110.1
C(5)-C(6)-Cl(2)	115.7(3)	H(12A)-C(12)-H(12B)	108.4
C(7)-C(6)-Cl(2)	114.6(3)	C(12)-C(13)-H(13A)	109.5
C(6)-C(7)-C(8)	128.5(4)	C(12)-C(13)-H(13B)	109.5
C(6)-C(7)-H(7)	115.7	H(13A)-C(13)-H(13B)	109.5

C(12)-C(13)-H(13C)	109.5
H(13A)-C(13)-H(13C)	109.5
H(13B)-C(13)-H(13C)	109.5
O(3)-C(14)-O(4)	121.0(4)
O(3)-C(14)-C(3)	125.6(4)
O(4)-C(14)-C(3)	113.4(3)
O(4)-C(15)-C(16)	107.3(3)
O(4)-C(15)-H(15A)	110.2
C(16)-C(15)-H(15A)	110.2
O(4)-C(15)-H(15B)	110.2
C(16)-C(15)-H(15B)	110.2
H(15A)-C(15)-H(15B)	108.5
C(15)-C(16)-H(16A)	109.5
C(15)-C(16)-H(16B)	109.5
H(16A)-C(16)-H(16B)	109.5
C(15)-C(16)-H(16C)	109.5
H(16A)-C(16)-H(16C)	109.5
H(16B)-C(16)-H(16C)	109.5

**Table 5.** Anisotropic displacement parameters ( $\text{\AA}^2 \times 10^3$ ) for **I.1**. The anisotropic displacement factor exponent takes the form:  $-2\pi^2 [h^2 a^{*2} U_{11} + \dots + 2 h k a^* b^* U_{12}]$ .

	$U_{11}$	$U_{22}$	$U_{33}$	$U_{23}$	$U_{13}$	$U_{12}$
Cl(1)	24(1)	12(1)	18(1)	1(1)	3(1)	3(1)
Cl(2)	28(1)	14(1)	21(1)	2(1)	-1(1)	3(1)
O(1)	40(2)	14(2)	25(2)	3(1)	2(2)	7(1)
O(2)	22(2)	12(2)	17(2)	3(1)	4(1)	2(1)
O(3)	32(2)	21(2)	19(2)	2(1)	6(1)	4(1)
O(4)	19(2)	14(2)	18(2)	-3(1)	4(1)	5(1)
C(1)	16(2)	13(2)	14(2)	-3(2)	-1(2)	-3(2)
C(2)	16(2)	22(2)	14(2)	-5(2)	0(2)	-6(2)
C(3)	14(2)	16(2)	19(2)	-7(2)	-2(2)	-1(2)
C(4)	15(2)	20(2)	12(2)	-3(2)	1(2)	-6(2)
C(5)	18(2)	20(2)	16(2)	1(2)	0(2)	-1(2)
C(6)	17(2)	13(2)	22(2)	1(2)	-4(2)	0(2)
C(7)	17(2)	20(2)	14(2)	-3(2)	0(2)	-3(2)
C(8)	16(2)	16(2)	13(2)	-4(2)	1(2)	-6(2)
C(9)	15(2)	14(2)	13(2)	-3(2)	-1(2)	-3(2)
C(10)	12(2)	14(2)	16(2)	-2(2)	1(2)	-1(2)
C(11)	18(2)	11(2)	17(2)	-2(2)	-4(2)	1(2)
C(12)	18(2)	13(2)	17(2)	3(2)	-2(2)	-4(2)
C(13)	22(2)	13(2)	27(2)	4(2)	-1(2)	2(2)



C(14)	17(2)	15(2)	18(2)	-1(2)	-2(2)	-1(2)
C(15)	15(2)	18(2)	15(2)	-2(2)	3(2)	2(2)
C(16)	16(2)	19(2)	18(2)	-4(2)	-1(2)	3(2)

---

**Table 6.** Hydrogen coordinates ( $\times 10^4$ ) and isotropic displacement parameters ( $\text{\AA}^2 \times 10^3$ ) for **I.1**.

	x	y	z	U(eq)
H(4)	0.7617	0.4875	0.0842	0.018
H(5)	0.4743	0.6423	0.0753	0.022
H(7)	0.0425	0.6551	0.3340	0.020
H(8)	0.2056	0.5021	0.4095	0.018
H(12A)	0.1866	0.1917	0.5927	0.020
H(12B)	0.5089	0.2236	0.6421	0.020
H(13A)	0.4940	0.0327	0.5750	0.032
H(13B)	0.4895	0.0499	0.6845	0.032
H(13C)	0.8278	0.0645	0.6181	0.032
H(15A)	1.5999	0.2080	0.0497	0.020
H(15B)	1.2757	0.1592	0.0188	0.020
H(16A)	1.7330	0.0623	0.1627	0.027
H(16B)	1.7486	0.0318	0.0572	0.027
H(16C)	1.4203	0.0133	0.1265	0.027

## **Appendix 2**

### **Crystallographic Data for Compound 1.6**

**Table 1.** Crystal data and structure refinement for **I.6**.

---

Empirical formula	$\text{C}_{34}\text{H}_{30}\text{AuO}_4\text{PS}_2$	
Formula weight	794.64	
Crystal system	Orthorhombic	
Space group	$Pca2_1$	
Unit cell dimensions	$a = 23.574(2) \text{ \AA}$	$\alpha = 90^\circ$
	$b = 11.1504(10) \text{ \AA}$	$\beta = 90^\circ$
	$c = 23.342(2) \text{ \AA}$	$\gamma = 90^\circ$
Volume	$6135.7(9) \text{ \AA}^3$	
Z, Z'	8, 2	
Density (calculated)	$1.720 \text{ Mg/m}^3$	
Wavelength	$0.71073 \text{ \AA}$	
Temperature	$100(2) \text{ K}$	
$F(000)$	3136	
Crystal size	$0.32 \times 0.30 \times 0.12 \text{ mm}^3$	
Absorption coefficient	$5.022 \text{ mm}^{-1}$	
Absorption correction	Semi-empirical from equivalents	
Max. and min. transmission	0.5840 and 0.2964	
Theta range for data collection	$1.73$ to $25.50^\circ$	
Reflections collected	37712	
Independent reflections	10050 [ $R(\text{int}) = 0.0404$ ]	
Data / restraints / parameters	10050 / 1 / 768	

$wR(F^2 \text{ all data})$	$wR2 = 0.0721$
$R(F \text{ obsd data})$	$R1 = 0.0294$
Goodness-of-fit on $F^2$	0.998
Observed data [ $I > 2\sigma(I)$ ]	9157
Absolute structure parameter	0.240(6)
Largest and mean shift / s.u.	0.030 and 0.001
Largest diff. peak and hole	1.203 and -0.548 e/Å <sup>3</sup>

---


$$R_1 = \Sigma ||F_O| - |F_C|| / \Sigma |F_O|$$

$$wR_2 = \{ \Sigma [w(F_O^2 - F_C^2)^2] / \Sigma [w(F_O^2)^2] \}^{1/2}$$

**Table 2.** Atomic coordinates and equivalent isotropic displacement parameters for **I.6**. U(eq) is defined as one third of the trace of the orthogonalized  $U_{ij}$  tensor.

	x	y	z	U(eq)
Au(1A)	0.511393(8)	0.22633(2)	0.546817(10)	0.01557(7)
S(1A)	0.75786(7)	0.91000(17)	0.47579(10)	0.0251(4)
S(2A)	0.55849(7)	0.24323(15)	0.45997(8)	0.0179(4)
P(1A)	0.46345(7)	0.21203(15)	0.63066(9)	0.0149(4)
O(1A)	0.74025(19)	0.8309(4)	0.5987(2)	0.0236(11)
O(2A)	0.69756(19)	0.6607(4)	0.6216(2)	0.0232(11)
O(3A)	0.7198(2)	0.6713(5)	0.3262(2)	0.0332(13)
O(4A)	0.7378(2)	0.8551(4)	0.3603(2)	0.0265(12)
C(1A)	0.7030(3)	0.7079(6)	0.5239(3)	0.0156(16)
C(2A)	0.7206(3)	0.7738(6)	0.4760(3)	0.0190(16)
C(3A)	0.7044(3)	0.7116(7)	0.4256(3)	0.0209(17)
C(4A)	0.6498(3)	0.5259(6)	0.4043(3)	0.0191(16)
C(5A)	0.6172(3)	0.4266(6)	0.4150(3)	0.0194(16)
C(6A)	0.6004(3)	0.3744(6)	0.4672(3)	0.0168(15)
C(7A)	0.6166(3)	0.4156(6)	0.5209(3)	0.0195(16)
C(8A)	0.6473(2)	0.5144(5)	0.5360(3)	0.0178(14)
C(9A)	0.6731(3)	0.6044(6)	0.5035(3)	0.0179(15)
C(10A)	0.6737(3)	0.6077(6)	0.4417(3)	0.0184(16)
C(11A)	0.7158(3)	0.7405(7)	0.5823(4)	0.0223(19)
C(12A)	0.7105(3)	0.6860(7)	0.6821(3)	0.0246(18)

C(13A)	0.6874(3)	0.5826(6)	0.7165(3)	0.0248(17)
C(14A)	0.7205(3)	0.7417(6)	0.3660(3)	0.0235(17)
C(15A)	0.7605(3)	0.8880(8)	0.3049(3)	0.032(2)
C(16A)	0.7148(3)	0.9092(8)	0.2614(4)	0.037(2)
C(17A)	0.5108(2)	0.2192(6)	0.6929(4)	0.0181(18)
C(18A)	0.5569(3)	0.2974(6)	0.6900(3)	0.0191(15)
C(19A)	0.5915(3)	0.3127(7)	0.7369(3)	0.0224(16)
C(20A)	0.5812(3)	0.2497(7)	0.7857(4)	0.0271(17)
C(21A)	0.5366(3)	0.1711(7)	0.7885(4)	0.0293(18)
C(22A)	0.5005(3)	0.1564(8)	0.7427(4)	0.029(2)
C(23A)	0.4122(3)	0.3328(6)	0.6416(3)	0.0177(16)
C(24A)	0.3953(3)	0.4033(7)	0.5964(3)	0.0263(17)
C(25A)	0.3553(3)	0.4929(8)	0.6054(4)	0.035(2)
C(26A)	0.3331(3)	0.5116(7)	0.6590(3)	0.0233(17)
C(27A)	0.3496(3)	0.4428(7)	0.7045(4)	0.0263(18)
C(28A)	0.3896(3)	0.3530(6)	0.6966(3)	0.0208(15)
C(29A)	0.4230(3)	0.0748(6)	0.6387(3)	0.0152(16)
C(30A)	0.4504(3)	-0.0317(7)	0.6509(3)	0.0225(17)
C(31A)	0.4200(3)	-0.1379(7)	0.6550(3)	0.0227(17)
C(32A)	0.3619(3)	-0.1360(7)	0.6461(3)	0.0192(17)
C(33A)	0.3345(3)	-0.0315(6)	0.6334(3)	0.0186(15)
C(34A)	0.3644(2)	0.0747(6)	0.6298(3)	0.0161(15)
Au(1B)	0.257865(8)	0.72326(2)	0.539559(10)	0.01562(7)
S(1B)	0.01475(7)	1.40395(16)	0.62809(9)	0.0242(4)
S(2B)	0.21361(7)	0.73428(15)	0.62814(8)	0.0180(4)

P(1B)	0.30606(7)	0.71845(16)	0.45587(9)	0.0163(4)
O(1B)	0.02315(19)	1.3244(5)	0.5038(2)	0.0277(12)
O(2B)	0.07028(19)	1.1604(4)	0.4770(2)	0.0233(11)
O(3B)	0.0910(2)	1.1991(4)	0.7755(2)	0.0303(12)
O(4B)	0.0298(2)	1.3347(5)	0.7412(2)	0.0270(12)
C(1B)	0.0652(3)	1.1996(6)	0.5756(3)	0.0172(16)
C(2B)	0.0521(3)	1.2678(6)	0.6260(3)	0.0187(15)
C(3B)	0.0728(3)	1.2077(6)	0.6750(3)	0.0175(16)
C(4B)	0.1298(3)	1.0193(6)	0.6918(3)	0.0166(15)
C(5B)	0.1605(2)	0.9203(6)	0.6782(3)	0.0151(14)
C(6B)	0.1719(2)	0.8673(6)	0.6258(3)	0.0152(15)
C(7B)	0.1508(3)	0.9057(6)	0.5733(3)	0.0167(15)
C(8B)	0.1185(2)	1.0057(6)	0.5590(3)	0.0189(16)
C(9B)	0.0967(3)	1.0968(6)	0.5937(3)	0.0163(15)
C(10B)	0.1018(3)	1.1028(6)	0.6560(3)	0.0183(17)
C(11B)	0.0504(3)	1.2352(6)	0.5180(4)	0.0266(19)
C(12B)	0.0567(3)	1.1883(7)	0.4186(3)	0.0174(16)
C(13B)	0.0843(3)	1.0931(7)	0.3829(3)	0.0301(19)
C(14B)	0.0664(3)	1.2429(6)	0.7348(3)	0.0220(16)
C(15B)	0.0238(3)	1.3846(8)	0.7983(3)	0.029(2)
C(16B)	-0.0204(3)	1.4812(8)	0.7943(3)	0.033(2)
C(17B)	0.2607(2)	0.7276(6)	0.3932(4)	0.0165(17)
C(18B)	0.2127(3)	0.8015(6)	0.3957(3)	0.0206(16)
C(19B)	0.1786(3)	0.8156(7)	0.3488(3)	0.0237(17)
C(20B)	0.1904(3)	0.7560(7)	0.2985(3)	0.030(2)



C(21B)	0.2379(3)	0.6806(8)	0.2953(4)	0.034(2)
C(22B)	0.2722(3)	0.6668(7)	0.3431(3)	0.0224(16)
C(23B)	0.3553(3)	0.8438(6)	0.4489(3)	0.0146(16)
C(24B)	0.3921(3)	0.8679(6)	0.4941(3)	0.0220(16)
C(25B)	0.4326(3)	0.9586(6)	0.4891(3)	0.0222(16)
C(26B)	0.4335(3)	1.0265(7)	0.4419(3)	0.0240(18)
C(27B)	0.3959(3)	1.0072(7)	0.3959(4)	0.0248(17)
C(28B)	0.3579(3)	0.9141(6)	0.4004(3)	0.0221(16)
C(29B)	0.3485(3)	0.5842(6)	0.4458(3)	0.0165(15)
C(30B)	0.3214(3)	0.4730(7)	0.4441(4)	0.0241(18)
C(31B)	0.3518(3)	0.3694(7)	0.4368(4)	0.031(2)
C(32B)	0.4111(3)	0.3736(7)	0.4343(3)	0.0220(18)
C(33B)	0.4389(3)	0.4827(6)	0.4382(3)	0.0226(16)
C(34B)	0.4079(3)	0.5857(7)	0.4438(3)	0.0202(16)

---

**Table 3.** Bond lengths [Å] for **I.6**.

Au(1A)-P(1A)	2.2655(19)	C(5A)-C(6A)	1.408(10)
Au(1A)-S(2A)	2.3190(19)	C(5A)-H(5A)	0.9500
S(1A)-C(2A)	1.755(7)	C(6A)-C(7A)	1.389(10)
S(1A)-H(1A)	1.20(8)	C(7A)-C(8A)	1.365(9)
S(2A)-C(6A)	1.772(7)	C(7A)-H(7A)	0.9500
P(1A)-C(29A)	1.813(7)	C(8A)-C(9A)	1.398(9)
P(1A)-C(23A)	1.827(7)	C(8A)-H(8A)	0.9500
P(1A)-C(17A)	1.833(8)	C(9A)-C(10A)	1.441(10)
O(1A)-C(11A)	1.223(9)	C(12A)-C(13A)	1.507(10)
O(2A)-C(11A)	1.348(9)	C(12A)-H(12A)	0.9900
O(2A)-C(12A)	1.473(9)	C(12A)-H(12B)	0.9900
O(3A)-C(14A)	1.217(9)	C(13A)-H(13A)	0.9800
O(4A)-C(14A)	1.336(8)	C(13A)-H(13B)	0.9800
O(4A)-C(15A)	1.447(9)	C(13A)-H(13C)	0.9800
C(1A)-C(2A)	1.401(10)	C(15A)-C(16A)	1.500(11)
C(1A)-C(9A)	1.434(10)	C(15A)-H(15A)	0.9900
C(1A)-C(11A)	1.442(11)	C(15A)-H(15B)	0.9900
C(2A)-C(3A)	1.417(11)	C(16A)-H(16A)	0.9800
C(3A)-C(10A)	1.417(10)	C(16A)-H(16B)	0.9800
C(3A)-C(14A)	1.479(11)	C(16A)-H(16C)	0.9800
C(4A)-C(5A)	1.370(9)	C(17A)-C(22A)	1.380(11)
C(4A)-C(10A)	1.383(10)	C(17A)-C(18A)	1.397(9)
C(4A)-H(4A)	0.9500	C(18A)-C(19A)	1.376(10)

C(18A)-H(18A)	0.9500	C(32A)-C(33A)	1.365(10)
C(19A)-C(20A)	1.360(11)	C(32A)-H(32A)	0.9500
C(19A)-H(19A)	0.9500	C(33A)-C(34A)	1.380(9)
C(20A)-C(21A)	1.370(10)	C(33A)-H(33A)	0.9500
C(20A)-H(20A)	0.9500	C(34A)-H(34A)	0.9500
C(21A)-C(22A)	1.376(11)	Au(1B)-P(1B)	2.260(2)
C(21A)-H(21A)	0.9500	Au(1B)-S(2B)	2.3191(19)
C(22A)-H(22A)	0.9500	S(1B)-C(2B)	1.756(7)
C(23A)-C(24A)	1.375(10)	S(1B)-H(1B)	1.15(8)
C(23A)-C(28A)	1.407(10)	S(2B)-C(6B)	1.780(7)
C(24A)-C(25A)	1.390(10)	P(1B)-C(17B)	1.815(8)
C(24A)-H(24A)	0.9500	P(1B)-C(29B)	1.816(7)
C(25A)-C(26A)	1.373(11)	P(1B)-C(23B)	1.823(7)
C(25A)-H(25A)	0.9500	O(1B)-C(11B)	1.229(9)
C(26A)-C(27A)	1.368(11)	O(2B)-C(11B)	1.354(9)
C(26A)-H(26A)	0.9500	O(2B)-C(12B)	1.434(8)
C(27A)-C(28A)	1.388(9)	O(3B)-C(14B)	1.216(9)
C(27A)-H(27A)	0.9500	O(4B)-C(14B)	1.347(8)
C(28A)-H(28A)	0.9500	O(4B)-C(15B)	1.451(8)
C(29A)-C(30A)	1.381(9)	C(1B)-C(9B)	1.429(10)
C(29A)-C(34A)	1.397(9)	C(1B)-C(2B)	1.434(10)
C(30A)-C(31A)	1.386(10)	C(1B)-C(11B)	1.444(11)
C(30A)-H(30A)	0.9500	C(2B)-C(3B)	1.412(10)
C(31A)-C(32A)	1.386(9)	C(3B)-C(10B)	1.426(10)
C(31A)-H(31A)	0.9500	C(3B)-C(14B)	1.458(10)

C(4B)-C(5B)	1.357(9)	C(18B)-C(19B)	1.369(10)
C(4B)-C(10B)	1.413(9)	C(18B)-H(18B)	0.9500
C(4B)-H(4B)	0.9500	C(19B)-C(20B)	1.378(11)
C(5B)-C(6B)	1.386(10)	C(19B)-H(19B)	0.9500
C(5B)-H(5B)	0.9500	C(20B)-C(21B)	1.401(11)
C(6B)-C(7B)	1.391(10)	C(20B)-H(20B)	0.9500
C(7B)-C(8B)	1.392(9)	C(21B)-C(22B)	1.385(11)
C(7B)-H(7B)	0.9500	C(21B)-H(21B)	0.9500
C(8B)-C(9B)	1.396(9)	C(22B)-H(22B)	0.9500
C(8B)-H(8B)	0.9500	C(23B)-C(28B)	1.378(10)
C(9B)-C(10B)	1.462(10)	C(23B)-C(24B)	1.394(10)
C(12B)-C(13B)	1.498(10)	C(24B)-C(25B)	1.394(9)
C(12B)-H(12C)	0.9900	C(24B)-H(24B)	0.9500
C(12B)-H(12D)	0.9900	C(25B)-C(26B)	1.336(11)
C(13B)-H(13D)	0.9800	C(25B)-H(25B)	0.9500
C(13B)-H(13E)	0.9800	C(26B)-C(27B)	1.408(10)
C(13B)-H(13F)	0.9800	C(26B)-H(26B)	0.9500
C(15B)-C(16B)	1.501(11)	C(27B)-C(28B)	1.374(10)
C(15B)-H(15C)	0.9900	C(27B)-H(27B)	0.9500
C(15B)-H(15D)	0.9900	C(28B)-H(28B)	0.9500
C(16B)-H(16D)	0.9800	C(29B)-C(30B)	1.396(9)
C(16B)-H(16E)	0.9800	C(29B)-C(34B)	1.401(8)
C(16B)-H(16F)	0.9800	C(30B)-C(31B)	1.369(10)
C(17B)-C(22B)	1.379(11)	C(30B)-H(30B)	0.9500
C(17B)-C(18B)	1.401(9)	C(31B)-C(32B)	1.400(10)

C(31B)-H(31B)	0.9500	C(33B)-C(34B)	1.368(10)
C(32B)-C(33B)	1.385(10)	C(33B)-H(33B)	0.9500
C(32B)-H(32B)	0.9500	C(34B)-H(34B)	0.9500

---

**Table 4.** Bond angles [°] for **I.6**.

P(1A)-Au(1A)-S(2A)	178.56(6)	C(4A)-C(5A)-C(6A)	130.5(7)
C(2A)-S(1A)-H(1A)	97(3)	C(4A)-C(5A)-H(5A)	114.7
C(6A)-S(2A)-Au(1A)	104.5(2)	C(6A)-C(5A)-H(5A)	114.7
C(29A)-P(1A)-C(23A)	105.1(3)	C(7A)-C(6A)-C(5A)	124.5(6)
C(29A)-P(1A)-C(17A)	105.9(3)	C(7A)-C(6A)-S(2A)	120.8(5)
C(23A)-P(1A)-C(17A)	105.1(3)	C(5A)-C(6A)-S(2A)	114.6(5)
C(29A)-P(1A)-Au(1A)	114.3(2)	C(8A)-C(7A)-C(6A)	130.3(7)
C(23A)-P(1A)-Au(1A)	113.5(3)	C(8A)-C(7A)-H(7A)	114.9
C(17A)-P(1A)-Au(1A)	112.2(2)	C(6A)-C(7A)-H(7A)	114.9
C(11A)-O(2A)-C(12A)	117.4(6)	C(7A)-C(8A)-C(9A)	132.1(7)
C(14A)-O(4A)-C(15A)	116.3(6)	C(7A)-C(8A)-H(8A)	114.0
C(2A)-C(1A)-C(9A)	107.5(6)	C(9A)-C(8A)-H(8A)	114.0
C(2A)-C(1A)-C(11A)	124.1(6)	C(8A)-C(9A)-C(1A)	127.6(7)
C(9A)-C(1A)-C(11A)	128.3(6)	C(8A)-C(9A)-C(10A)	124.5(7)
C(1A)-C(2A)-C(3A)	109.1(6)	C(1A)-C(9A)-C(10A)	107.9(6)
C(1A)-C(2A)-S(1A)	127.1(6)	C(4A)-C(10A)-C(3A)	125.4(7)
C(3A)-C(2A)-S(1A)	123.8(6)	C(4A)-C(10A)-C(9A)	127.7(7)
C(2A)-C(3A)-C(10A)	108.5(7)	C(3A)-C(10A)-C(9A)	106.9(7)
C(2A)-C(3A)-C(14A)	126.8(7)	O(1A)-C(11A)-O(2A)	118.8(7)
C(10A)-C(3A)-C(14A)	124.5(7)	O(1A)-C(11A)-C(1A)	127.0(7)
C(5A)-C(4A)-C(10A)	130.3(7)	O(2A)-C(11A)-C(1A)	114.1(6)
C(5A)-C(4A)-H(4A)	114.9	O(2A)-C(12A)-C(13A)	106.8(6)
C(10A)-C(4A)-H(4A)	114.9	O(2A)-C(12A)-H(12A)	110.4

C(13A)-C(12A)-H(12A)	110.4	C(22A)-C(17A)-C(18A)	119.7(7)
O(2A)-C(12A)-H(12B)	110.4	C(22A)-C(17A)-P(1A)	122.6(5)
C(13A)-C(12A)-H(12B)	110.4	C(18A)-C(17A)-P(1A)	117.6(6)
H(12A)-C(12A)-H(12B)	108.6	C(19A)-C(18A)-C(17A)	120.0(7)
C(12A)-C(13A)-H(13A)	109.5	C(19A)-C(18A)-H(18A)	120.0
C(12A)-C(13A)-H(13B)	109.5	C(17A)-C(18A)-H(18A)	120.0
H(13A)-C(13A)-H(13B)	109.5	C(20A)-C(19A)-C(18A)	119.8(7)
C(12A)-C(13A)-H(13C)	109.5	C(20A)-C(19A)-H(19A)	120.1
H(13A)-C(13A)-H(13C)	109.5	C(18A)-C(19A)-H(19A)	120.1
H(13B)-C(13A)-H(13C)	109.5	C(19A)-C(20A)-C(21A)	120.6(8)
O(3A)-C(14A)-O(4A)	122.5(7)	C(19A)-C(20A)-H(20A)	119.7
O(3A)-C(14A)-C(3A)	124.7(7)	C(21A)-C(20A)-H(20A)	119.7
O(4A)-C(14A)-C(3A)	112.8(7)	C(20A)-C(21A)-C(22A)	120.9(8)
O(4A)-C(15A)-C(16A)	112.3(6)	C(20A)-C(21A)-H(21A)	119.5
O(4A)-C(15A)-H(15A)	109.2	C(22A)-C(21A)-H(21A)	119.5
C(16A)-C(15A)-H(15A)	109.2	C(21A)-C(22A)-C(17A)	119.0(7)
O(4A)-C(15A)-H(15B)	109.2	C(21A)-C(22A)-H(22A)	120.5
C(16A)-C(15A)-H(15B)	109.2	C(17A)-C(22A)-H(22A)	120.5
H(15A)-C(15A)-H(15B)	107.9	C(24A)-C(23A)-C(28A)	119.9(6)
C(15A)-C(16A)-H(16A)	109.5	C(24A)-C(23A)-P(1A)	120.4(6)
C(15A)-C(16A)-H(16B)	109.5	C(28A)-C(23A)-P(1A)	119.7(6)
H(16A)-C(16A)-H(16B)	109.5	C(23A)-C(24A)-C(25A)	119.5(7)
C(15A)-C(16A)-H(16C)	109.5	C(23A)-C(24A)-H(24A)	120.3
H(16A)-C(16A)-H(16C)	109.5	C(25A)-C(24A)-H(24A)	120.3
H(16B)-C(16A)-H(16C)	109.5	C(26A)-C(25A)-C(24A)	120.4(7)

C(26A)-C(25A)-H(25A)	119.8	C(34A)-C(33A)-H(33A)	119.9
C(24A)-C(25A)-H(25A)	119.8	C(33A)-C(34A)-C(29A)	119.8(6)
C(27A)-C(26A)-C(25A)	121.0(7)	C(33A)-C(34A)-H(34A)	120.1
C(27A)-C(26A)-H(26A)	119.5	C(29A)-C(34A)-H(34A)	120.1
C(25A)-C(26A)-H(26A)	119.5	P(1B)-Au(1B)-S(2B)	176.20(6)
C(26A)-C(27A)-C(28A)	119.6(7)	C(2B)-S(1B)-H(1B)	97(4)
C(26A)-C(27A)-H(27A)	120.2	C(6B)-S(2B)-Au(1B)	105.4(2)
C(28A)-C(27A)-H(27A)	120.2	C(17B)-P(1B)-C(29B)	105.5(3)
C(27A)-C(28A)-C(23A)	119.6(7)	C(17B)-P(1B)-C(23B)	105.0(3)
C(27A)-C(28A)-H(28A)	120.2	C(29B)-P(1B)-C(23B)	105.6(3)
C(23A)-C(28A)-H(28A)	120.2	C(17B)-P(1B)-Au(1B)	113.5(2)
C(30A)-C(29A)-C(34A)	119.4(6)	C(29B)-P(1B)-Au(1B)	114.1(2)
C(30A)-C(29A)-P(1A)	120.1(5)	C(23B)-P(1B)-Au(1B)	112.3(2)
C(34A)-C(29A)-P(1A)	120.4(5)	C(11B)-O(2B)-C(12B)	117.5(6)
C(29A)-C(30A)-C(31A)	120.5(6)	C(14B)-O(4B)-C(15B)	117.1(6)
C(29A)-C(30A)-H(30A)	119.7	C(9B)-C(1B)-C(2B)	107.2(7)
C(31A)-C(30A)-H(30A)	119.7	C(9B)-C(1B)-C(11B)	128.3(6)
C(30A)-C(31A)-C(32A)	119.2(7)	C(2B)-C(1B)-C(11B)	124.4(6)
C(30A)-C(31A)-H(31A)	120.4	C(3B)-C(2B)-C(1B)	109.7(6)
C(32A)-C(31A)-H(31A)	120.4	C(3B)-C(2B)-S(1B)	124.1(6)
C(33A)-C(32A)-C(31A)	120.8(7)	C(1B)-C(2B)-S(1B)	126.1(6)
C(33A)-C(32A)-H(32A)	119.6	C(2B)-C(3B)-C(10B)	107.7(7)
C(31A)-C(32A)-H(32A)	119.6	C(2B)-C(3B)-C(14B)	127.7(7)
C(32A)-C(33A)-C(34A)	120.3(6)	C(10B)-C(3B)-C(14B)	124.5(7)
C(32A)-C(33A)-H(33A)	119.9	C(5B)-C(4B)-C(10B)	130.3(7)



C(5B)-C(4B)-H(4B)	114.8	C(13B)-C(12B)-H(12C)	110.5
C(10B)-C(4B)-H(4B)	114.8	O(2B)-C(12B)-H(12D)	110.5
C(4B)-C(5B)-C(6B)	131.0(7)	C(13B)-C(12B)-H(12D)	110.5
C(4B)-C(5B)-H(5B)	114.5	H(12C)-C(12B)-H(12D)	108.7
C(6B)-C(5B)-H(5B)	114.5	C(12B)-C(13B)-H(13D)	109.5
C(5B)-C(6B)-C(7B)	125.3(6)	C(12B)-C(13B)-H(13E)	109.5
C(5B)-C(6B)-S(2B)	115.8(5)	H(13D)-C(13B)-H(13E)	109.5
C(7B)-C(6B)-S(2B)	118.8(5)	C(12B)-C(13B)-H(13F)	109.5
C(6B)-C(7B)-C(8B)	130.8(7)	H(13D)-C(13B)-H(13F)	109.5
C(6B)-C(7B)-H(7B)	114.6	H(13E)-C(13B)-H(13F)	109.5
C(8B)-C(7B)-H(7B)	114.6	O(3B)-C(14B)-O(4B)	121.6(7)
C(7B)-C(8B)-C(9B)	130.2(7)	O(3B)-C(14B)-C(3B)	126.3(6)
C(7B)-C(8B)-H(8B)	114.9	O(4B)-C(14B)-C(3B)	112.1(6)
C(9B)-C(8B)-H(8B)	114.9	O(4B)-C(15B)-C(16B)	106.6(6)
C(8B)-C(9B)-C(1B)	127.1(7)	O(4B)-C(15B)-H(15C)	110.4
C(8B)-C(9B)-C(10B)	125.4(6)	C(16B)-C(15B)-H(15C)	110.4
C(1B)-C(9B)-C(10B)	107.5(6)	O(4B)-C(15B)-H(15D)	110.4
C(4B)-C(10B)-C(3B)	125.6(7)	C(16B)-C(15B)-H(15D)	110.4
C(4B)-C(10B)-C(9B)	126.6(6)	H(15C)-C(15B)-H(15D)	108.6
C(3B)-C(10B)-C(9B)	107.8(6)	C(15B)-C(16B)-H(16D)	109.5
O(1B)-C(11B)-O(2B)	119.2(8)	C(15B)-C(16B)-H(16E)	109.5
O(1B)-C(11B)-C(1B)	126.9(7)	H(16D)-C(16B)-H(16E)	109.5
O(2B)-C(11B)-C(1B)	113.9(6)	C(15B)-C(16B)-H(16F)	109.5
O(2B)-C(12B)-C(13B)	106.1(6)	H(16D)-C(16B)-H(16F)	109.5
O(2B)-C(12B)-H(12C)	110.5	H(16E)-C(16B)-H(16F)	109.5

C(22B)-C(17B)-C(18B)	118.9(7)	C(26B)-C(25B)-H(25B)	120.3
C(22B)-C(17B)-P(1B)	122.7(5)	C(24B)-C(25B)-H(25B)	120.3
C(18B)-C(17B)-P(1B)	118.3(6)	C(25B)-C(26B)-C(27B)	122.1(7)
C(19B)-C(18B)-C(17B)	120.6(7)	C(25B)-C(26B)-H(26B)	119.0
C(19B)-C(18B)-H(18B)	119.7	C(27B)-C(26B)-H(26B)	119.0
C(17B)-C(18B)-H(18B)	119.7	C(28B)-C(27B)-C(26B)	117.8(8)
C(18B)-C(19B)-C(20B)	120.5(7)	C(28B)-C(27B)-H(27B)	121.1
C(18B)-C(19B)-H(19B)	119.8	C(26B)-C(27B)-H(27B)	121.1
C(20B)-C(19B)-H(19B)	119.8	C(27B)-C(28B)-C(23B)	121.5(7)
C(19B)-C(20B)-C(21B)	119.7(7)	C(27B)-C(28B)-H(28B)	119.3
C(19B)-C(20B)-H(20B)	120.1	C(23B)-C(28B)-H(28B)	119.3
C(21B)-C(20B)-H(20B)	120.1	C(30B)-C(29B)-C(34B)	117.8(6)
C(22B)-C(21B)-C(20B)	119.4(8)	C(30B)-C(29B)-P(1B)	118.9(5)
C(22B)-C(21B)-H(21B)	120.3	C(34B)-C(29B)-P(1B)	123.0(5)
C(20B)-C(21B)-H(21B)	120.3	C(31B)-C(30B)-C(29B)	121.0(6)
C(17B)-C(22B)-C(21B)	120.9(7)	C(31B)-C(30B)-H(30B)	119.5
C(17B)-C(22B)-H(22B)	119.6	C(29B)-C(30B)-H(30B)	119.5
C(21B)-C(22B)-H(22B)	119.6	C(30B)-C(31B)-C(32B)	119.9(7)
C(28B)-C(23B)-C(24B)	118.9(7)	C(30B)-C(31B)-H(31B)	120.1
C(28B)-C(23B)-P(1B)	122.6(6)	C(32B)-C(31B)-H(31B)	120.1
C(24B)-C(23B)-P(1B)	118.5(5)	C(33B)-C(32B)-C(31B)	120.0(7)
C(25B)-C(24B)-C(23B)	120.2(7)	C(33B)-C(32B)-H(32B)	120.0
C(25B)-C(24B)-H(24B)	119.9	C(31B)-C(32B)-H(32B)	120.0
C(23B)-C(24B)-H(24B)	119.9	C(34B)-C(33B)-C(32B)	119.4(6)
C(26B)-C(25B)-C(24B)	119.4(7)	C(34B)-C(33B)-H(33B)	120.3

C(32B)-C(33B)-H(33B)	120.3
C(33B)-C(34B)-C(29B)	121.8(7)
C(33B)-C(34B)-H(34B)	119.1
C(29B)-C(34B)-H(34B)	119.1

**Table 5.** Anisotropic displacement parameters ( $\text{\AA}^2 \times 10^3$ ) for **I.6**. The anisotropic displacement factor exponent takes the form:  $-2\pi^2 [h^2 a^{*2}U_{11} + \dots + 2 h k a^* b^* U_{12}]$ .

	$U_{11}$	$U_{22}$	$U_{33}$	$U_{23}$	$U_{13}$	$U_{12}$
Au(1A)	14(1)	17(1)	15(1)	0(1)	1(1)	-2(1)
S(1A)	27(1)	18(1)	30(1)	-1(1)	7(1)	-6(1)
S(2A)	18(1)	21(1)	15(1)	-1(1)	1(1)	-5(1)
P(1A)	14(1)	16(1)	15(1)	1(1)	1(1)	1(1)
O(1A)	23(2)	21(3)	26(3)	-1(2)	-5(2)	-11(2)
O(2A)	25(2)	24(3)	21(3)	-2(2)	-4(2)	-7(2)
O(3A)	45(3)	25(3)	29(4)	-1(3)	15(3)	-8(3)
O(4A)	36(3)	24(3)	19(3)	5(2)	7(2)	-10(2)
C(1A)	10(3)	16(4)	21(4)	-2(3)	0(3)	-3(3)
C(2A)	14(3)	17(4)	26(4)	-3(3)	6(3)	5(3)
C(3A)	25(4)	19(4)	19(4)	4(3)	0(3)	7(3)
C(4A)	21(3)	21(4)	15(4)	-1(3)	5(3)	4(3)
C(5A)	15(3)	24(4)	18(4)	-5(3)	-3(3)	2(3)
C(6A)	14(3)	20(4)	16(4)	8(3)	-1(3)	0(3)
C(7A)	25(3)	17(4)	17(4)	3(3)	0(3)	-2(3)
C(8A)	13(3)	27(3)	14(4)	1(3)	-4(3)	-2(2)
C(9A)	16(3)	18(4)	19(4)	4(3)	2(3)	7(3)
C(10A)	12(3)	22(4)	21(4)	-1(3)	-1(3)	7(3)
C(11A)	7(3)	15(4)	45(6)	8(3)	-1(3)	-3(3)

C(12A)	26(4)	31(5)	17(4)	-9(3)	-9(3)	1(3)
C(13A)	28(3)	21(4)	25(5)	-1(3)	-5(3)	-3(3)
C(14A)	24(4)	19(4)	27(5)	4(3)	3(3)	-3(3)
C(15A)	34(5)	35(5)	28(6)	6(4)	3(3)	-16(4)
C(16A)	46(5)	31(5)	34(5)	-6(4)	14(4)	11(4)
C(17A)	14(3)	19(4)	22(5)	-1(3)	3(3)	3(3)
C(18A)	27(3)	8(3)	22(4)	3(3)	-5(3)	2(3)
C(19A)	20(3)	20(4)	27(5)	-4(3)	-1(3)	0(3)
C(20A)	24(3)	39(5)	18(4)	0(4)	-4(3)	4(3)
C(21A)	21(4)	42(5)	24(4)	10(4)	-2(3)	2(3)
C(22A)	17(3)	44(5)	27(5)	6(4)	6(3)	-5(3)
C(23A)	15(3)	12(4)	27(5)	-6(3)	-1(3)	-5(3)
C(24A)	25(4)	34(5)	20(4)	8(3)	8(3)	7(3)
C(25A)	37(4)	45(5)	24(5)	22(4)	-1(4)	13(4)
C(26A)	25(4)	15(4)	31(5)	-4(4)	3(3)	3(3)
C(27A)	20(3)	35(5)	24(5)	-9(4)	-1(3)	0(3)
C(28A)	22(3)	24(4)	16(4)	7(3)	-2(3)	2(3)
C(29A)	17(3)	17(4)	11(4)	-1(3)	3(3)	-2(3)
C(30A)	10(3)	31(5)	26(5)	4(3)	1(3)	7(3)
C(31A)	21(3)	22(4)	26(5)	4(3)	2(3)	4(3)
C(32A)	20(4)	21(4)	17(4)	-3(3)	8(3)	-7(3)
C(33A)	18(3)	27(4)	11(4)	-3(3)	1(3)	2(3)
C(34A)	19(3)	10(3)	19(4)	-1(3)	-5(3)	5(3)
Au(1B)	14(1)	17(1)	16(1)	0(1)	1(1)	2(1)
S(1B)	29(1)	18(1)	26(1)	0(1)	-1(1)	5(1)

S(2B)	18(1)	19(1)	17(1)	3(1)	2(1)	4(1)
P(1B)	14(1)	17(1)	18(1)	-2(1)	2(1)	1(1)
O(1B)	25(2)	31(3)	27(3)	1(2)	-5(2)	3(2)
O(2B)	29(3)	22(3)	19(3)	-3(2)	-2(2)	6(2)
O(3B)	42(3)	26(3)	23(3)	-6(2)	-1(3)	12(2)
O(4B)	29(3)	31(3)	22(3)	-2(2)	2(2)	12(2)
C(1B)	11(3)	17(4)	23(4)	-7(3)	-1(3)	-5(3)
C(2B)	17(3)	15(4)	24(4)	-3(3)	-2(3)	-6(3)
C(3B)	12(3)	20(4)	21(4)	1(3)	1(3)	-6(3)
C(4B)	19(3)	22(4)	8(4)	-1(3)	-6(3)	-6(3)
C(5B)	16(3)	19(4)	11(4)	2(3)	-5(3)	4(3)
C(6B)	10(3)	17(4)	19(4)	2(3)	0(3)	-7(2)
C(7B)	16(3)	21(4)	14(4)	-5(3)	0(3)	-2(3)
C(8B)	16(3)	22(4)	19(4)	1(3)	-5(3)	-2(3)
C(9B)	17(3)	14(4)	18(4)	0(3)	1(3)	-1(3)
C(10B)	15(3)	12(4)	29(5)	0(3)	-5(3)	0(3)
C(11B)	24(4)	10(4)	46(5)	-3(3)	-5(3)	3(3)
C(12B)	17(3)	23(4)	12(4)	8(3)	-5(3)	4(3)
C(13B)	32(4)	38(5)	21(5)	-3(4)	-13(3)	4(4)
C(14B)	18(3)	23(4)	26(5)	1(3)	3(3)	1(3)
C(15B)	34(4)	32(5)	21(6)	-6(3)	5(3)	3(4)
C(16B)	35(4)	32(5)	33(6)	4(3)	17(4)	11(3)
C(17B)	15(3)	14(4)	21(5)	-1(3)	1(3)	-9(3)
C(18B)	22(3)	20(4)	20(4)	-5(3)	5(3)	1(3)
C(19B)	25(4)	23(4)	23(5)	2(3)	1(3)	7(3)

C(20B)	33(4)	29(5)	28(6)	7(3)	-4(3)	0(4)
C(21B)	34(5)	36(4)	31(6)	-10(4)	5(4)	2(3)
C(22B)	21(3)	29(4)	17(4)	-4(3)	1(3)	-3(3)
C(23B)	15(3)	9(3)	20(4)	0(3)	7(3)	3(3)
C(24B)	29(4)	17(4)	20(4)	-4(3)	1(3)	-5(3)
C(25B)	17(3)	25(4)	24(5)	-3(3)	-2(3)	-5(3)
C(26B)	21(4)	17(4)	34(5)	-15(4)	0(3)	-5(3)
C(27B)	23(3)	23(4)	29(5)	2(3)	2(3)	3(3)
C(28B)	19(3)	21(4)	27(5)	-5(3)	-1(3)	3(3)
C(29B)	10(3)	23(4)	16(4)	-6(3)	2(3)	-1(3)
C(30B)	14(3)	22(4)	37(5)	-3(4)	3(3)	-8(3)
C(31B)	33(4)	15(4)	45(6)	-6(4)	-2(4)	-1(3)
C(32B)	27(4)	16(4)	23(5)	0(3)	4(3)	4(3)
C(33B)	17(3)	26(4)	25(4)	0(3)	0(3)	0(3)
C(34B)	18(3)	22(4)	20(4)	3(3)	3(3)	-3(3)

---

**Table 6.** Hydrogen coordinates ( $\times 10^4$ ) and isotropic displacement parameters ( $\text{\AA}^2 \times 10^3$ ) for **I.6**.

	x	y	z	U(eq)
H(1A)	0.762(3)	0.920(6)	0.527(3)	0.030
H(4A)	0.6570	0.5410	0.3649	0.023
H(5A)	0.6039	0.3863	0.3818	0.023
H(7A)	0.6044	0.3673	0.5521	0.023
H(8A)	0.6520	0.5239	0.5762	0.021
H(12A)	0.6924	0.7620	0.6942	0.030
H(12B)	0.7520	0.6931	0.6878	0.030
H(13A)	0.6460	0.5796	0.7124	0.037
H(13B)	0.6972	0.5934	0.7570	0.037
H(13C)	0.7039	0.5074	0.7025	0.037
H(15A)	0.7859	0.8233	0.2912	0.039
H(15B)	0.7836	0.9618	0.3090	0.039
H(16A)	0.6865	0.9644	0.2772	0.056
H(16B)	0.6966	0.8328	0.2518	0.056
H(16C)	0.7315	0.9441	0.2268	0.056
H(18A)	0.5645	0.3401	0.6556	0.023
H(19A)	0.6225	0.3671	0.7353	0.027
H(20A)	0.6051	0.2601	0.8180	0.032
H(21A)	0.5305	0.1262	0.8225	0.035
H(22A)	0.4689	0.1038	0.7454	0.035
H(24A)	0.4108	0.3909	0.5593	0.032



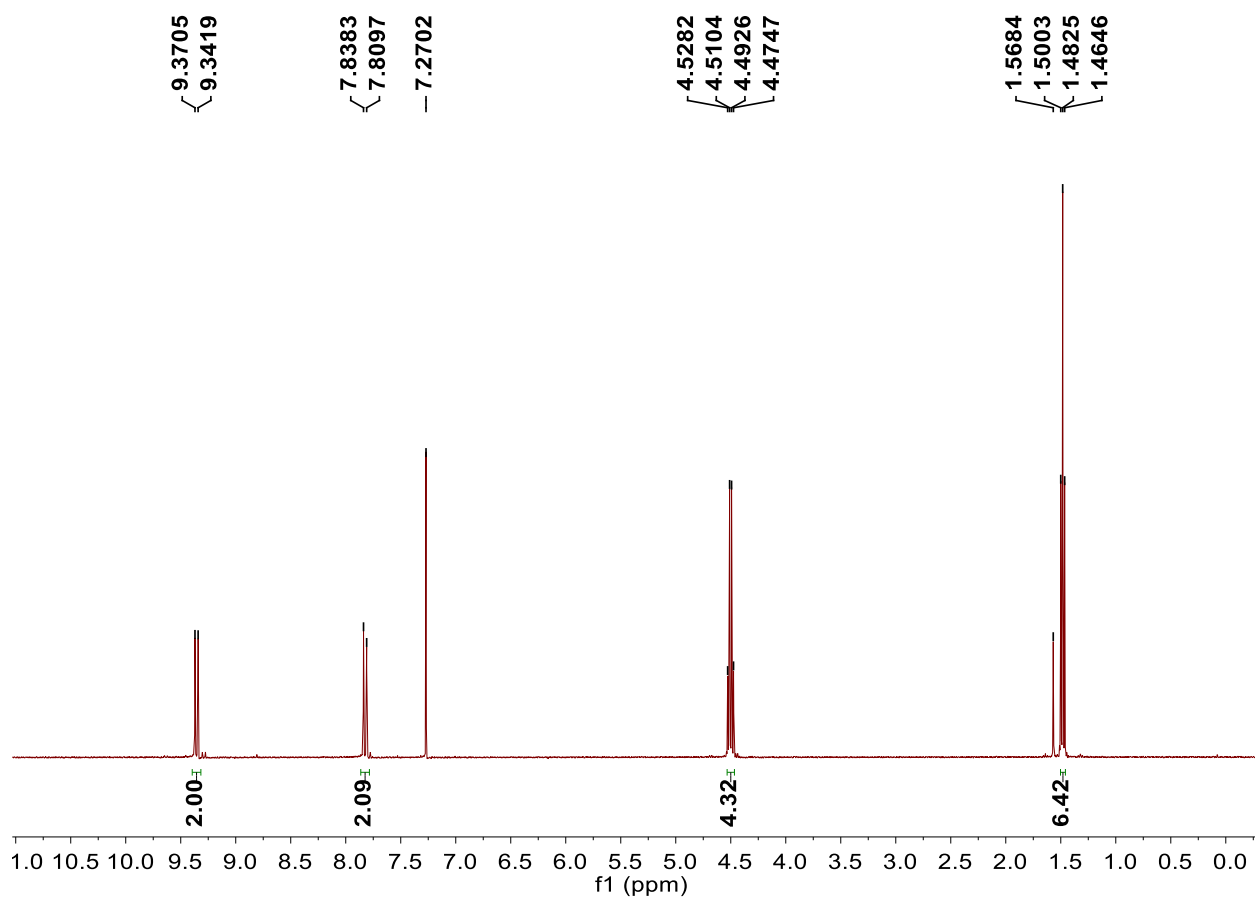
H(25A)	0.3432	0.5415	0.5742	0.042
H(26A)	0.3059	0.5734	0.6646	0.028
H(27A)	0.3338	0.4563	0.7414	0.032
H(28A)	0.4017	0.3054	0.7280	0.025
H(30A)	0.4903	-0.0323	0.6566	0.027
H(31A)	0.4389	-0.2109	0.6637	0.027
H(32A)	0.3408	-0.2084	0.6490	0.023
H(33A)	0.2947	-0.0319	0.6269	0.022
H(34A)	0.3452	0.1474	0.6214	0.019
H(1B)	0.019(3)	1.428(6)	0.580(3)	0.029
H(4B)	0.1266	1.0349	0.7316	0.020
H(5B)	0.1770	0.8806	0.7101	0.018
H(7B)	0.1601	0.8552	0.5418	0.020
H(8B)	0.1098	1.0132	0.5194	0.023
H(12C)	0.0716	1.2685	0.4082	0.021
H(12D)	0.0151	1.1880	0.4128	0.021
H(13D)	0.1253	1.0932	0.3899	0.045
H(13E)	0.0770	1.1091	0.3423	0.045
H(13F)	0.0686	1.0146	0.3932	0.045
H(15C)	0.0603	1.4186	0.8116	0.035
H(15D)	0.0117	1.3218	0.8256	0.035
H(16D)	-0.0552	1.4478	0.7778	0.050
H(16E)	-0.0064	1.5461	0.7697	0.050
H(16F)	-0.0283	1.5128	0.8326	0.050
H(18B)	0.2038	0.8422	0.4303	0.025

H(19B)	0.1464	0.8668	0.3509	0.028
H(20B)	0.1665	0.7660	0.2660	0.036
H(21B)	0.2464	0.6393	0.2608	0.040
H(22B)	0.3040	0.6147	0.3412	0.027
H(24B)	0.3897	0.8225	0.5285	0.026
H(25B)	0.4592	0.9721	0.5189	0.027
H(26B)	0.4604	1.0897	0.4393	0.029
H(27B)	0.3967	1.0569	0.3629	0.030
H(28B)	0.3330	0.8979	0.3694	0.027
H(30B)	0.2814	0.4691	0.4480	0.029
H(31B)	0.3326	0.2948	0.4334	0.037
H(32B)	0.4322	0.3017	0.4299	0.026
H(33B)	0.4792	0.4859	0.4369	0.027
H(34B)	0.4272	0.6604	0.4464	0.024

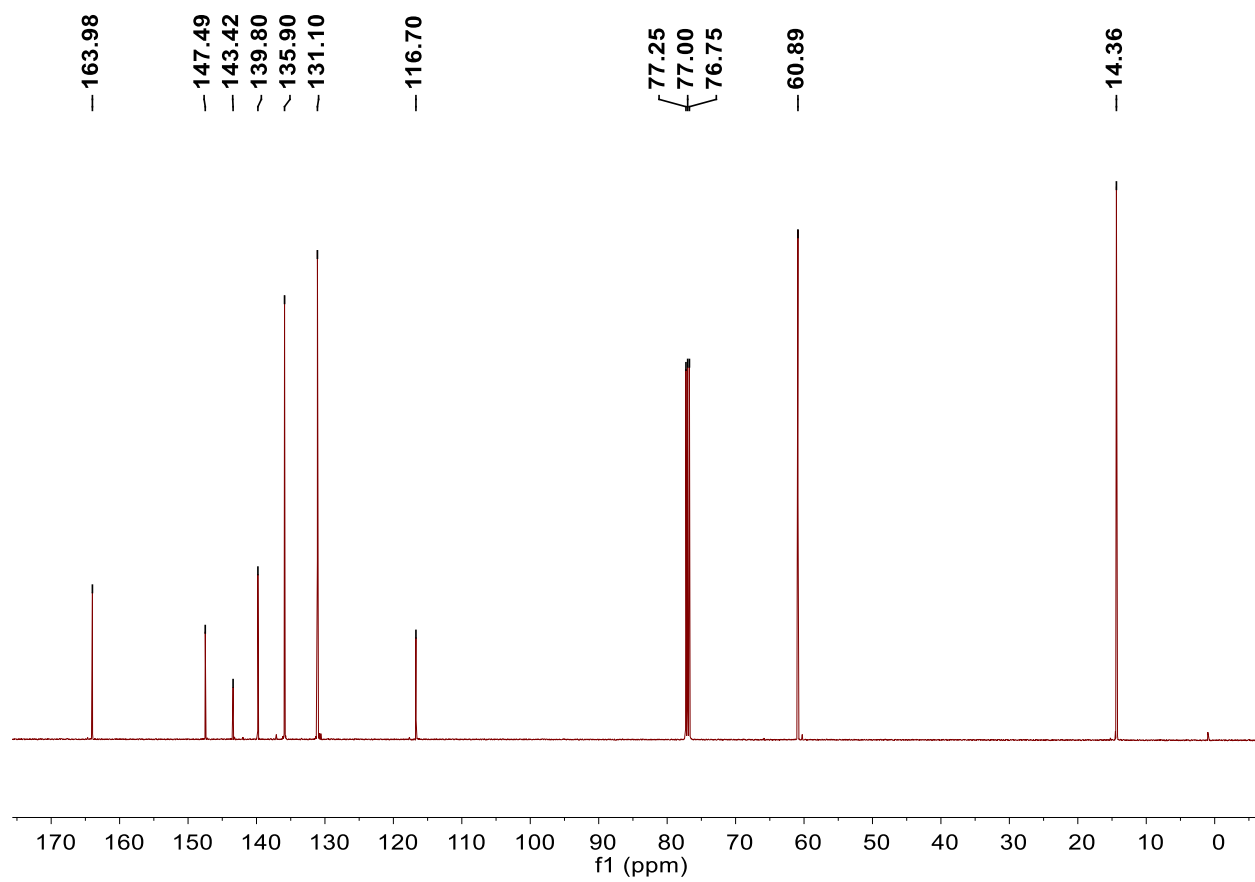
---

## **Appendix 3**

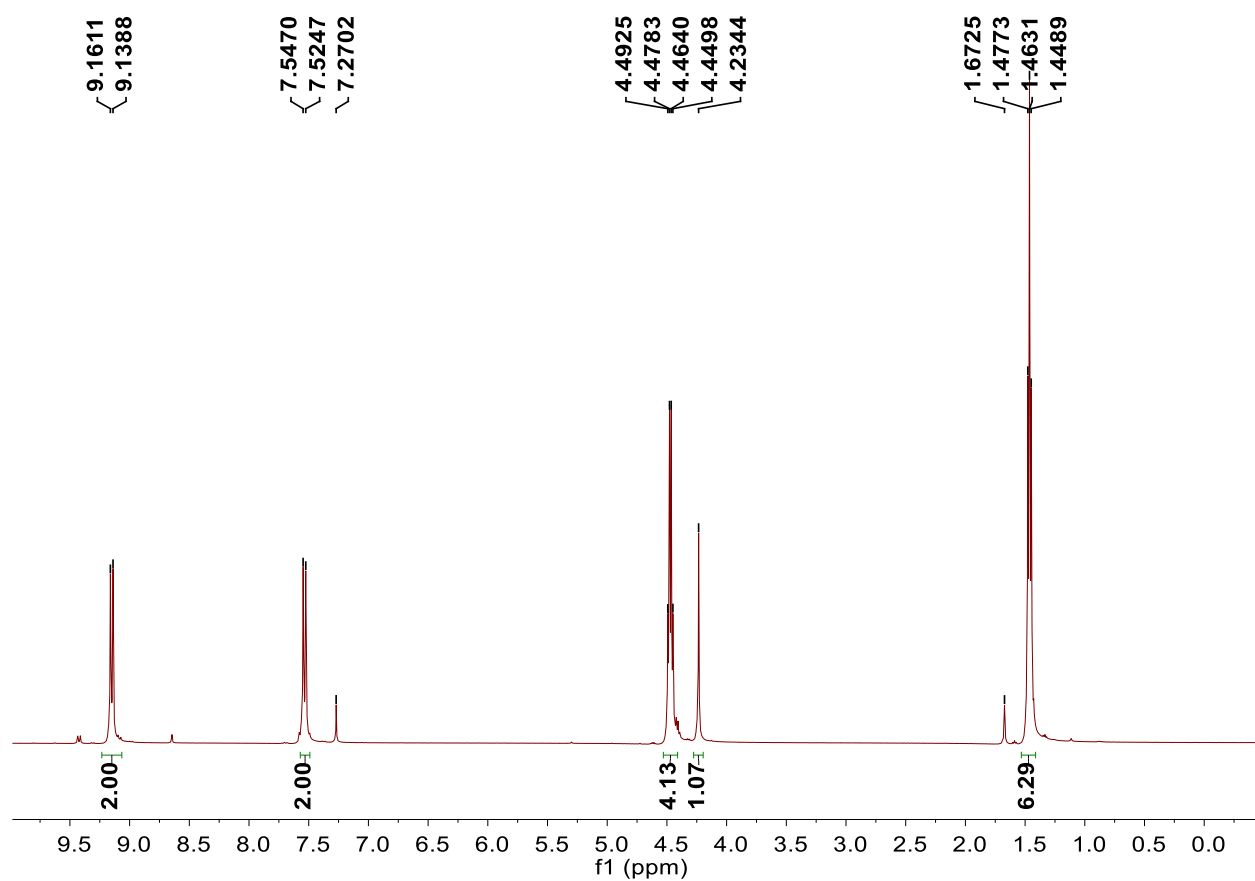
### **NMR Spectra of Selected Compounds from Chapter I**



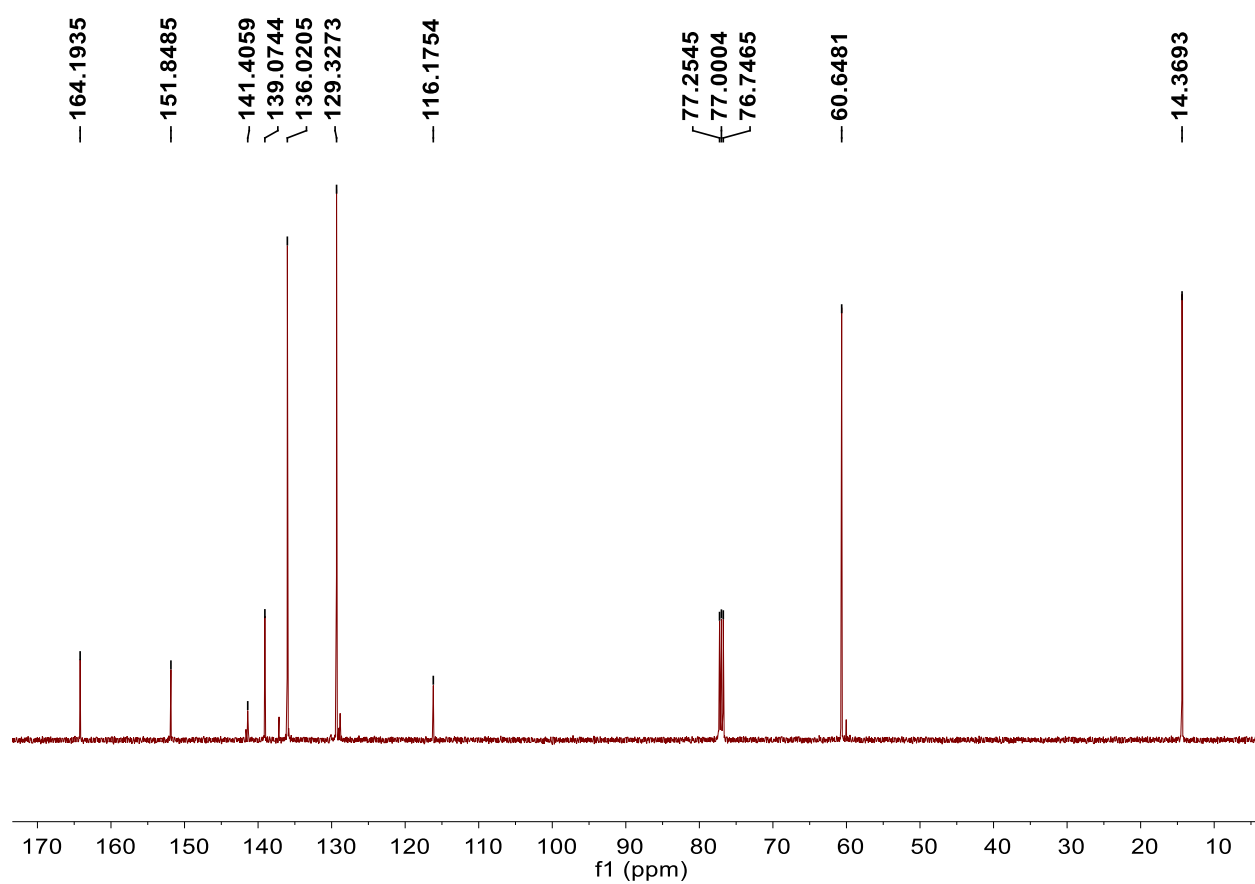
<sup>1</sup>H NMR of 1.1 in CDCl<sub>3</sub>



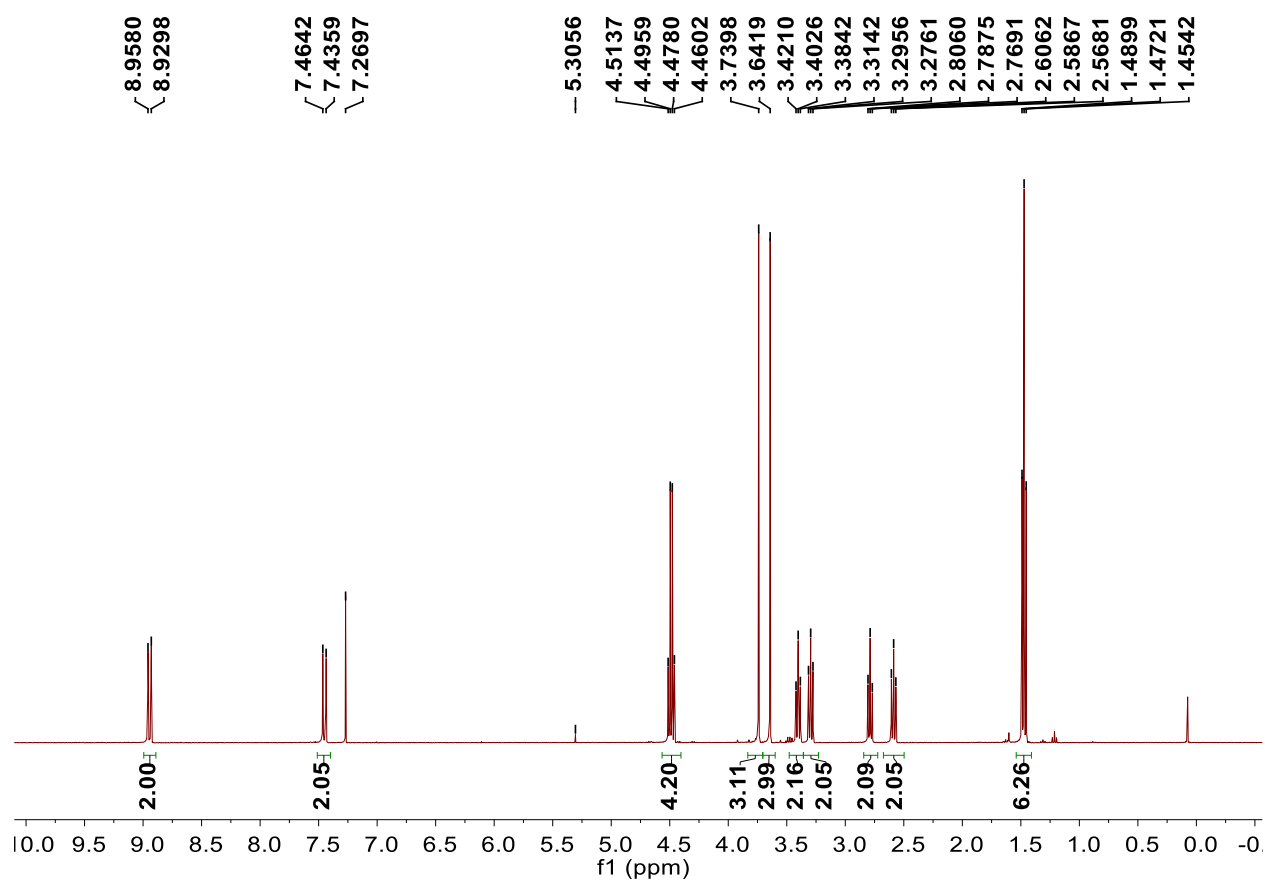
<sup>13</sup>C NMR of I.1 in CDCl<sub>3</sub>



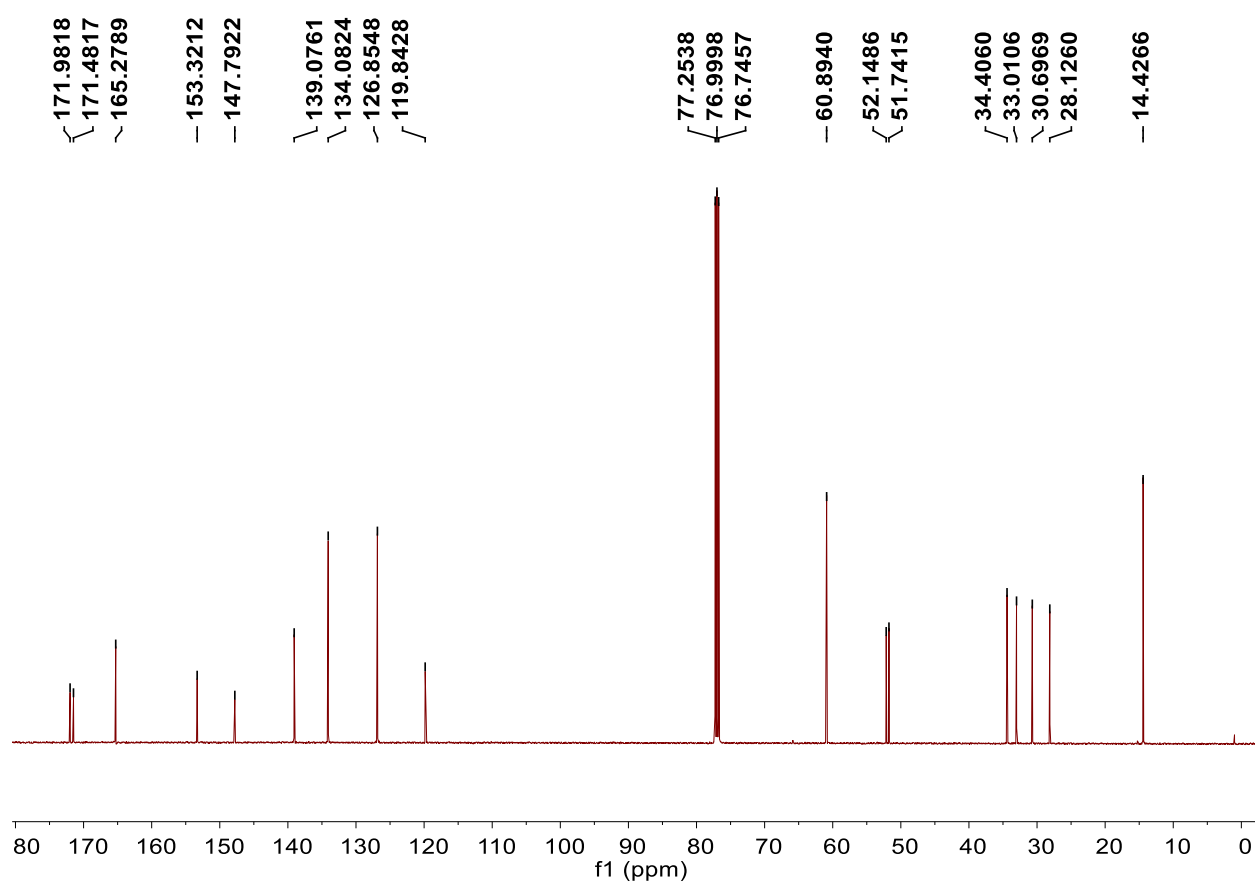
<sup>1</sup>H NMR of 1.2 in CDCl<sub>3</sub>



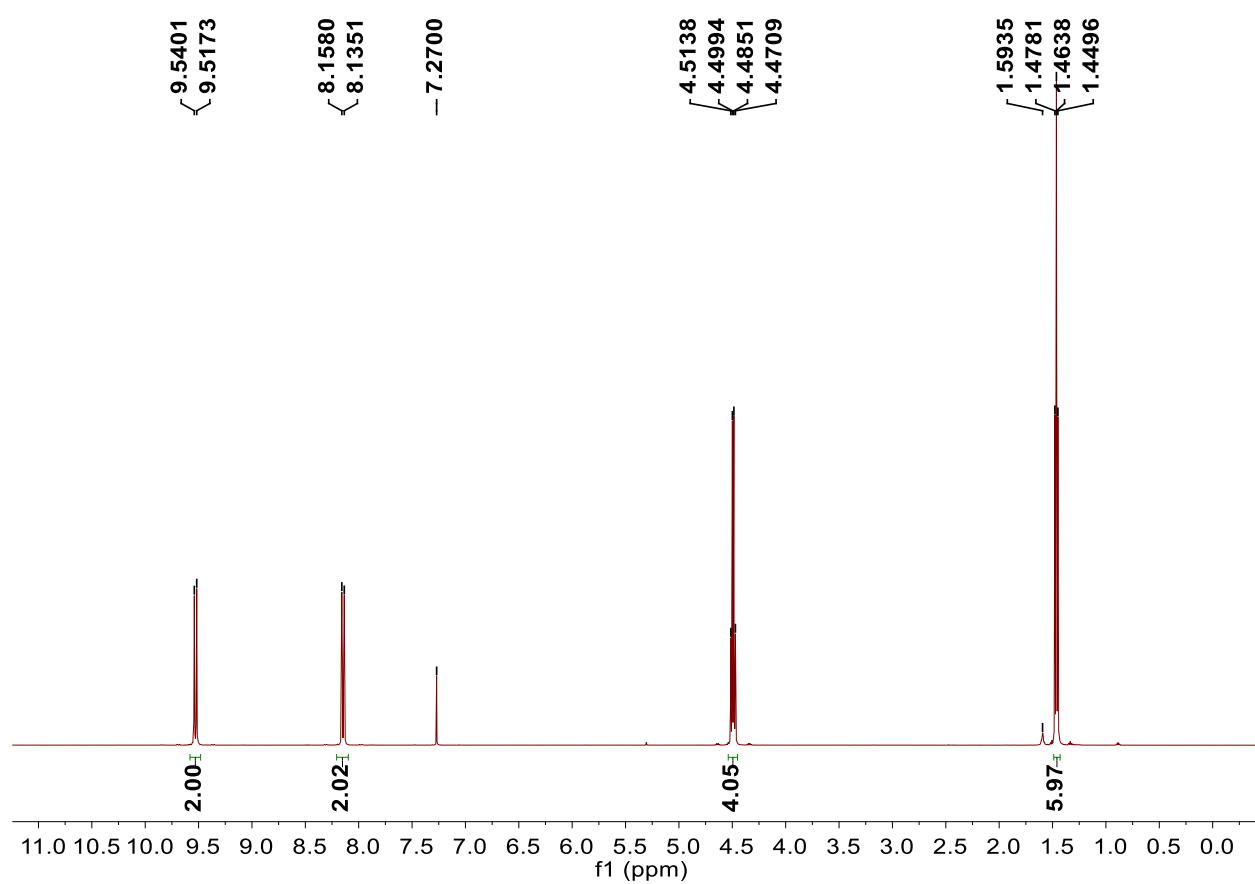
<sup>13</sup>C NMR of 1.2 in CDCl<sub>3</sub>



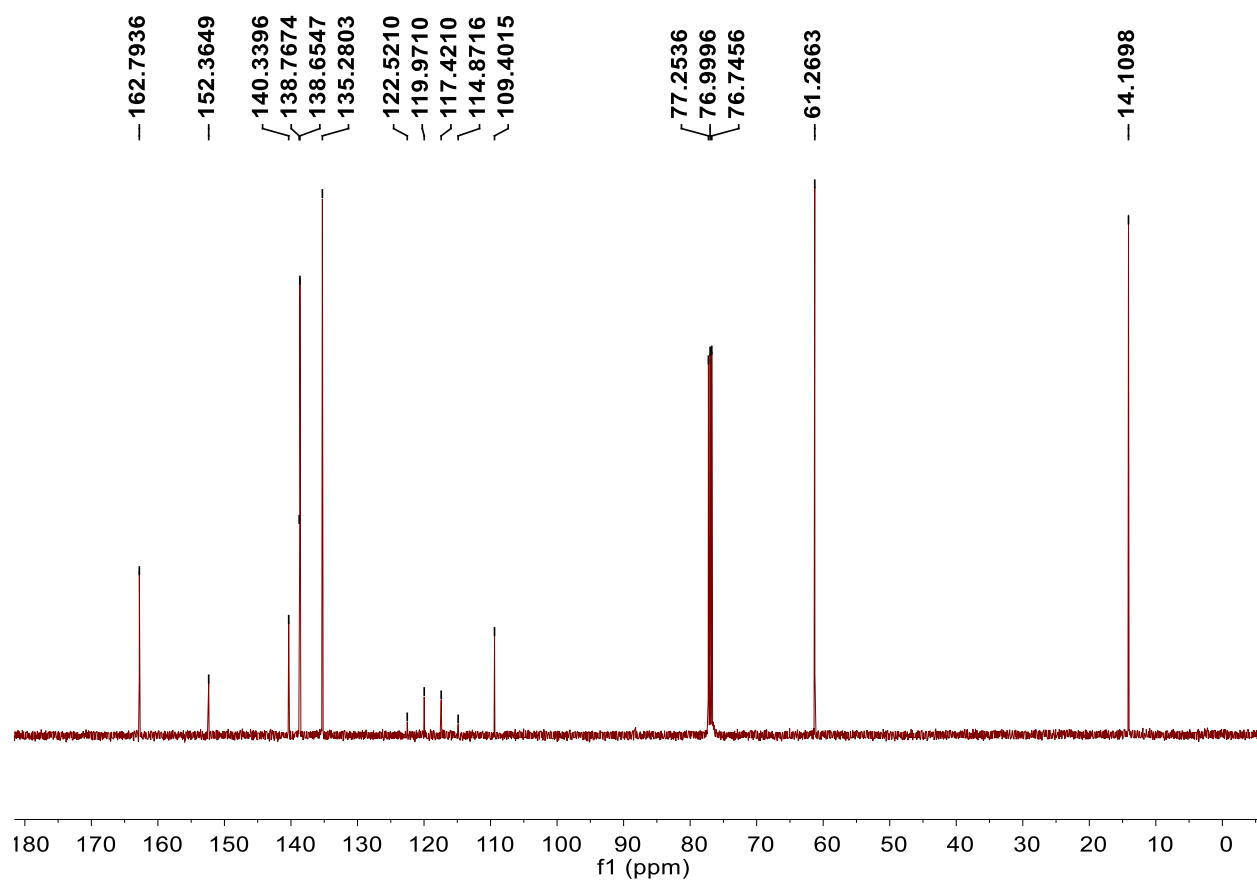




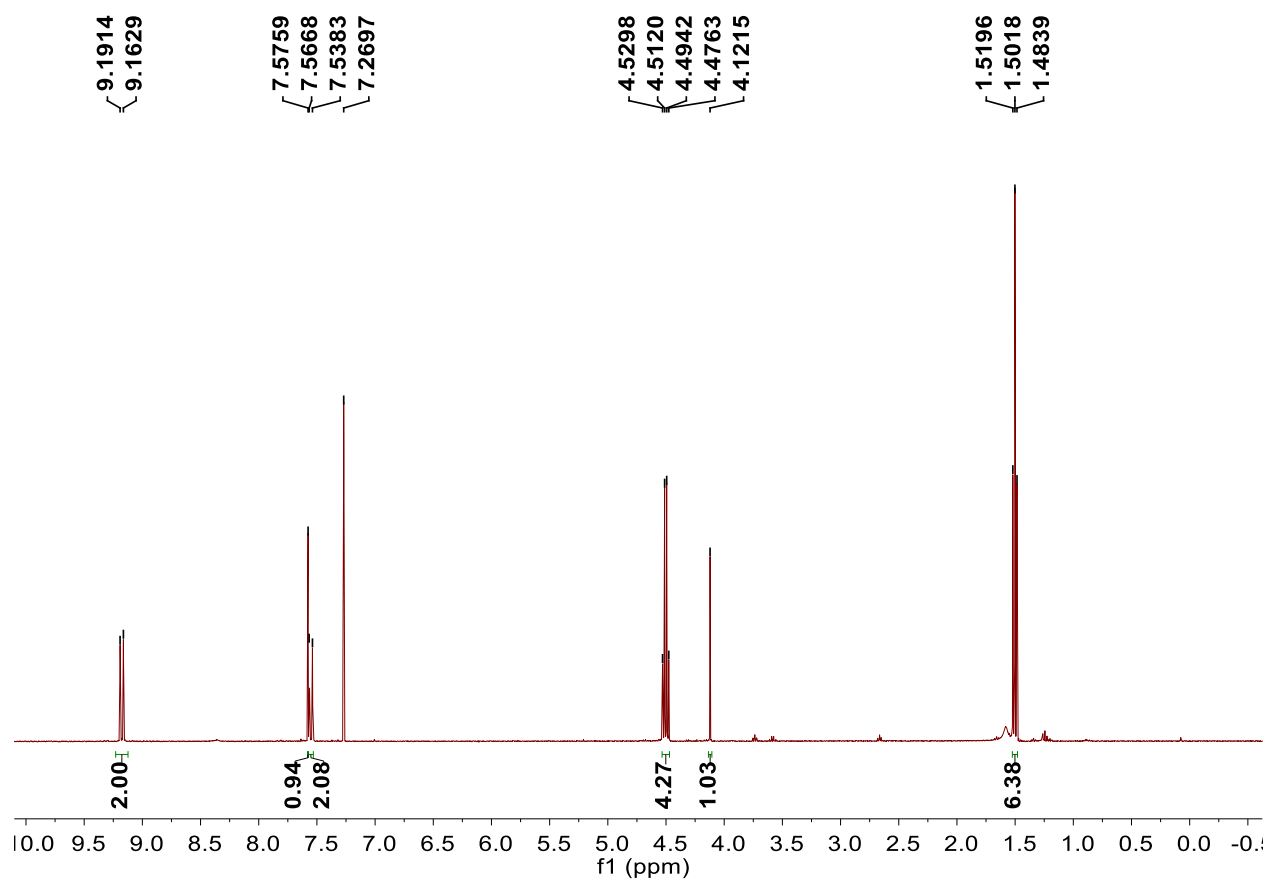
$^{13}\text{C}$  NMR of 1.3 in  $\text{CDCl}_3$



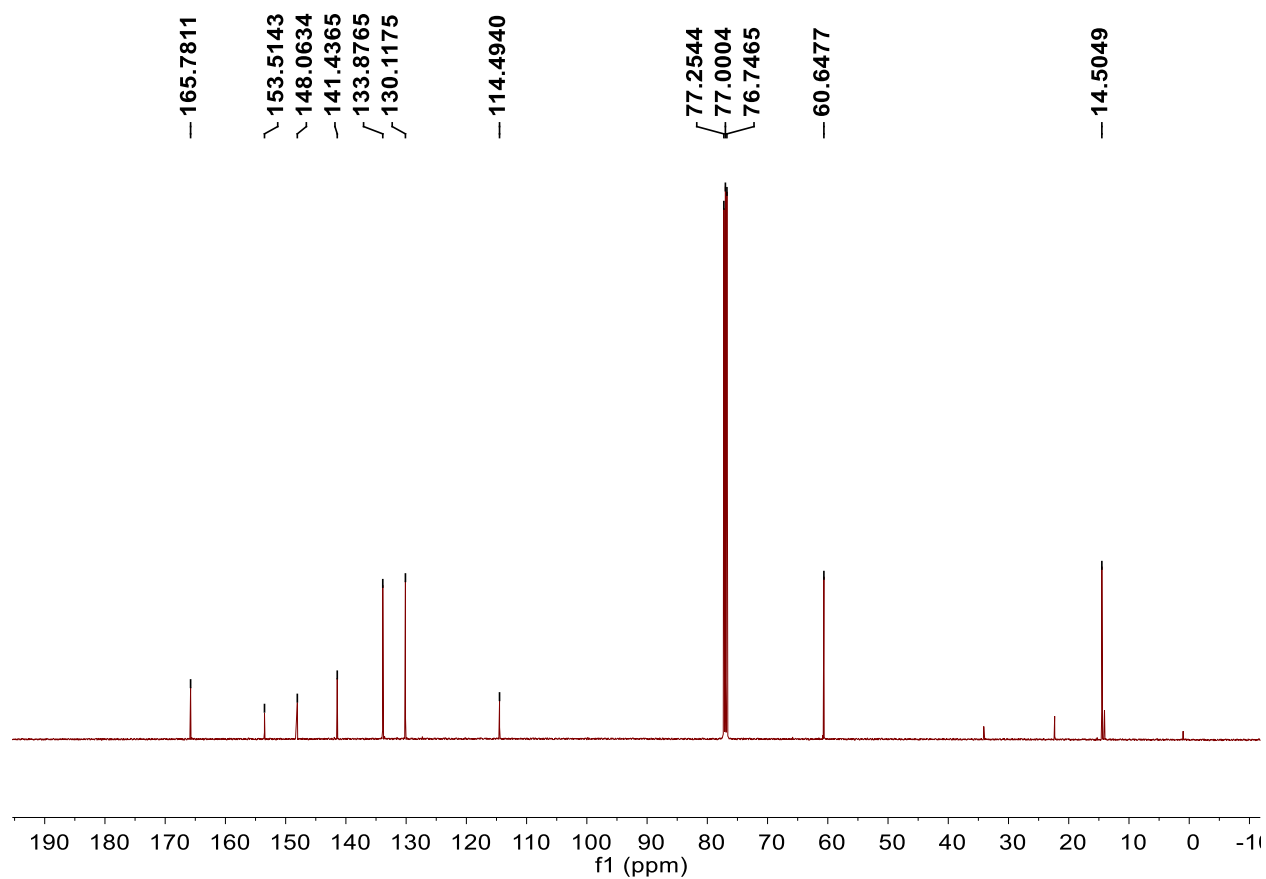
$^1\text{H}$  NMR of 1.4 in  $\text{CDCl}_3$



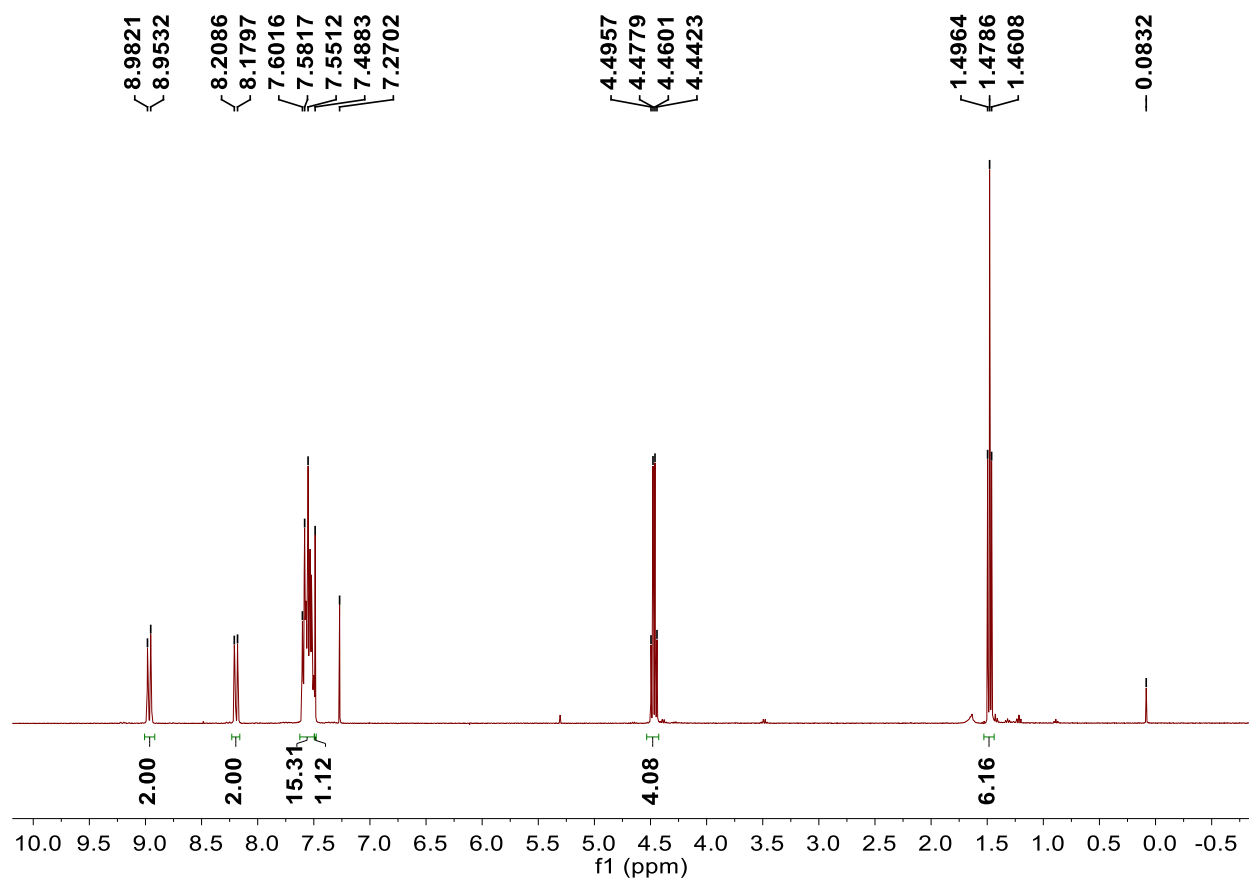
<sup>13</sup>C NMR of I.4 in CDCl<sub>3</sub>



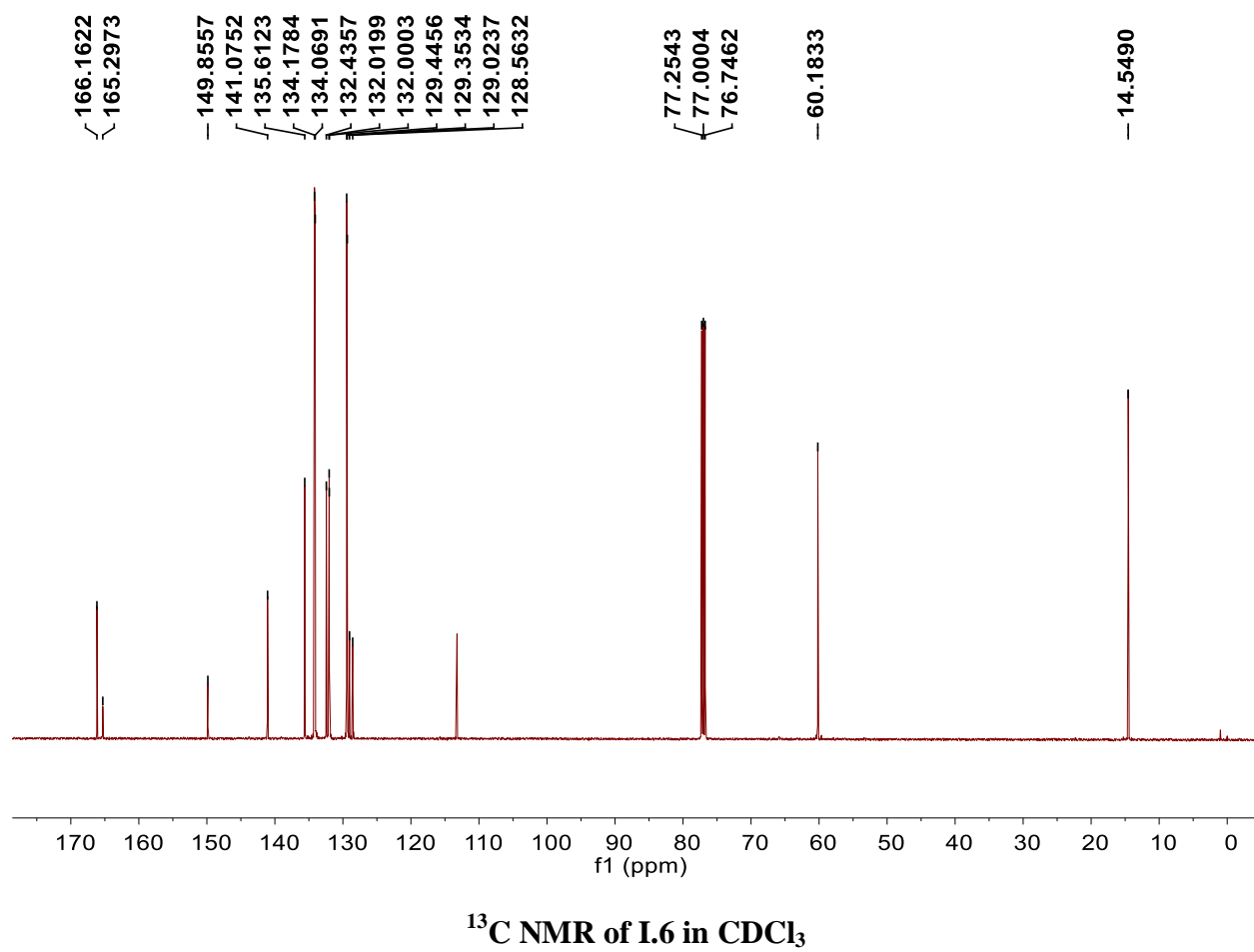
<sup>1</sup>H NMR of 1.5 in CDCl<sub>3</sub>

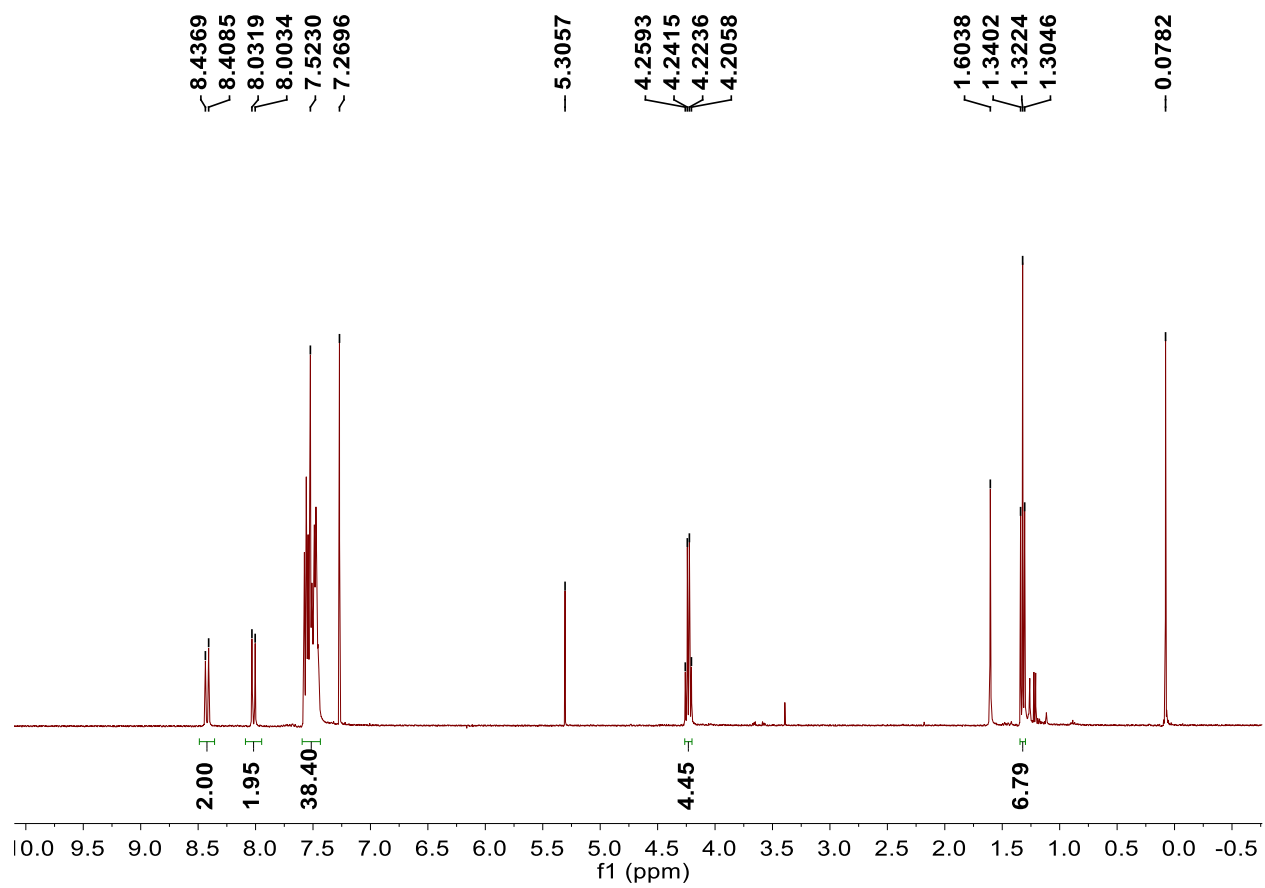


<sup>13</sup>C NMR of 1.5 in CDCl<sub>3</sub>

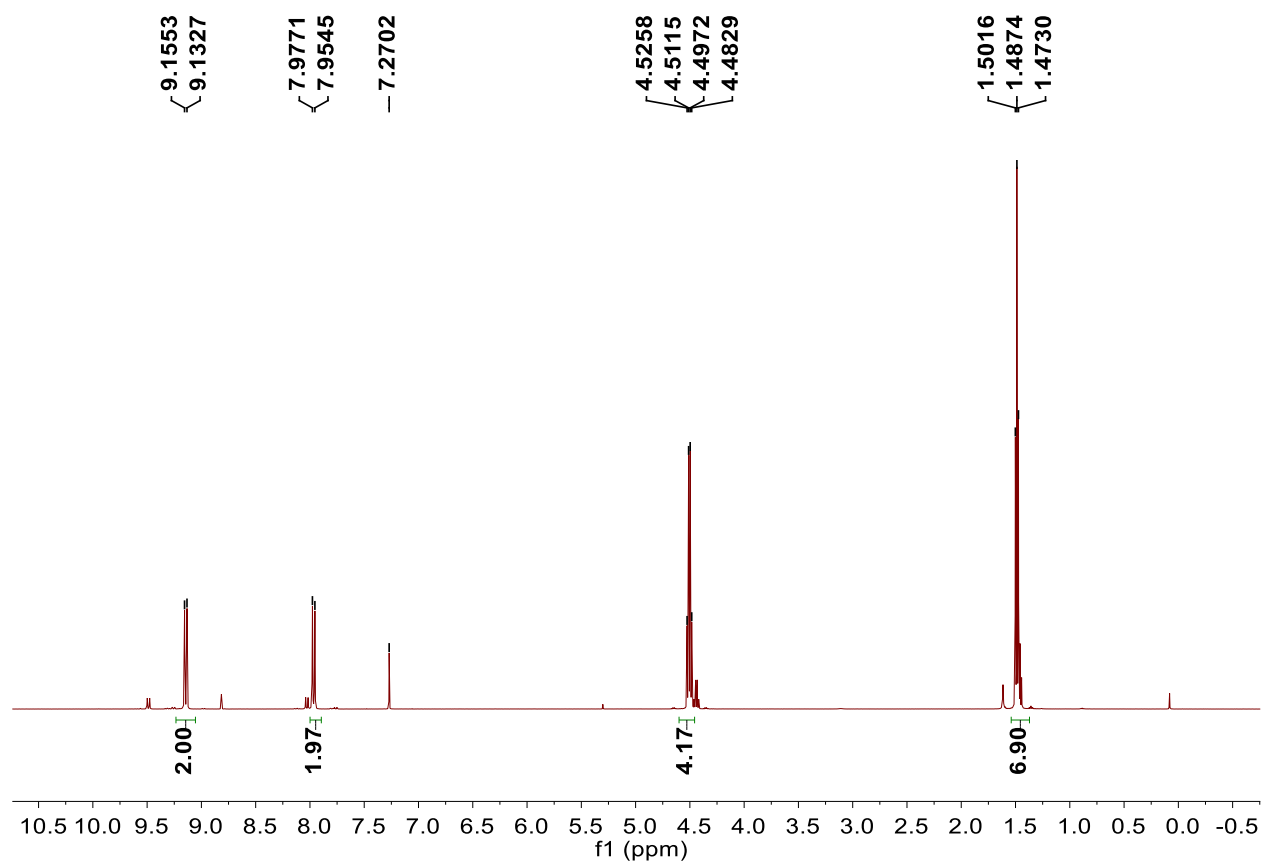


<sup>1</sup>H NMR of L.6 in CDCl<sub>3</sub>

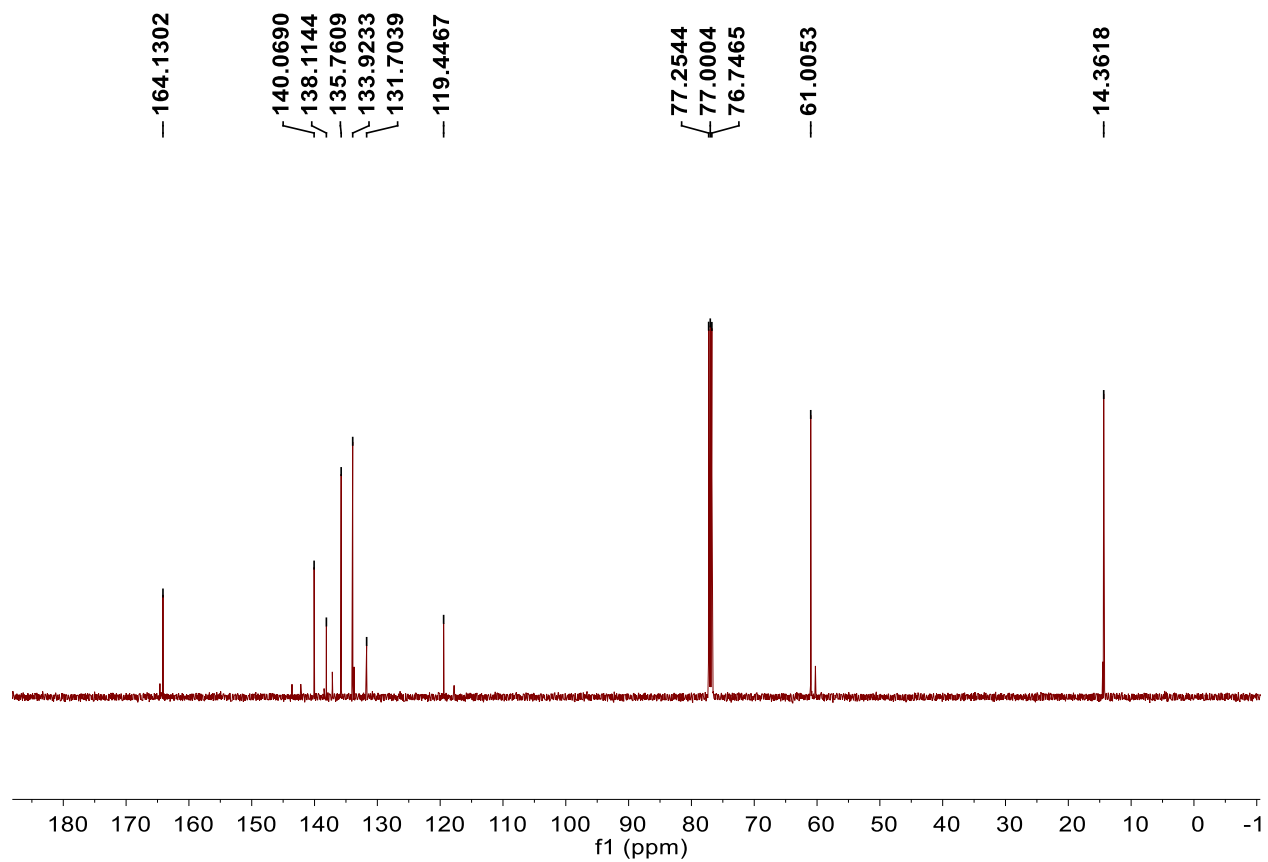








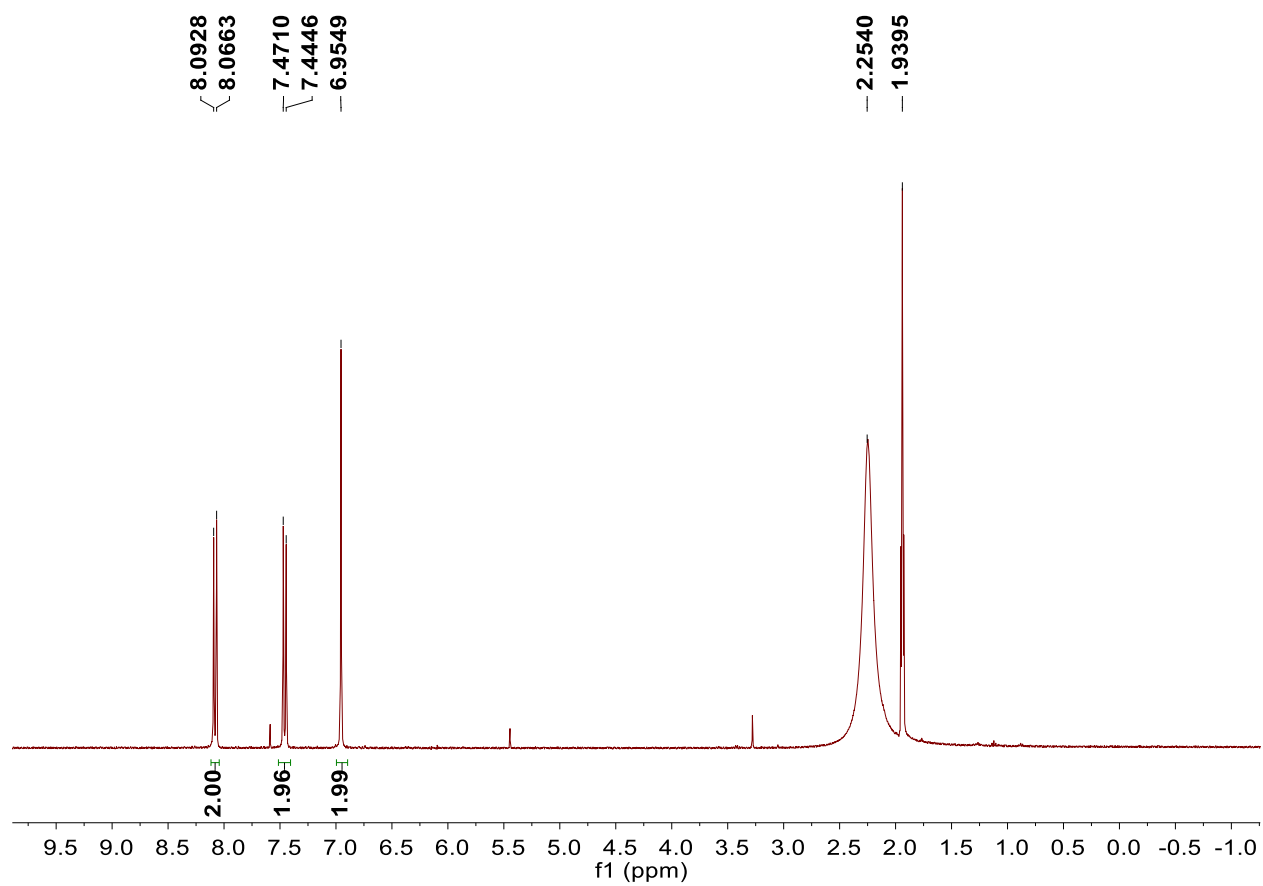
<sup>1</sup>H NMR of 1.8 in CDCl<sub>3</sub>



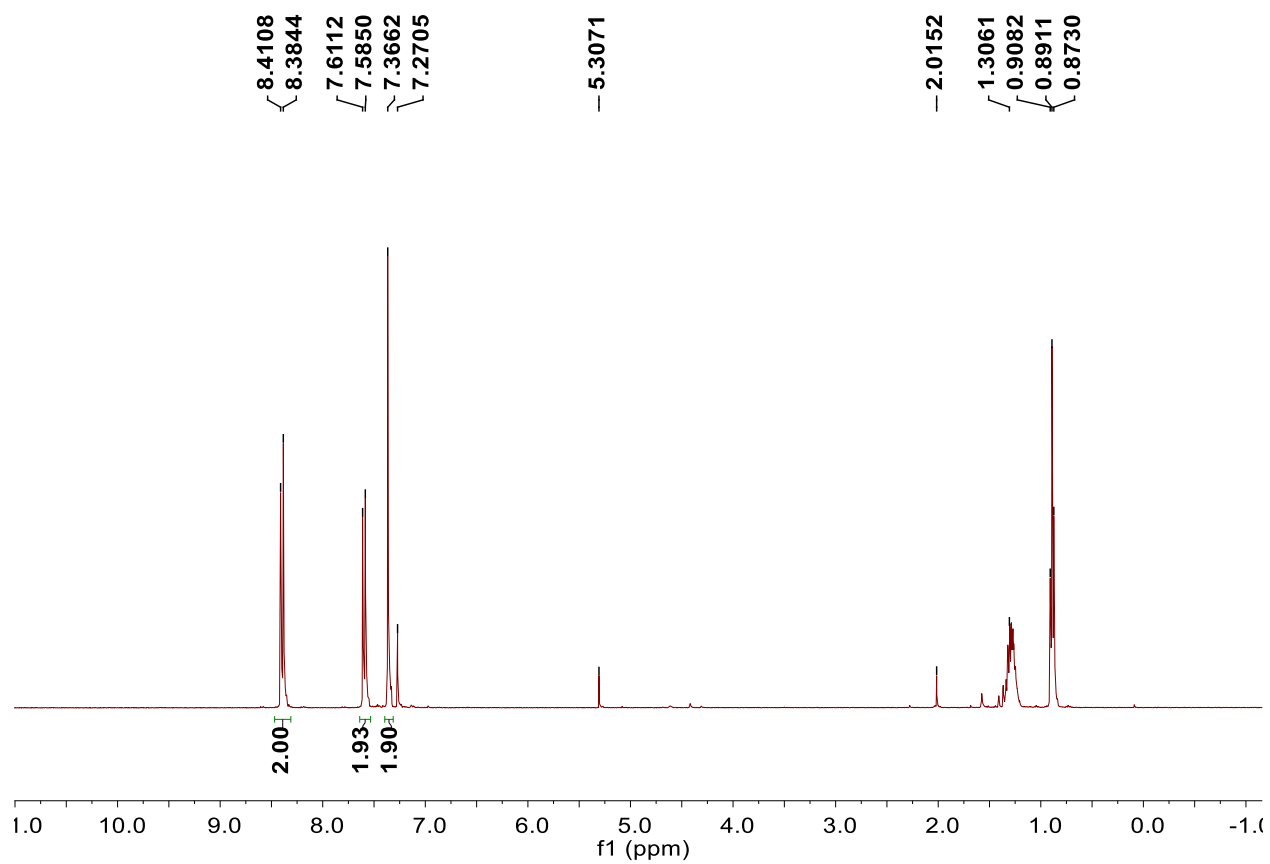
$^{13}\text{C}$  NMR of L.8 in  $\text{CDCl}_3$

## **Appendix 4**

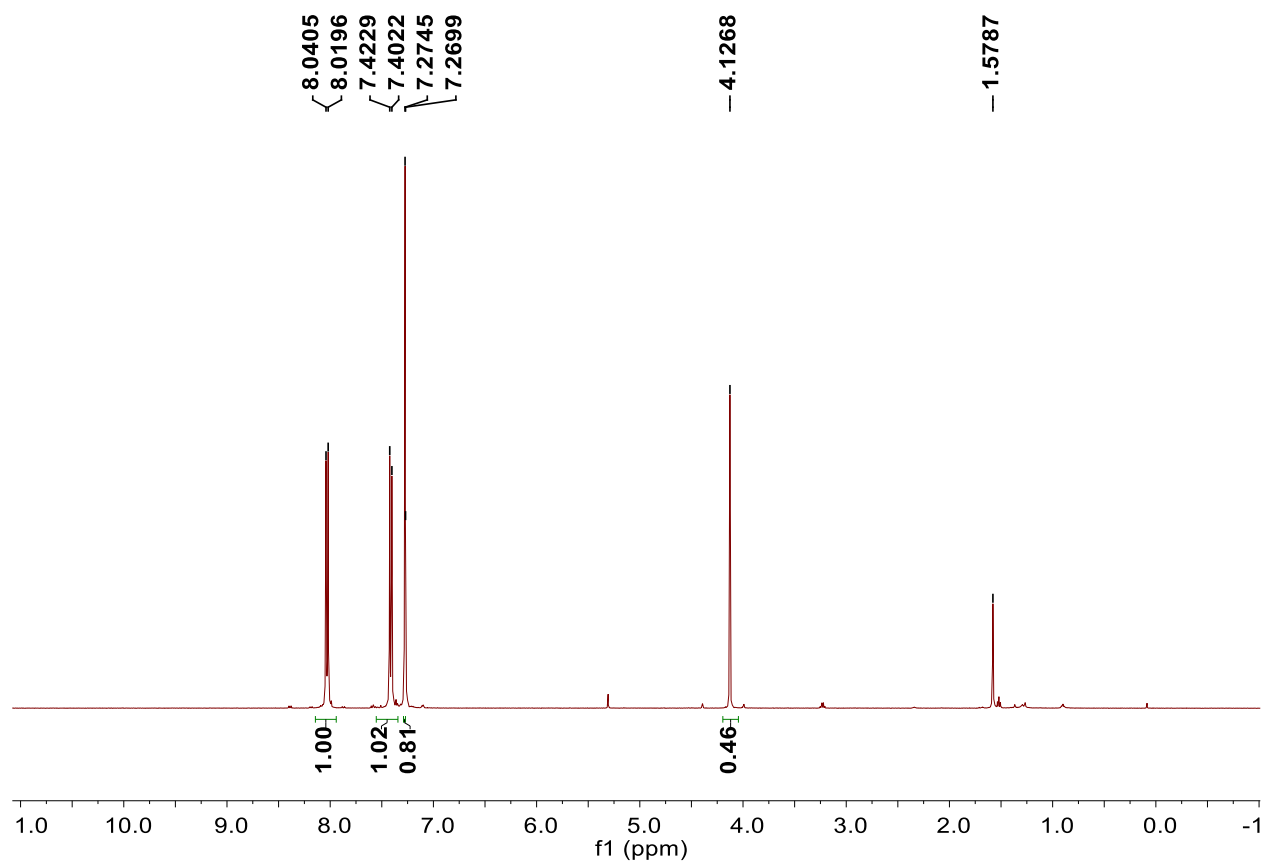
### **NMR Spectra of Selected Compounds from Chapter II**



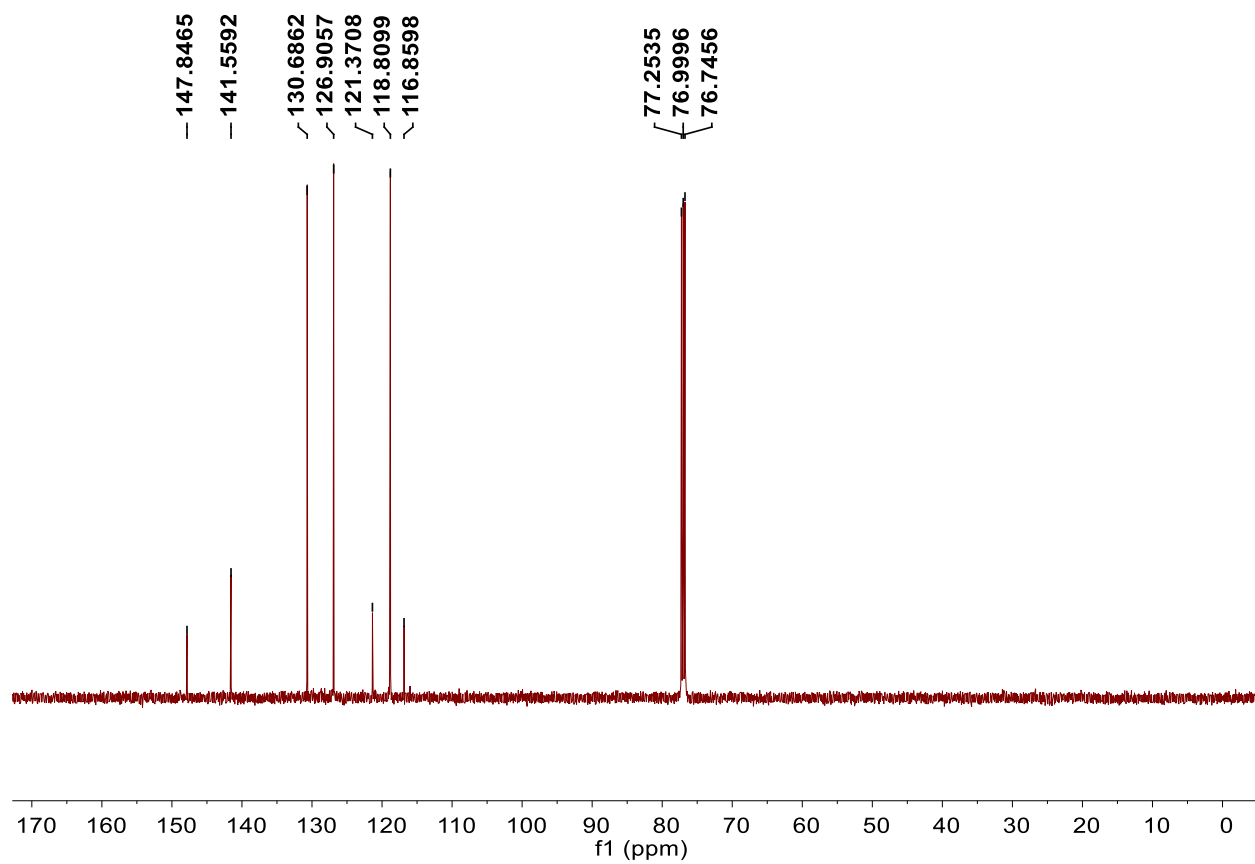
<sup>1</sup>H NMR 11.2 in CD<sub>3</sub>CN



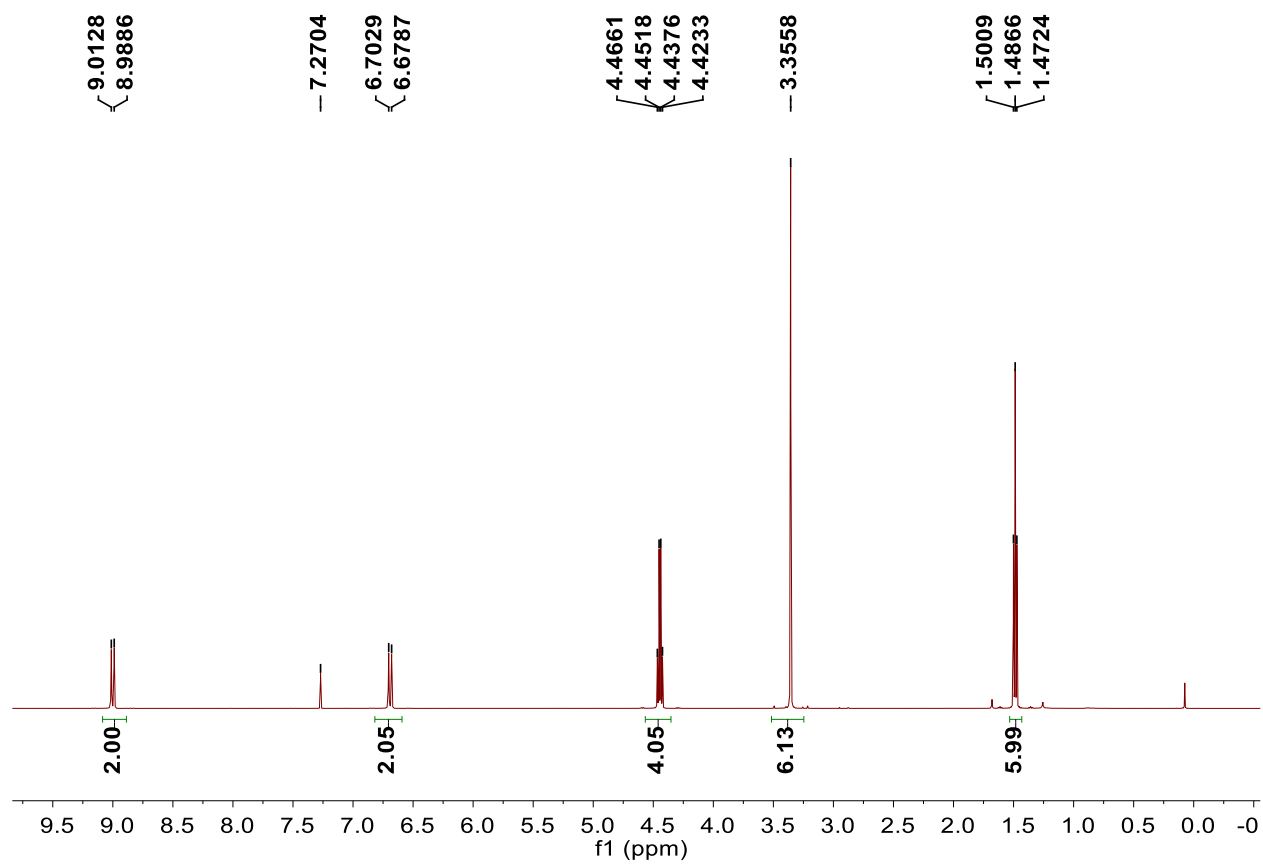
<sup>1</sup>H NMR IL.3 in CDCl<sub>3</sub>



<sup>1</sup>H NMR IL.4 in CDCl<sub>3</sub>

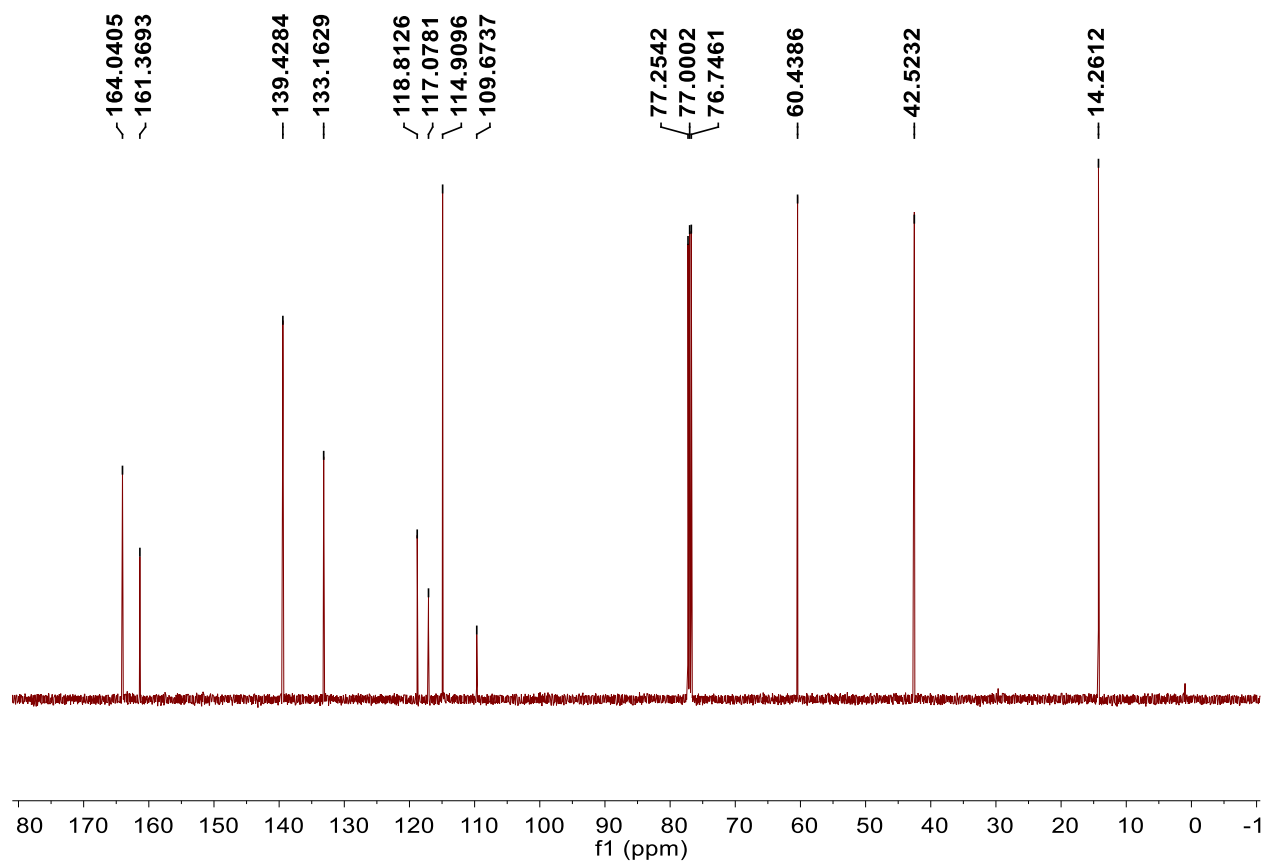


$^{13}\text{C}$  NMR II.4 in  $\text{CDCl}_3$

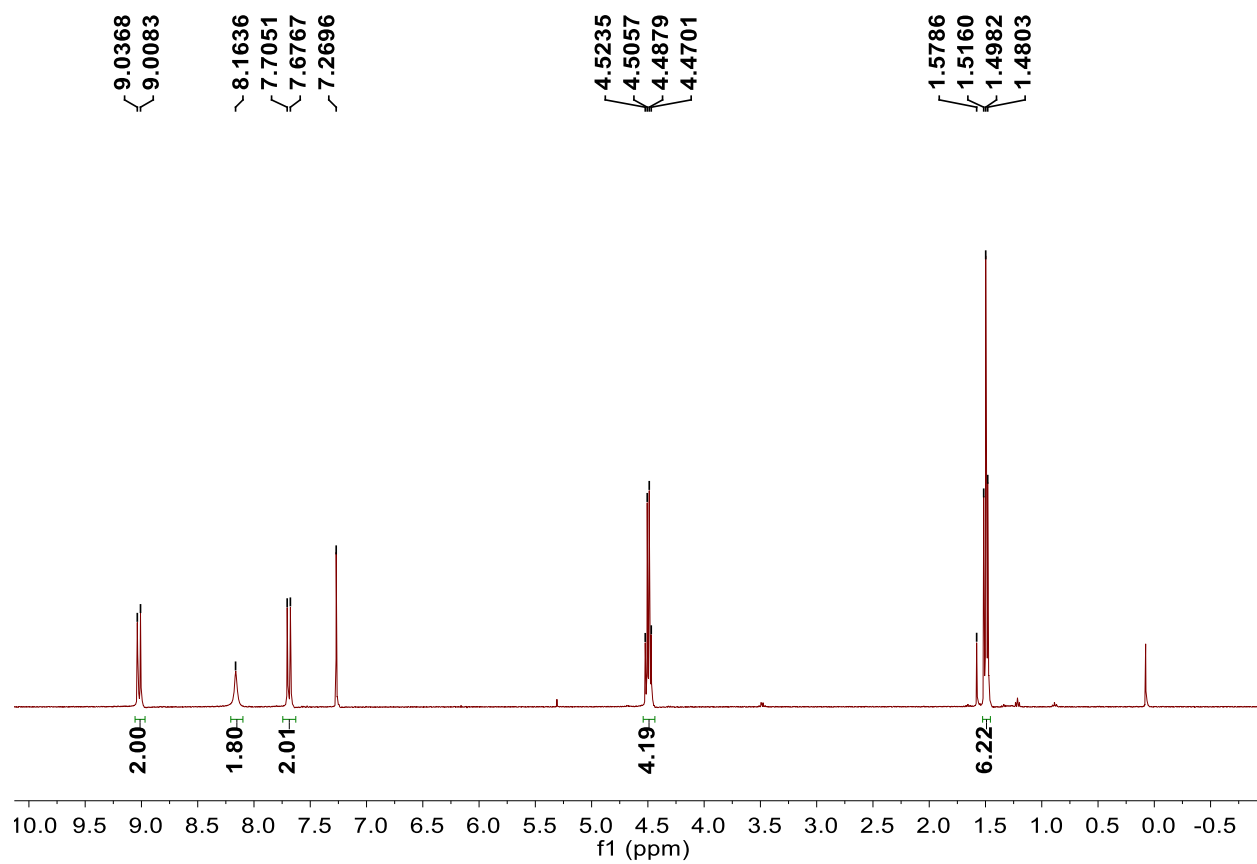


<sup>1</sup>H NMR 11.5 in CDCl<sub>3</sub>

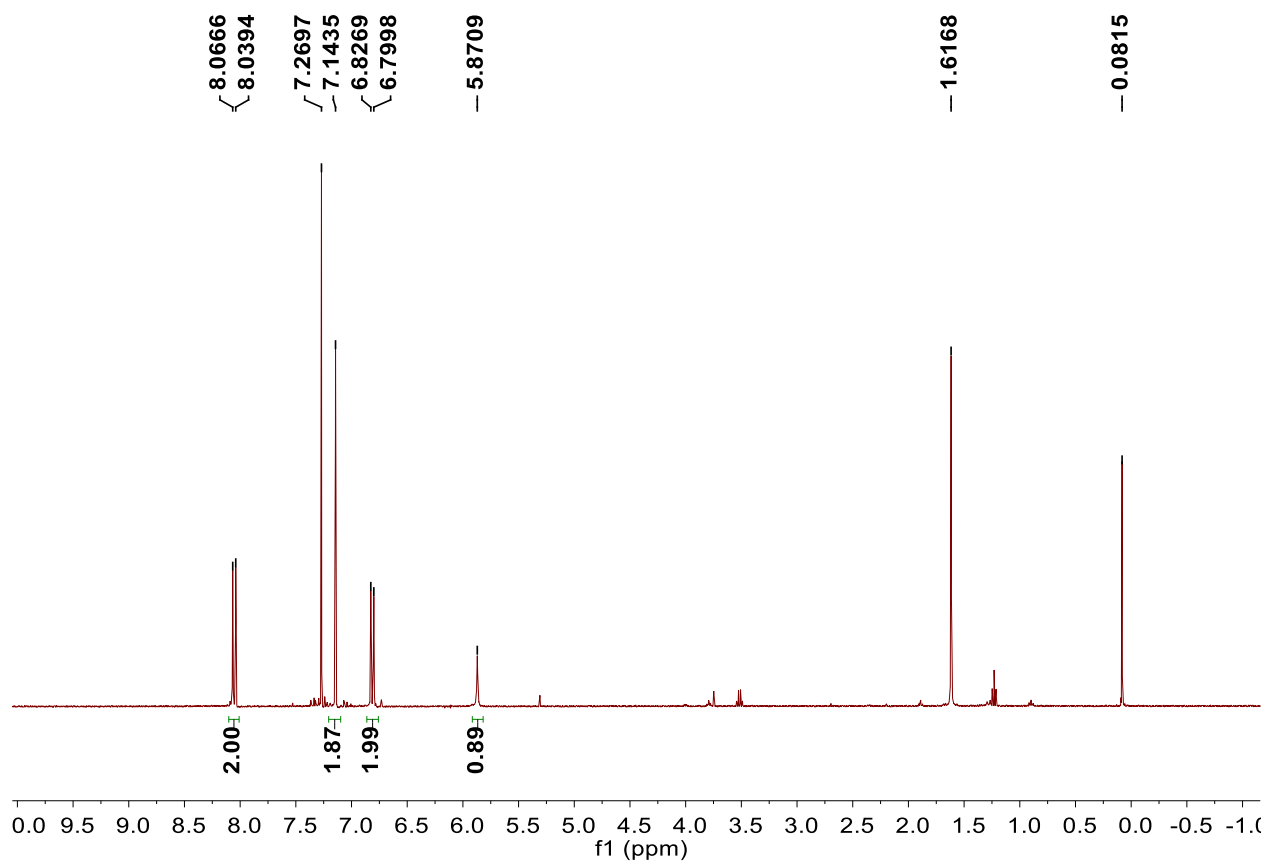




$^{13}\text{C}$  NMR II.5 in  $\text{CDCl}_3$



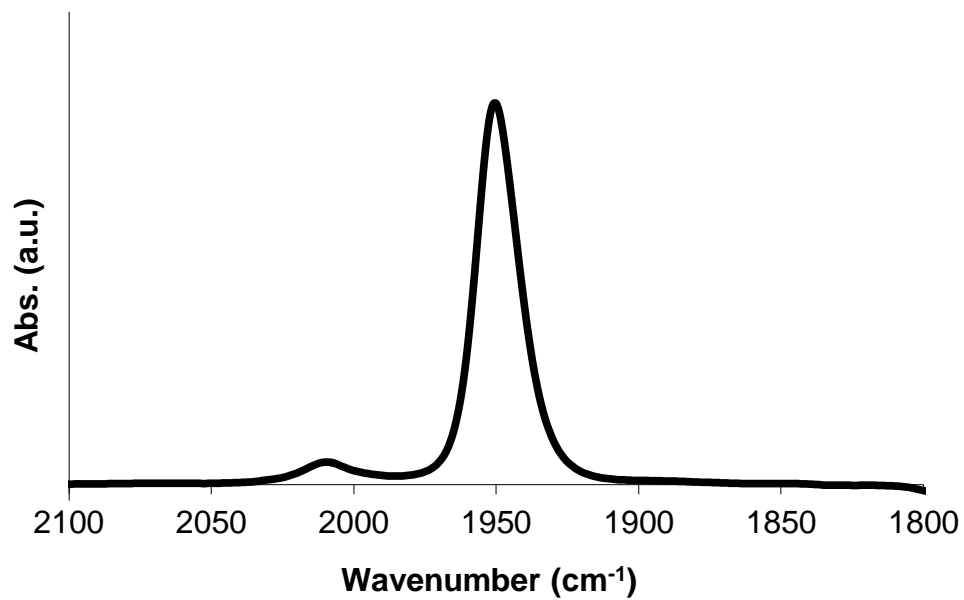
<sup>1</sup>H NMR IL.6 in CDCl<sub>3</sub>



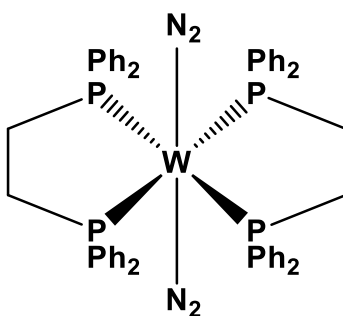
<sup>1</sup>H NMR 11.10 in CDCl<sub>3</sub>

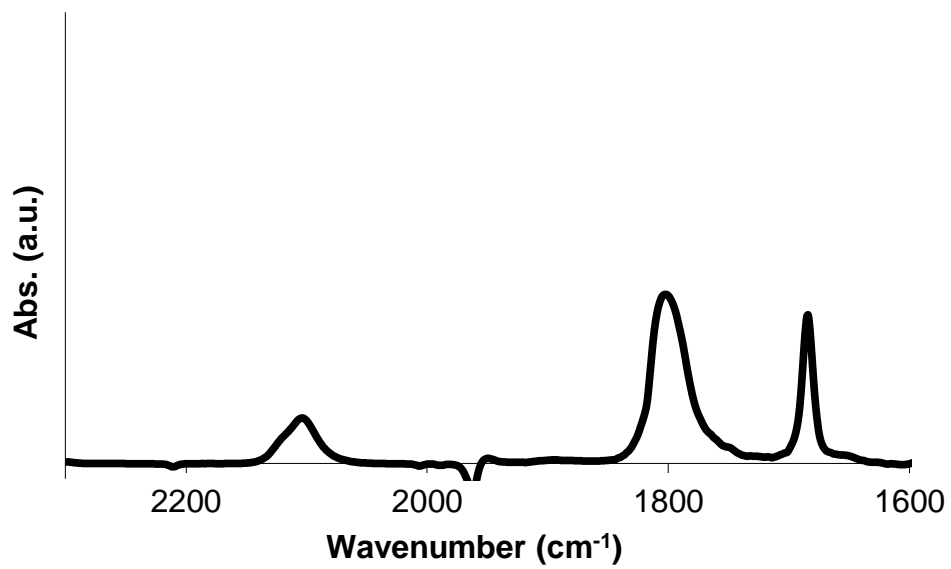
## **Appendix 5**

### **FTIR Spectra of Selected Compounds**

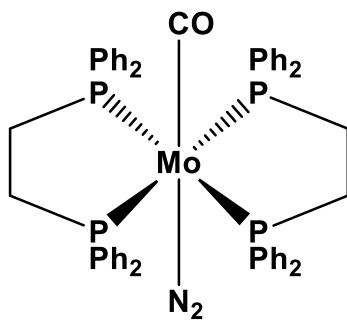


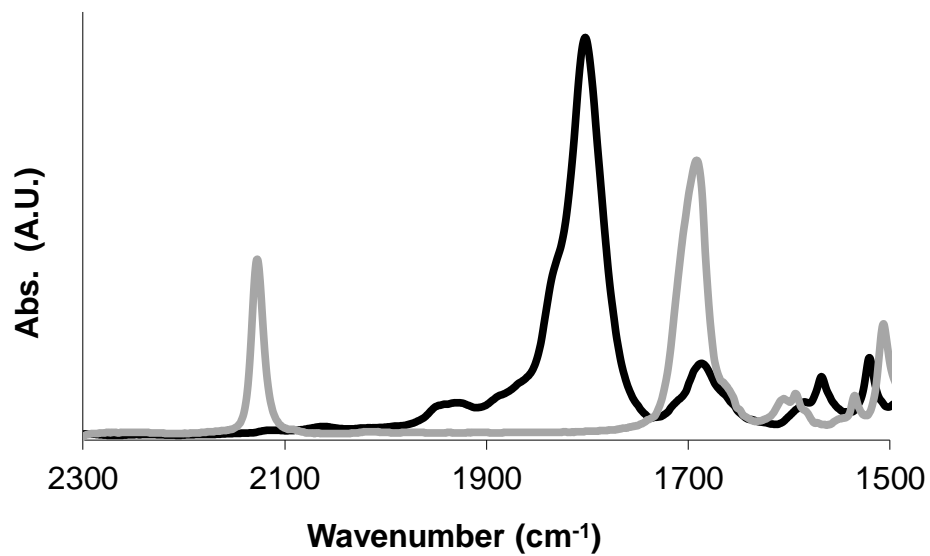
FTIR of  $[\text{W}(\text{N}_2)_2(\text{dppe})_2]$  in THF



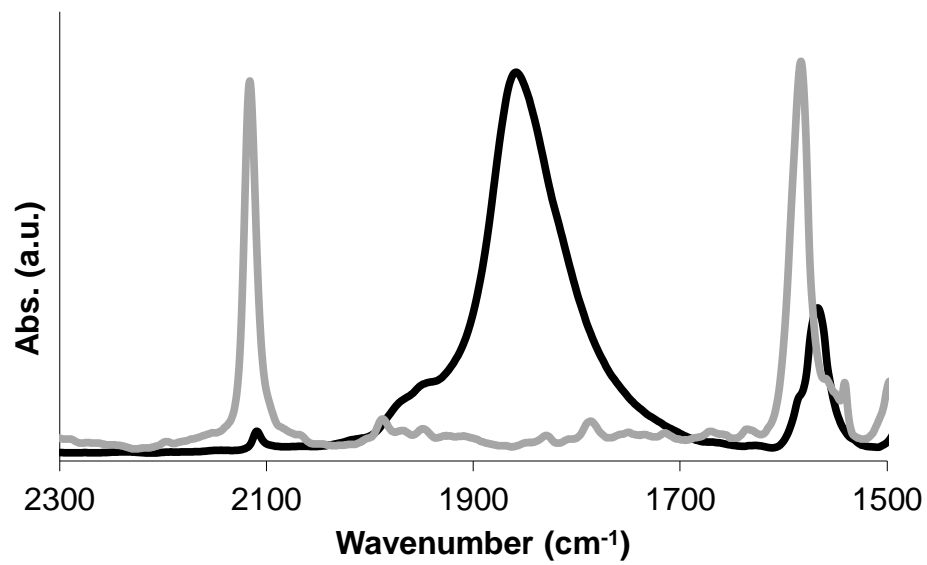


FTIR of  $[\text{Mo}(\text{CO})(\text{N}_2)(\text{dppe})_2]$  in THF



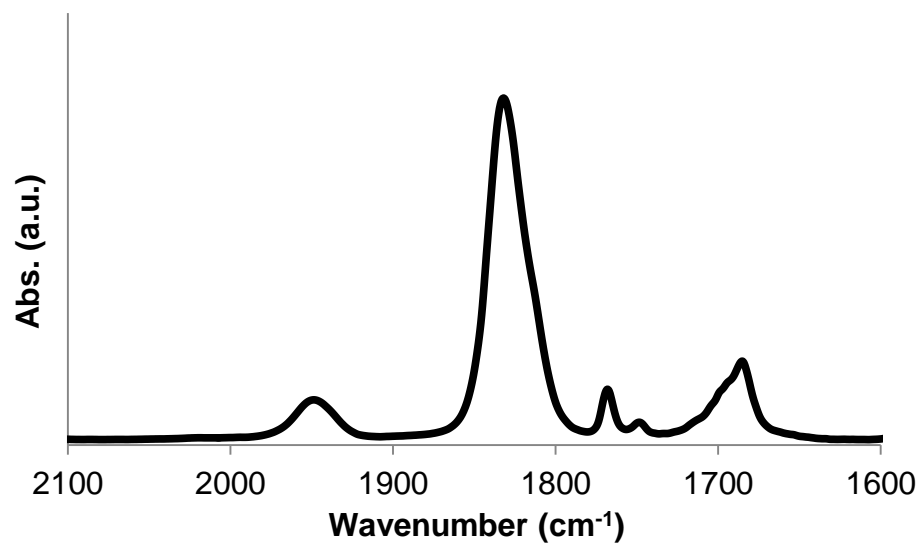


FTIR spectra of **III.1** (black) and the corresponding free isocyanide ligand (grey) in THF.

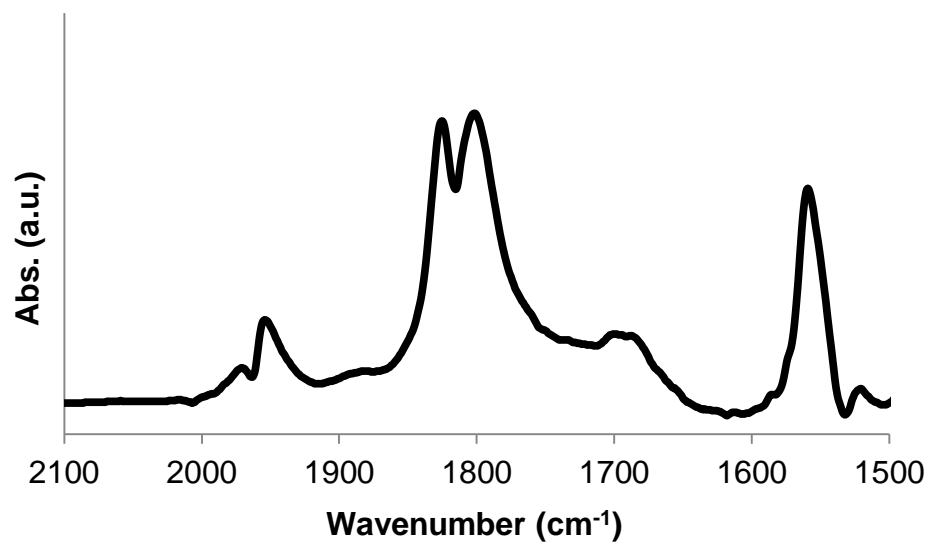


FTIR spectra of **III.2** (black) and the corresponding free isocyanide ligand (grey) in THF.





FTIR spectrum **III.4** in THF



FTIR spectrum of **III.5** in THF